https://doi.org/10.1070/RCR5027

Computational NMR of natural products

Valentin A. Semenov, Leonid B. Krivdin

A.E.Favorsky Irkutsk Institute of Chemistry, Siberian Branch of the Russian Academy of Sciences, ul. Favorskogo 1, 664033 Irkutsk, Russian Federation

This review generalizes diverse computational NMR studies of different natural products involving true alkaloids (indole, quinolizidine, pyrrolizidine, piperidine, indolizidine, quinoline, isoquinoline, indoloquinoline, and guanidine alkaloids), pseudoalkaloids (terpenes and steroids), quinones, lactones, lactams, flavonoids, and many others. The diverse computational protocols employed in each particular case are thoroughly discussed with a special emphasis on their structural and stereochemical applications.
The bibliography includes 165 references.

Dedicated to Professor Gary Martin in view of his outstanding contribution to the field of Nuclear Magnetic Resonance of natural products.

Contents

1. Introduction 2
2. Quantum chemical calculations of NMR chemical shifts: a general overview 2
   2.1. Level of theory and quality of basis set 2
   2.2. Solvent effects 3
   2.3. Zero-point vibration corrections 3
   2.4. Relativistic effects 3
   2.5. Conversion of calculated shielding constants into NMR chemical shifts scale 4
   2.6. Identification of stereochemical misassignments 4
3. True alkaloids 5
   3.1. Indole alkaloids 5
      3.1.1. Monoterpene indole alkaloids 6
      3.1.2. Dimeric monoterpene indole alkaloids 10
      3.1.3. Trimeric monoterpene indole alkaloids 10
   3.2. Quinolizidine alkaloids 12
   3.3. Pyrrolizidine alkaloids 14
   3.4. Piperidine alkaloids 14
   3.5. Indolizidine alkaloids 14
   3.6. Quinoline and isoquinoline alkaloids 15
   3.7. Indoloquinoline alkaloids 15
   3.8. Guanidine alkaloids 15
4. Pseudoalkaloids 16
   4.1. Terpenes 16
   4.2. Steroids 19
5. Quinones 20
6. Miscellaneous 20
   6.1. Lactones 20
   6.2. Lactams 23
   6.3. Organoelement natural products 25
   6.4. Peptides 25
   6.5. Mixed types 26
7. Conclusion 31
8. List of acronyms and designations 32
9. References 32

V.A.Semenov. PhD in chemistry, graduated from Irkutsk State University (Department of Chemistry) in 2009 and received his PhD in 2016 from A.E.Favorsky Irkutsk Institute of Chemistry. He is currently a Head of the NMR Laboratory at the same Institute.
His research interests focus on the high-level quantum-chemical calculations of NMR spectral parameters being substantiated by over 30 research papers in chemical and physical international journals.
E-mail: semenov@irioch.irk.ru
L.B.Krivdin graduated from M.V.Lomonosov Moscow State University in 1977, received his PhD in 1982 from the Irkutsk State University, which was followed by a postdoctoral fellowship at Flinders University of South Australia in the group of Professor Ernst Della (1990–1991). He received his DSc in 1989 and Full Professor in 1993.
His research interests focus on computation of NMR parametres being substantiated with some 400 research publications, including approximately 20 reviews and book chapters. Under his scientific supervision, 12 PhD dissertations were defended in the interim of 1989 until present. Professor Krivdin visited 50 countries being invited as a visiting professor of a number of different universities involving those in Russia, the United States, Australia, Argentina, the United Kingdom, Poland, France and many others around the world. He is currently a Chief Researcher in the NMR Laboratory at A.E.Favorsky Irkutsk Institute of Chemistry and a Chair of Chemistry at Angarsk State Technical University.
E-mail: krivdin55@gmail.com

The present review is dedicated to ***Professor Gary Martin*** *from Seton Hall University and Stevens Institute of Technology, USA, in view of his outstanding contribution to the field of Nuclear Magnetic Resonance of natural products. Gary Martin, the 2018 recipient of the Schoolery Award, holds a PhD degree in Pharmaceutical Sciences. He is doing his research in NMR spectroscopy of natural products and is now investigating the utilization of NMR pulse sequences for the unequivocal confirmation of molecular constitution and configuration using anisotropic NMR data - residual dipolar couplings and residual chemical shift anisotropy. He is the author of approximately 350 publications, including books, book chapters, reviews, and research papers. Some a decade ago, Gary Martin adopted the position of a Co-Editor-in-Chief of Magnetic Resonance in Chemistry, a leading NMR periodical appreciated worldwide. It was not without his efforts, which sharply increased the impact factor of the journal. The topic of the present review is among the main, so to say, passions of Gary, and my sincere hope is that it will be of some practical value to many scientists all over the world working in this field.*

Leonid Krivdin

Received 07 June 2021

© 2022 Uspekhi Khimii, ZIOC RAS, Russian Academy of Sciences and IOP Publishing Limited

1. Introduction

Synthetic methods applied for the production of natural products and more complex biological species, including carbohydrates, peptides, deoxyribonucleic and ribonucleic acids, and small peptides, have enormously progressed in the last decade. Indeed, we are now witnessing unprecedented progress in this area involving structural aspects of modern organic and bioorganic chemistry. In parallel with those achievements, a common practice of modern structural studies deals with numerous revisions and reestablishments of the originally proposed erroneous structures. On the other hand, we are currently witnessing numerous unsuccessful attempts to synthesize natural products extracted from different natural sources, such as trees, plants, seaweed, and corals, which calls for the development of modern means of their structural identification.

At present, marked progress in modern NMR techniques and instrumentation is observed.[1] In this line, NMR-oriented calculations at different levels of theory,[2–19] together with those dealing with the computational aspects of the most common NMR isotopes,[20–31] are rapidly developing penetrating different areas of chemistry involving, in particular, biochemical studies of natural products.[32–37]

Presented material is arranged in three basic sections: the first one dealing with the calculation of NMR chemical shifts and spin-spin coupling constants of true alkaloids; the second one concerning the computational NMR of pseudoalkaloids like terpenes and steroids; and the third one comprising the computational NMR of miscellaneous natural compounds, such as lactones, lactams and peptides. A good deal of interest is focused on stereoelectronic effects and their applications to structural and stereochemical studies of natural products.

2. Quantum chemical calculations of NMR chemical shifts: a general overview

Considering the characteristic features of the calculation of NMR chemical shifts of natural products, several factors should be noted that affect the accuracy of theoretical calculations in comparison with experiments. For an adequate description of the electronic system, it is necessary to solve a number of problems aimed at eliminating errors arising in quantum chemical calculations. Among them are solvent and relativistic effects, as well as the general factors affecting the accuracy of calculating magnetic resonance parameters, which are the level of theory and quality of the basis set, vibrational corrections, and finally the so-called 'geometric factor'.

2.1. Level of theory and quality of basis set

When calculating second-order molecular magnetic properties, such as chemical shifts and spin-spin coupling constants, it is of major importance to take into account electron correlation, which is determined by the level of theory of a particular method. This is the insufficient description of electron correlation, which is the main source of errors in the calculation of chemical shifts and spin-spin coupling constants.

Pure *ab initio* methods, when used in combination with a sufficiently large basis set, can yield highly accurate numerical results. However, the calculation of large molecules such as natural products at the non-empirical level is an extremely resource-demanding process. Therefore, it is quite natural that small compounds containing no heavy nuclei remain the prime object of high-precision *ab initio* methods. For this reason, calculation of NMR chemical shifts of biological molecules with significant molecular weight could be performed with less expensive methods, such as density functional theory (DFT).[38]

The DFT method is much more economical than any of the non-empirical calculations because the former uses a function that depends only on three spatial coordinates, while the many-electron wave function of a system with N electrons, used in the non-empirical methods, operates with $3N$ variables. At that, the complexity of the calculation increases in proportion to the degree to which the excited states are taken into account.

The practical interest to the DFT method for chemists is that it is a highly economical alternative to any of the *ab initio* methods. With a correct choice of the DFT functional used for calculation of shielding constants, it is possible to approach the accuracy of the MP2 theory, the former with a significant reduction of the computational cost, which is comparable to the uncorrelated Hartree-Fock method.

Analysis of publications on theoretical calculations of NMR parameters of natural products of the last two decades suggests that the overwhelming majority of works have been performed within the framework of various DFT functionals. Most often, the preference is given to a classical hybrid functional B3LYP[39] and the family of hybrid functionals based on the Perdew-Wang exchange corrections, such as B3PW91[40] and mPW1PW91.[41] Exchange-correlation functionals of Perdew, Burke and Ernzerhof, PBE*n*[42] are also used rather frequently. It is much less common to come across more complex double hybrid multiparameter functionals, as well as functionals using dispersion corrections such as ωB97X-D.[43]

The choice of the basis set of functions describing atomic orbitals is also an important factor of the level and quality of the quantum-chemical calculation of the NMR properties. The basis set must meet the requirements of the particular problem, must have sufficient dimensions, and be flexible for describing the molecular properties of the considered electronic system. Based on this consideration, the following two factors can be used as the main criteria when choosing the basis for the calculation of NMR spectral parameters: rapid convergence to the complete basis set (CBS)[44] limit and optimization of the basis set for the calculation of spectral properties.

The latter is determined by the inclusion of special tight functions, which correctly describe the distribution of electron density near atomic nuclei. In this line, for the calculation of coupling constants, specialized basis sets are used, which are extended with tight *s*- and *p*-functions. Among the most popular specialized basis sets optimized for the calculation of NMR shielding constants (chemical shifts) is the pcS-*n* family of basis sets developed by Jensen.[45]

In addition, a sufficient level of valence splitting, enlarged with polarization and diffusion functions for a correct description of the valence part of the electron shell, is required. Diffuse functions are large and have a sufficient distance from the nucleus, which provides an adequate description of the electron density distribution in ionic and complex systems, as well as the lone pairs of heteroatoms. However, despite a wide variety of known specialized basis

sets, one of the most popular in calculating NMR chemical shifts is the standard two- and three-fold valence split Pople 6-31G[46] and 6-311G,[47] which is mainly due to their simplicity and, as a result, low computational cost.

It is also worth mentioning the approach, which is known as the locally dense basis set (LDBS) scheme.[48] The main idea of this approach is that one or a group of nuclei of interest is described by an extended high-quality basis set, while the rest of the nuclei in the molecule are described on a much smaller and much more economical basis. The LDBS approach allows a significant reduction in computational cost (of up to several orders of magnitude in terms of processing time!) with only a slight loss in accuracy. In addition, the principal feature of this approach is that it permits the calculation of chemical shifts at a high level of theory for large molecules, for which it is impossible to use complete basis sets owing to the exceeding the limit of particular software packages in terms of the number of basis functions of atomic orbitals.

2.2. Solvent effects

The most popular methods for modeling solvation effects can be divided into two large groups — the implicit/continuum models, developed to take into account nonspecific solvation, and models with an explicitly specified solvent in the computational space, also called the 'supermolecular model', allowing us to take into account specific interactions with the environment.

Empirical parameters, which define the solvent as a continuous isotropic field, play a key role in models of implicit solvent accounting. The main one is the dielectric constant ε. The change in the solvent field can be taken into account within the polarizable continuum model (PCM) developed by Tomasi and coworkers.[49] The PCM model is characterized as a quasi-non-empirical method for calculating the energy of solvation, accounting for nonspecific interactions between the dielectric solvent and substrate. Solvent effects calculated within the PCM scheme are constrained not to take into account any specific solvation effects. It can be applied at all levels of quantum chemical calculation. Another advantage of this model lies in the fact that its machine resource costs are much lower than those of the models of explicit accounting of the solvent.

However, the use of continuum models with the consideration of the solvent as an isotropic continuous medium does not account for specific non-covalent interactions between the molecules of solvent and solute. To describe such contacts, it is necessary to use an approach that describes the solvent-substrate molecular cluster in an explicit way. The supermolecular model allows one to estimate the influence of solvation effects on the NMR chemical shift quite accurately. Ideally, the number of solvent molecules in the calculation space should be as large as possible, but increasing the number of calculated electronic systems leads to an enormous increase in computational cost.

2.3. Zero-point vibration corrections

Regarding the accuracy of the calculated NMR chemical shifts, one should mention the influence of the zero-point vibrations of atomic nuclei (ZPV).[50] To search for the sought mean values of the internal coordinates of nuclei, it is necessary to calculate the deviations of geometric parameters of a molecule in the equilibrium state over all excited states until the effective geometry is found, at which all deviations are averaged.

It should be borne in mind that calculation of the corrections to the zero-point vibrations of nuclei is an extremely resource-demanding process requiring multifold iterations of calculated NMR shielding constants for a large set of anharmonic contributions, that is, the different sets of geometric parameters. A reasonable compromise in this case can be found by calculating shielding constants for the equilibrium geometry at a high level of theory and evaluating vibrational corrections at the DFT level with simplified basis sets.[51] However, even such a hybrid approach is extremely resource demanding and allows the calculation of vibrational corrections only for the simplest molecules.

In practice, when calculating ^{1}H and ^{13}C NMR chemical shifts of natural products, the influence of vibrational corrections is often neglected since they are rather small, being comparable to a total calculation error.

2.4. Relativistic effects

The main relativistic corrections to the nonrelativistic Hamiltonian that affect the NMR shielding constant are defined as the classical scalar Darwin and spin-orbit corrections. The results of numerous studies of the heavy atom effects on the second-order molecular properties indicate that both scalar relativistic and spin-orbit effects result in a significant change in the magnitude of the NMR shielding constant of 'heavy' elements of a third and higher periods. On the other hand, for the elements of the first two periods, relativistic corrections are negligible and are of no practical importance when performing quantum-chemical calculations of NMR chemical shifts.

An exception is the so-called 'heavy-atom effect on the light atom shielding' (HALA),[52] which is due to the presence of a 'heavy' atom attached to a 'light' atom. The spin density induced by the external magnetic field around the heavy atom nucleus is transferred through the chemical bond between heavy and light atoms. In this case, it perturbs the Fermi-contact and spin-dipole contributions to the wave function Hamiltonian of the near-nuclear electrons of the lighter atom.

The HALA effects in the calculated values of NMR shielding constants of light nuclei can reach significant values. In this case, considering relativistic effects for a light atom is of principle importance.[53] The HALA effects for carbon atoms are very well known, as exemplified by the normal halogen dependence (NHD).[54] Moreover, the values of ^{13}C and ^{1}H NMR chemical shifts in the molecules of natural products can be significantly influenced by the closely located atoms of heavier elements such as selenium, tellurium, and transition metals.

The most complete theory, capable of describing relativistic effects, is the formalism of the four-component one-electron Dirac equation, known as the 'fully relativistic four-component framework'.[55] Since calculation, performed according to the four-component relativistic scheme, is an extremely resource-demanding task, several two-component approximations were developed to simplify this procedure. One of the most popular approximations is the zero-order regular approximation (ZORA), which considers the main relativistic corrections, including the most essential spin-orbit correction.[56] Indeed, calculations of the NMR shielding constants of heavy nuclei by this method at the DFT level demonstrate good agreement with the exper-

imental results. At the same time, which is of major importance, the resource intensity of this computational scheme is one of the lowest among the methods taking into account relativistic corrections.[57]

Among the most popular approximations of the two-component Hamiltonian, an alternative to ZORA is the Douglas-Kroll (DK) method, modified and developed by the Hess group[58] (abbreviated as 'DKH'). The DKH method is recommended as a reliable tool for the calculation of relativistic corrections for heavy nuclei.[59]

2.5. Conversion of calculated shielding constants into NMR chemical shifts scale

Despite the seeming simplicity of the conversion of calculated shielding constants into chemical shifts (which is done for comparison with experiment), this operation has many pitfalls and ambiguities. In common practice, there are several statistical methods for converting calculated shielding constants into chemical shifts. The simplest of them consists of calculating shielding constants in a compound under study (σ_i, ppm) and in a standard (σ_{st}, ppm) at the same level of theory. At that, theoretical chemical shifts (δ_i, ppm) are calculated as $\delta_i = \sigma_{st} - \sigma_i$.

To verify the adequacy of the applied calculation scheme, the mean absolute error (MAE) and root mean square deviation (RMSD) are evaluated according to Equations (1) and (2), respectively:

$$\mathrm{MAE} = \frac{\sum_{i=1}^{n} |\delta_{exp} - \delta_i|}{n} \quad (1)$$

$$\mathrm{RMSD} = \sqrt{\frac{\sum_{i=1}^{n} (\delta_{exp} - \delta_i)^2}{n}} \quad (2)$$

where δ_{exp} and δ_i represent the experimental and calculated chemical shifts for each of the n nuclei.

In practice, when recalculating shielding constants into chemical shifts, well-approved statistical techniques are used to compensate for a systematic calculation error associated mainly with the standard used in the experiment. All of them are based on a model, which implies the construction of a linear correlation regression of calculated shielding constants against experimental chemical shifts. At that, experimentally determined chemical shifts are plotted along the abscissa, while calculated shielding constants are plotted on the ordinate (Fig. 1 *a*).

As a result of this correlation, a linear regression equation is determined in the form of $\sigma_{calc} = b - a\delta_{exp}$,

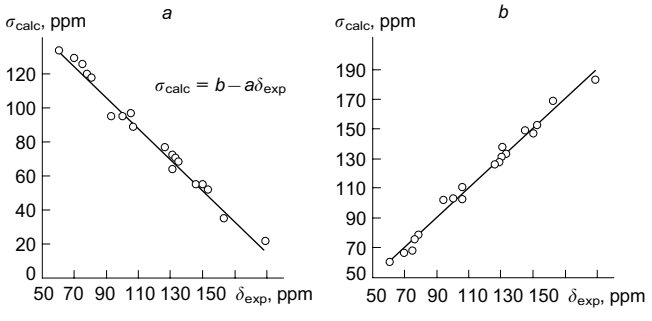


Figure 1. Correlation of calculated shielding constants *vs* experimental NMR chemical shifts (*a*) and correlation of calculated *vs* experimental NMR chemical shifts (*b*).

where constant b is essentially a 'zero chemical shift', corresponding to a shielding constant of the nucleus under study in a potential reference compound. The scaling coefficient a presents a systematic calculation error and can be used to determine the correction factor for the solvent effects, ZPV corrections, relativistic effects, and other accuracy factors. Then, using the slope a and intercept b, one could apply the linear scaling procedure with the estimation of the corrected mean absolute error (CMAE) determined as

$$\mathrm{CMAE} = \frac{\sum_{i=1}^{n} |\delta_{exp} - [(\sigma_{calc} - b)/a]|}{n} \quad (3)$$

where σ_{calc} are the unscaled shielding constants for each of n nuclei, and a and b are the slope and intercept of the linear regression shown in Fig. 1 *a*. At the final step of this statistical treatment, a correlation is deduced between experimental and calculated chemical shifts using the equation $\delta_{calc} = (\sigma_{calc} - b)/a$ (see Fig. 1 *b*).

2.6. Identification of stereochemical misassignments

Recently, much more sophisticated statistical procedures were developed aimed at the comparison of experimental and calculated data when simulated chemical shifts for two or more isomers of a natural product may be very similar, preventing their unambiguous assignment to a particular structure. Such approaches combine quantum chemical calculations of NMR chemical shifts with more complicated data processing, providing a higher level of confidence compared to the simple statistical parameters discussed in the previous Section 2.5. These new workflows, which are based on statistical processing by virtue of Student's *t*-test, are currently considered the most accurate and important alternative tools for solving a number of difficult structural and stereochemical assignments from a theoretical point of view.

Initial approaches such as CP*n* (Ref. 60) and DP4 (Ref. 61) have shown that calculation of NMR chemical shifts combined with diastereomer probability is a powerful tool for determining stereochemistry in complex cases where only one set of experimental data is available. The DP4 method is much more successful at making correct assignments with a high rate of confidence than probabilities based only on MAE and/or correlation coefficient and RMSD. When assigning a higher probability to the correct structure, this is a much more efficient scheme than the probability of a random guess.

Later, different variations of this methodology were created, including Py-DP4,[62] DP4+,[63] DP4.2,[64] *J*-DP4,[65] and DiCE.[66] Among those, the most popular is the DP4+ modification proposed by Sarotti and coworkers,[63] where in addition to the scaled chemical shifts, the inclusion of unscaled data was implemented (see previous Section). As a result, it is much more efficient in performing correct assignments and has larger confidence than probabilities based on the scaled chemical shifts. Moreover, the use of higher levels of theory in the procedure of calculating NMR parameters resulted in a significant improvement in the overall performance of the DP4+ approach compared to the original DP4 method of Smith and Goodman.[61]

Recently, on the basis of the diastereomer probability distribution formalism, more complex techniques have been developed, including the use of feed-forward artificial neural networks (ANNs), such as DFT+ML,[67]

ANN-PRA,[68,69] and DP4-AI.[70] Within a framework of these techniques, calculated shielding constants together with experimental NMR data are subjected to correlation analysis. Furthermore, the obtained set of statistical descriptors is used as the input vectors for the ANN input layer. Ultimately, using the results of a pattern recognition analysis, a conclusion is made about the correctness or incorrectness of the initially established stereochemical structure of a compound under study.

3. True alkaloids

One of the most known and representative classes of natural products are the alkaloids of natural (mostly plant) origin involving nitrogen-containing heterocycles — the so-called 'true alkaloids'. It is long and very well known that most of these compounds provide marked physiological activity. Some of them inhibit, or, on the contrary, excite the nervous system, others paralyze nerve endings, dilate or constrict blood vessels, third have anesthetic effect, *etc*. A wide variety of isolated natural alkaloids predetermined the development of quantum chemistry used for solving the problems of their structural identification. A vast number of studies over the past several years have been devoted to the revision of the structure and configurations of numerous natural products together with the reassignment of their NMR spectra. We start this review with the most interesting and informative results in this area dealing with the most impressive class of true alkaloids — indole alkaloids, numbering more than 4000 known compounds.

3.1. Indole alkaloids

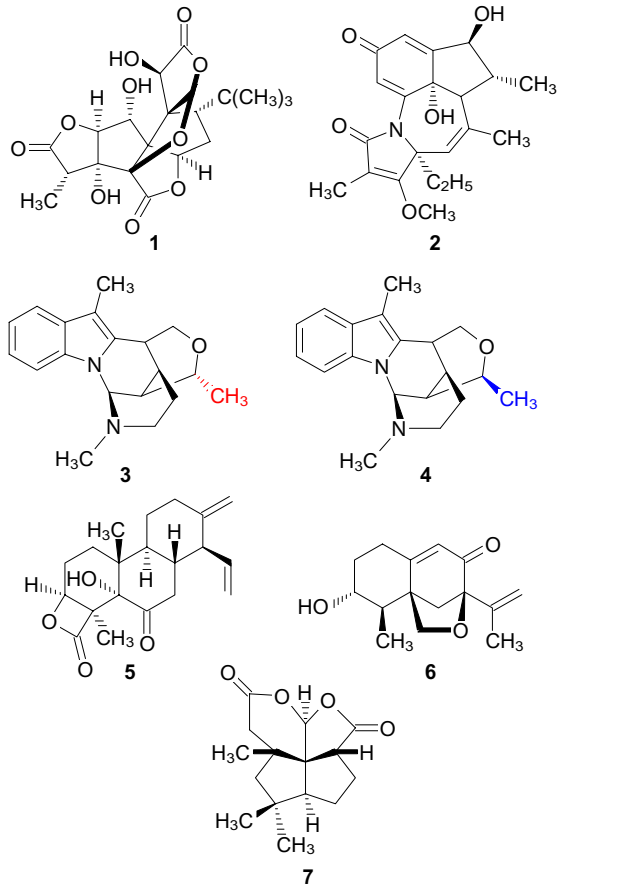
Recently, Kutateladze and Mukhina[71] reported the modification of a fast and reliable method for the multiparametric scaling of Fermi contact contributions to proton-proton spin-spin coupling constants in ^{1}H NMR spectra to achieve fast and accurate prediction. This procedure was demonstrated on a series of 475 experimental spin-spin coupling constants for a set of 919 coupling constants from a diverse collection of natural products, including indole alkaloids, exemplified here with ginkgolide B (**1**), tetrapetalone A-Me aglycon (**2**), alstoscholarisine A (**3**), alstoscholarisine E (**4**), hawaiinolide A (**5**), penicilleremophilane B (**6**), and penifulvin A (**7**).

Performed calculations of ^{1}H–^{1}H spin–spin coupling constants resulted in a mean accuracy of 0.29 Hz with the maximum absolute error not exceeding 1 Hz. An especially good result characterized by an MAE of only 0.23 Hz was achieved for nocardioazine A (**8**) (Fig. 2).

Described in a very recent communication by Hehre *et al.*,[72] was an efficient protocol for the calculation of ^{13}C NMR chemical shifts for natural products with multiple degrees of conformational freedom. An accuracy of ~4 ppm was achieved for about 1000 (!) diverse natural products, with the structures confirmed by X-ray crystallography and approximately 2300 natural products with the structures elucidated mainly by NMR and mass spectra.

In more detail, the authors proposed a scheme for empirically correcting ^{13}C NMR chemical shifts from the ωB97X-D/6-31G(d) DFT calculations. As an example of the latter, the following are the reassigned ^{13}C NMR chemical shifts of daldinone C (**9**), 13,18,20-epi-isochandonanthone (**10**), mycoleptodiscin A (**11**), 5-bromo-8-methoxy-1-methyl-β-carboline (**12**), and wortmin (**13**) (Fig. 3). Large

Structures 1–7



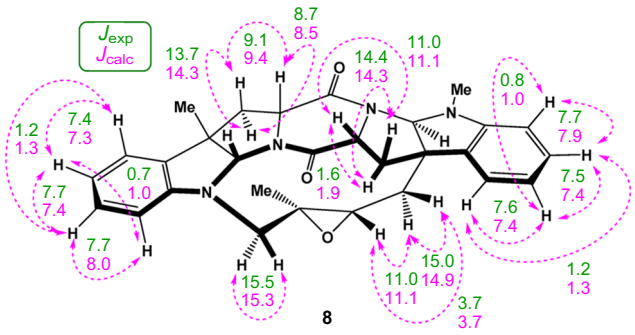


Figure 2. Calculated and experimental ^{1}H–^{1}H spin–spin coupling constants for nocardioazine A (**8**). Reproduced from Kutateladze and Mukhina[71] with the permission of the American Chemical Society.

deviations between the calculated and experimental ^{13}C NMR chemical shifts among diverse natural products are observed, which suggests that much caution should be taken into account when applying calculations at the DFT level.

Tran *et al.*[73] studied the extract of the marine sponge *Damiria* sp., which led to the isolation of two novel alkaloids named damirines A (**14**) and B (**15**). Their structures were elucidated by comprehensive NMR spectroscopic analyses and DFT calculations of their ^{13}C NMR chemical shifts. Reported damirines represent a new hexacyclic carbon-nitrogen framework comprising an indolo[3,2-*a*]carb-

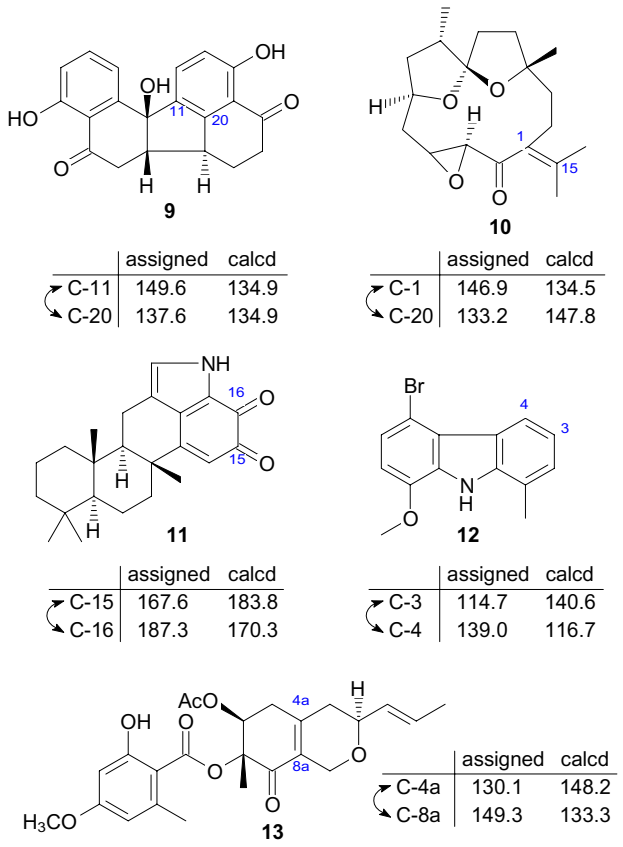
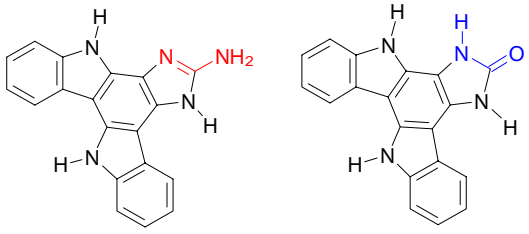


Figure 3. Calculated and experimental ^{13}C NMR chemical shifts for compounds **10**–**13**. Reproduced with minor editing privilege from Hehre *et al.*[72] with the permission of the American Chemical Society.

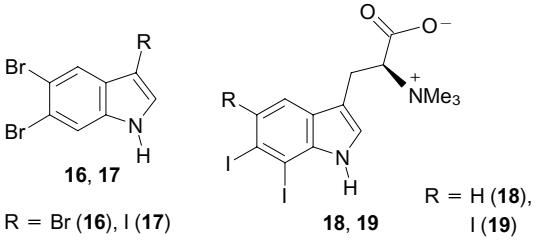
Structures 14, 15



azole fused with either an aminoimidazole or an imidazolone ring.

Casella *et al.*[74] studied a series of 81 molecules exemplified with brominated and iodinated indoles **16**–**19**. The authors emphasized the necessity of including relativistic corrections at the four-component level for the most accurate prediction of the ^{13}C NMR chemical shifts of the brominated and especially iodinated natural products.

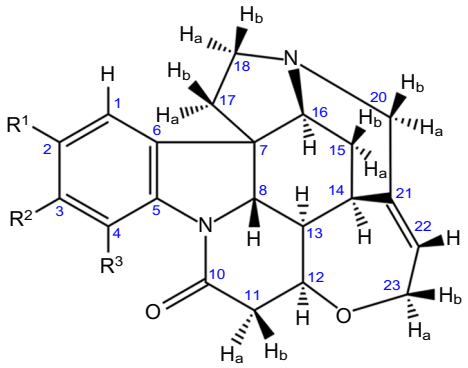
Structures 16–19



3.1.1. Monoterpene indole alkaloids

The study of toxic and carcinogenic substances represents one of the most demanding areas in human safety due to their hazard to public health. There is a great motivation to remove and/or incorporate those substances in other products instead of leaving them to contaminate the environment, which requires establishing versatile methods of their transformation based, for example, on proton transfer complexation.[75]

We start this section with a discussion of strychnine (**20**), a well-known toxic indole alkaloid. The molecule strychnine provides the entire array of 32 possible relative stereoisomers.[76] Strychnine attracts constant and unflagging attention from theoretical chemists dealing with the calculation of its NMR parameters (see, *e.g.*, recent papers [71, 72, 76–82] together with the most salient earlier contributions [83–87]). In this line, in three very recent publications from that series, the stereochemical analysis of strychnine and all its possible stereoisomers was performed based on the calculation of their ^{1}H and ^{13}C NMR chemical



20: $R^2 = R^2 = R^3 = H$;
21: $R^1 = OH$, $R^2 = R^3 = H$;
22: $R^1 = R^3 = H$, $R^2 = OH$;
23: $R^1 = R^2 = H$, $R^3 = OH$;
24: $R^1 = OCH_3$, $R^2 = R^3 = H$;
25: $R^1 = R^3 = H$, $R^2 = OCH_3$;
26: $R^1 = R^2 = OH$, $R^3 = H$;
27: $R^1 = OH$, $R^2 = OCH_3$, $R^3 = H$;
28: $R^1 = H$, $R^2 = OCH_3$, $R^3 = OH$;
29: $R^1 = R^2 = OCH_3$, $R^3 = H$

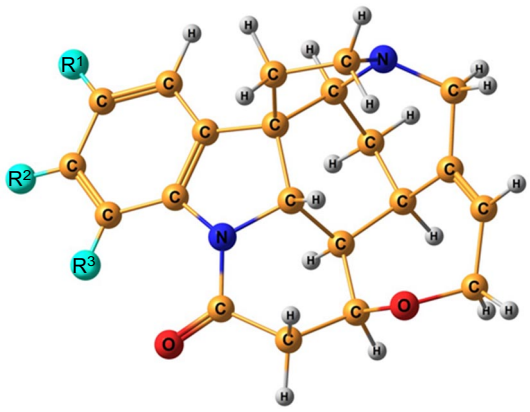


Figure 4. Atom numbering and stereochemical structure of strychnine **20** and a family of representative naturally occurring strychnos alkaloids **21**–**29**. Reproduced with minor editing privilege from Semenov and Krivdin [76] with the permission of Wiley.

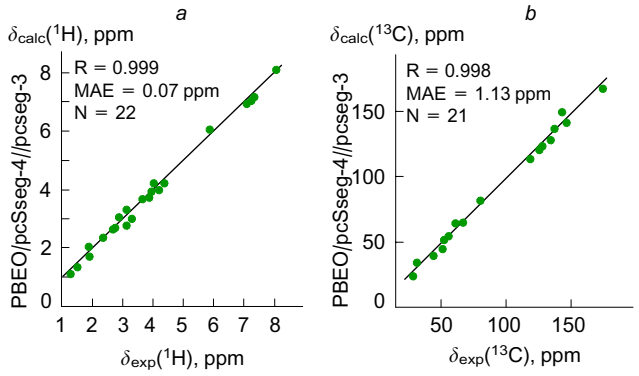


Figure 5. Correlation plots of the chemical shifts of strychnine **20** calculated using the PBE0/pcSseg-4//pcseg-3 LDBS scheme *vs* experiment for ^{1}H and ^{13}C NMR chemical shifts (*a* and *b*, respectively). Reproduced from Semenov and Krivdin[76] with the permission of Wiley.

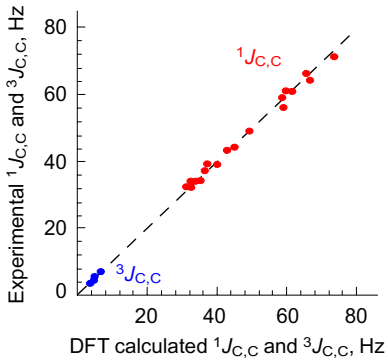


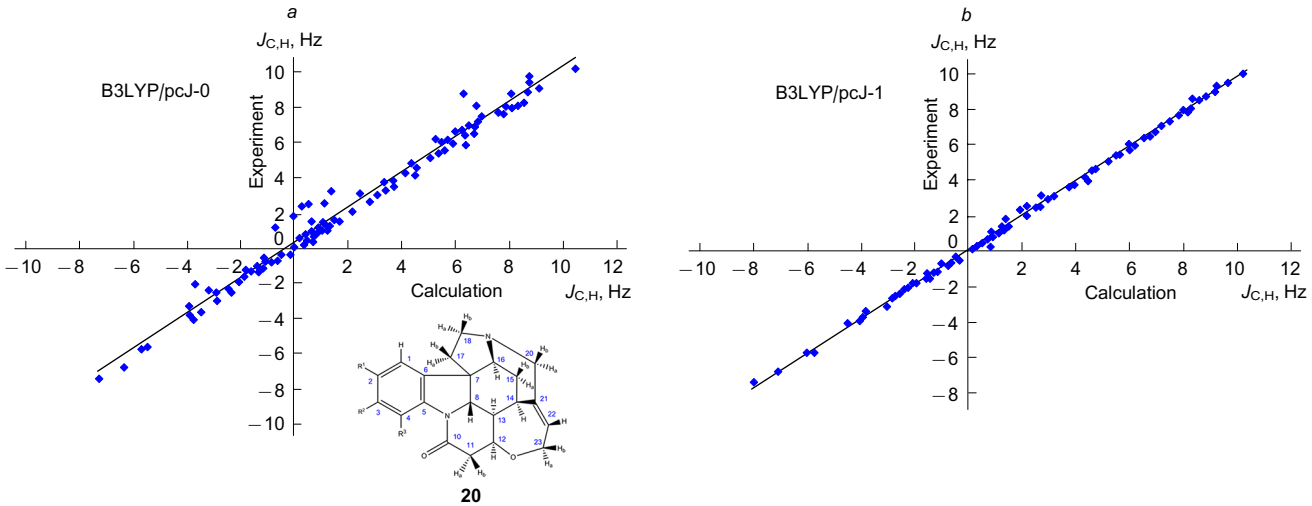
Figure 6. Correlation plot of experimental $^{13}C-^{13}C$ one-bond and vicinal spin–spin coupling constants of strychnine **20** *vs* their theoretical values calculated at the B3LYP/6-311+G(d,p) level. Reproduced with minor editing privilege from Williamson *et al.*[78] with the permission of the American Chemical Society.

shifts[76] together with the one-bond and vicinal carbon–carbon coupling constants (Fig. 4).[78,79]

For the ^{1}H and ^{13}C NMR chemical shifts, it was found that the most accurate scheme at the DFT level using the PBE0 functional was the combination of Jensen's basis sets pcSseg4//pcseg-3 (pcSseg4 on carbons and pcseg-3 elsewhere in the molecule).[76] The performed calculations were characterized by a mean absolute error of only 0.07 ppm in the range of about 7 ppm for protons and only 1.13 pm for ^{13}C NMR chemical shifts spread over the range of approximately 150 ppm (Fig. 5).

For the one-bond and vicinal carbon–carbon coupling constants, a combination of experimental and theoretical methods based on the establishment of carbon–carbon connectivity patterns enabled the tracing out of carbon skeleton of that alkaloid.[78] This is a very illustrative example showing that with the increasing molecular complexity resulting in the diminishing number of protons in the vicinity of a chiral center, the challenge of establishing the relative stereochemical configuration at the optical centers of a molecule dramatically increases. In that paper, the one-bond and vicinal carbon–carbon coupling constants of strychnine were calculated at the B3LYP/6-311+G(d,p) level in very good agreement with the experimental results (Fig. 6). The linear regression between experimental and DFT calculated values was described by a nearly ideal slope (0.98) and a very small intercept (0.33 Hz) for the whole number of 27 different $^1J_{C,C}$ and $^3J_{C,C}$ coupling constants. As a result, a standard error as small as 1.09 Hz was observed, which is comparable to the estimated experimental error.

Additionally, $^1J_{C,C}$ coupling constants were calculated for twelve diastereoisomers of strychnine.[79] On the basis of the unexpected but significant variations of these constants on the very slight conformational changes, a stereochemical analysis based solely on the use of those couplings of strychnine was performed to elucidate the correct diastereoisomer of this compound. The latter was characterized by an MAE of only 0.7 Hz, while for the rest of the diastereoisomers, the MAEs were in the range of 1–3 Hz. In those calculations, theoretical $^1J_{C,C}$ values were evaluated at the B3LYP/6-311+G(d,p) level of theory with the Fermi contact term calculated by adding tight polarization functions for *s* and *d* orbitals to the original 6-311+G(d,p) basis set.



20

Figure 7. Comparison of the calculated and experimental $J_{C,H}$ (122 values) of strychnine **20** for the pcJ-0 and pcJ-1 basis sets. Reproduced with minor editing privilege from Helgaker *et al.*[81] with the permission of the American Chemical Society.

Table 1. Statistical parameters of the calculated ^{1}H and ^{13}C NMR chemical shifts of strychnos alkaloids. Compiled from Semenov *et al.*[88]

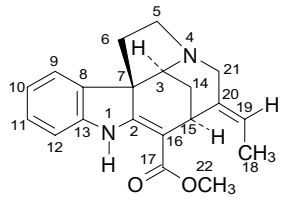
Compound	Range, ppm	Error range, ppm		Relative error (%)	Slope	Correlation coefficient	MAE, ppm
		from	to				
			^{1}H NMR chemical shifts				
20	1.21 – 8.08	−0.16	+0.15	1.2	1.11	0.999	0.08
29	1.22 – 7.82	−0.17	+0.14	1.2	1.09	0.998	0.08
			^{13}C NMR chemical shifts				
20	26.9 – 168.4	−6.7	+2.0	0.7	1.09	0.999	1.0
21	26.6 – 167.5	−9.0	+4.9	1.1	1.09	0.998	1.6
22	26.1 – 167.5	−6.7	+4.9	1.0	1.07	0.999	1.4
23	26.1 – 168.5	−6.7	+1.4	0.9	1.07	0.999	1.4
24	26.6 – 166.4	−6.2	+5.9	1.1	1.07	0.999	1.6
25	26.5 – 167.5	−6.3	+7.7	1.1	1.07	0.998	1.5
26	25.8 – 167.1	−7.3	+4.0	1.1	1.06	0.999	1.5
27	25.9 – 164.2	−9.3	+4.4	1.5	1.08	0.998	2.1
28	26.3 – 169.4	−8.9	+8.3	1.5	1.07	0.997	2.1
29	26.3 – 164.8	−9.1	+4.7	1.7	1.08	0.998	2.3

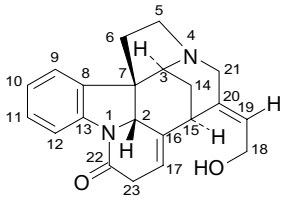
In continuation of these studies, geminal, vicinal, and longer-range carbon – hydrogen and carbon – carbon spin – spin coupling constants, $^{n}J_{C,H}$ and $^{n-1}J_{C,C}$, were calculated for strychnine compared to experiments.[82] In total, for 22 protons and 21 carbons of strychnine, 462 $^{n}J_{C,H}$ and 200 $^{n-1}J_{C,C}$ couplings were calculated at the DFT level. The reduced number of carbon – carbon couplings in comparison with the proton – carbon couplings is because each of the $^{n}J_{C,C}$ couplings between any pair of protonated carbons corresponds to the two different $^{n+1}J_{C,H}$ couplings and each of the methylene groups, so strychnine has roughly double the number of $J_{C,H}$ couplings compared with $J_{C,C}$.

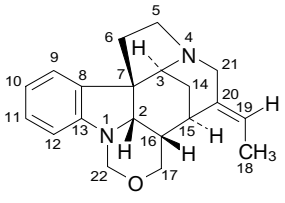
In the recent publication by Helgaker *et al.*,[81] the most common B3LYP exchange-correlation functional was employed with the rather popular Jensen's pcJ-1 basis set (Fig. 7).

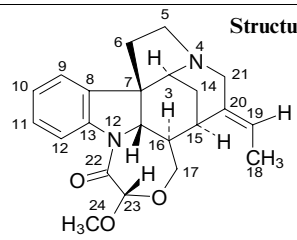
A further study of strychnine and its derivatives[88] involved a family of ten representative naturally occurring strychnos alkaloids, namely, strychnine (**20**) *per se*, 2-hydroxy- (**21**), 3-hydroxy- (**22**), 4-hydroxystrychnine (**23**), *β*-colubrine (**24**), α-colubrine (**25**), 2,3-dihydroxy- (**26**), 2-hydroxy-3-methoxy- (**27**), 4-hydroxy-3-methoxy-strychnine (**28**), and brucine (**29**), all derivatives possessing a strychnine carbon skeleton. Semenov *et al.*[88] employed the PBE0/pcSseg-2//pcseg-2 computational scheme for the calculation of their ^{1}H and ^{13}C NMR chemical shifts, as derived in the parent publication.[76]

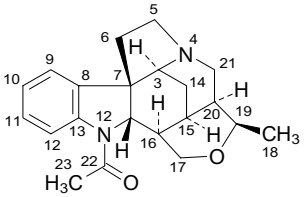
Structures 30 – 41

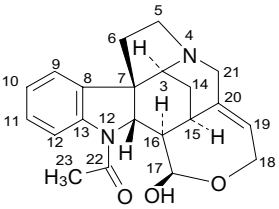

Akuammicine (**30**)

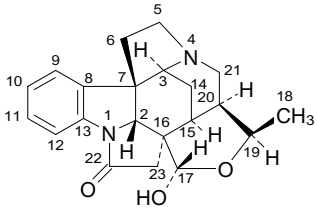

Isostrychnine (**31**)

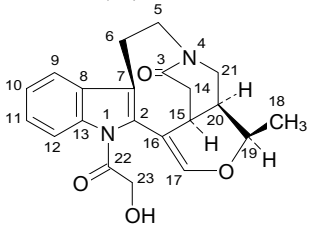

Rosibiline (**32**)

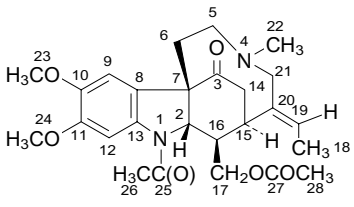

Tsilanine (**33**)

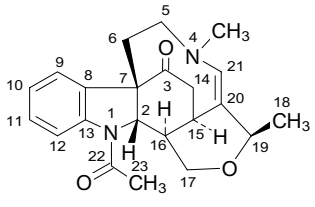

Spermostrychnine (**34**)

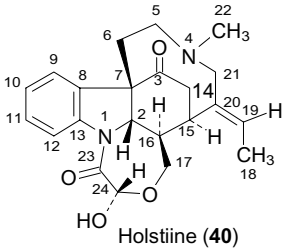

Diaboline (**35**)

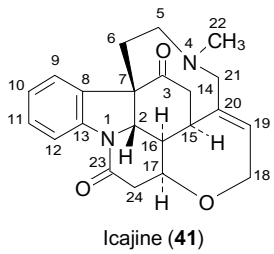

Cyclostrychnine (**36**)


Henningsamide (**37**)


Strychnosilidine (**38**)


Strychnobrasiline (**39**)


Holstiine (**40**)


Icajine (**41**)

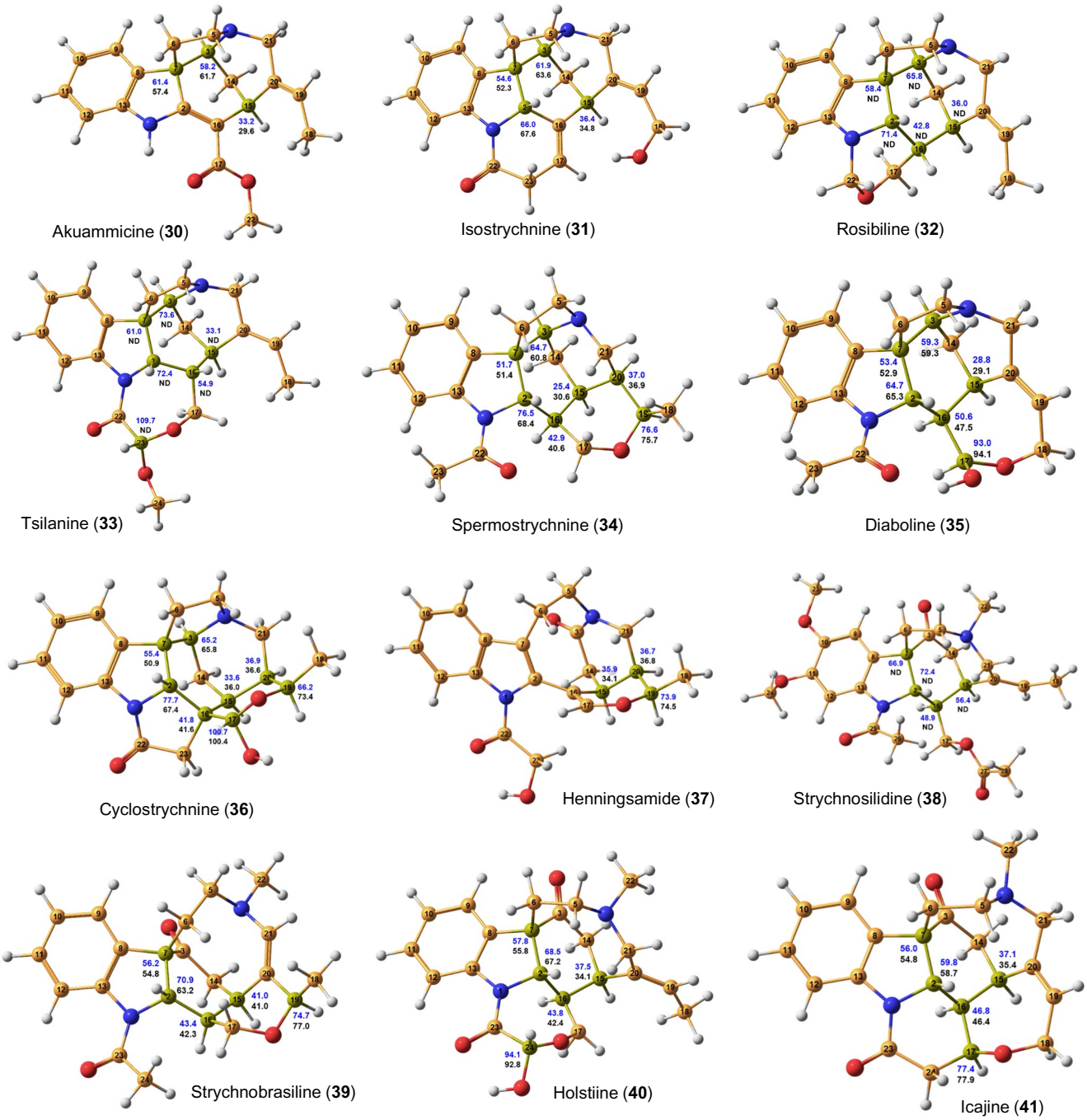


Figure 8. Stereochemical structures (all asymmetric centers are marked in light green) and calculated (marked in blue) and experimental (marked in black) ^{13}C NMR chemical shifts of compounds **30**–**41**. 'ND' stands for 'Not Determined'. Reproduced with minor editing privilege from Semenov *et al.*[89] with the permission of Wiley.

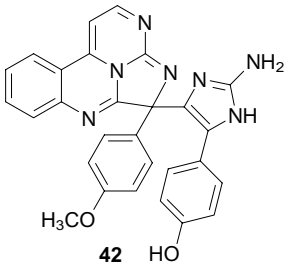
Table 1 lists the statistical parameters of the established correlations between the calculated and experimental ^{1}H and ^{13}C NMR chemical shifts of strychnos alkaloids **20**–**29**.

In the next communication from that series,[89] the PBE0/pcSseg-2//pcseg-2 calculations of ^{1}H and ^{13}C NMR chemical shifts were performed for a classical series of twelve strychnos alkaloids, such as akuammicine (**30**), isostrychnine (**31**), rosibiline (**32**), tsilanine (**33**), spermostrychnine (**34**), diaboline (**35**), cyclostrychnine (**36**), henningsamide (**37**), strychnosilidine (**38**), strychnobrasiline (**39**), holstiine (**40**), and icajine (**41**). The 3D structures of compounds **30**–**41** along with the calculated and experimental ^{13}C NMR chemical shifts are presented in Fig. 8.

Regarding computational ^{13}C NMR data, it should first be noted that for these twelve strychnines, established earlier absolute configurations of all 62 asymmetric centers (see Fig. 8) corresponded well to the results of the performed calculations, and in some particular cases, the reassignments of the individual resonances were reported.

Recently, Sauri *et al.*[90] established the structure of the natural alkaloid eudistidine-C (**42**). The observed $^{4}J_{C,H}$ and $^{5}J_{C,H}$ couplings were in reasonably good agreement with the B3LYP/6-311+G(d,p) calculations.

Structure 42

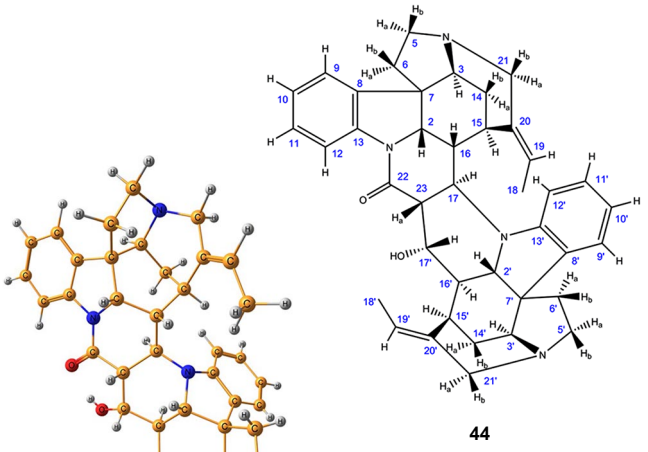


42

Magalhães *et al.*[91] reported a new glucosyl sarpagan alkaloid — 21(*R**)-(*O*-β-glucosyl)-hydroxy-sarpagan-17-oic acid (**43**) arising from tryptamine and secologanin. The biogenetic pathway to compound **43** from tryptamine and secologanin along with eleven accompanying alkaloids, which were isolated from a soluble alkaloidal fraction of the ethanol extract of *Rauvolfia ligustrina*, is shown in Fig. 9. All these structures were elucidated by a variety of spectroscopic methods and DFT calculations of their ^{1}H and ^{13}C NMR chemical shifts. The geometries of all structures were optimized using the mPW1PW91 functional in combination with Pople's 6-31G(d,p) basis set, while all NMR isotropic shielding constants were calculated at the same level of theory in methanol medium simulated with the IEF-PCM solvation method.

3.1.2. Dimeric monoterpene indole alkaloids

Recently, Semenov and Krivdin[92] reported ^{1}H and ^{13}C NMR chemical shifts of strychnobaillonine (**44**). This alkaloid has the stereochemical structure of 2*S*, 3*S*, 7*R*, 15*R*, 16*R*, 17*R*, 23*R*, 2′*S*, 3′*S*, 7'*R*, 15′*R*, 16′*R*, 17′*S*, which was optimized at the M06-2X/aug-cc-pVQZ level (Fig. 10). Very good agreement was achieved at this level between the calculated and experimental ^{1}H (Fig. 11 *a*,*c*) and ^{13}C (Fig. 11 *b*) NMR chemical shifts.



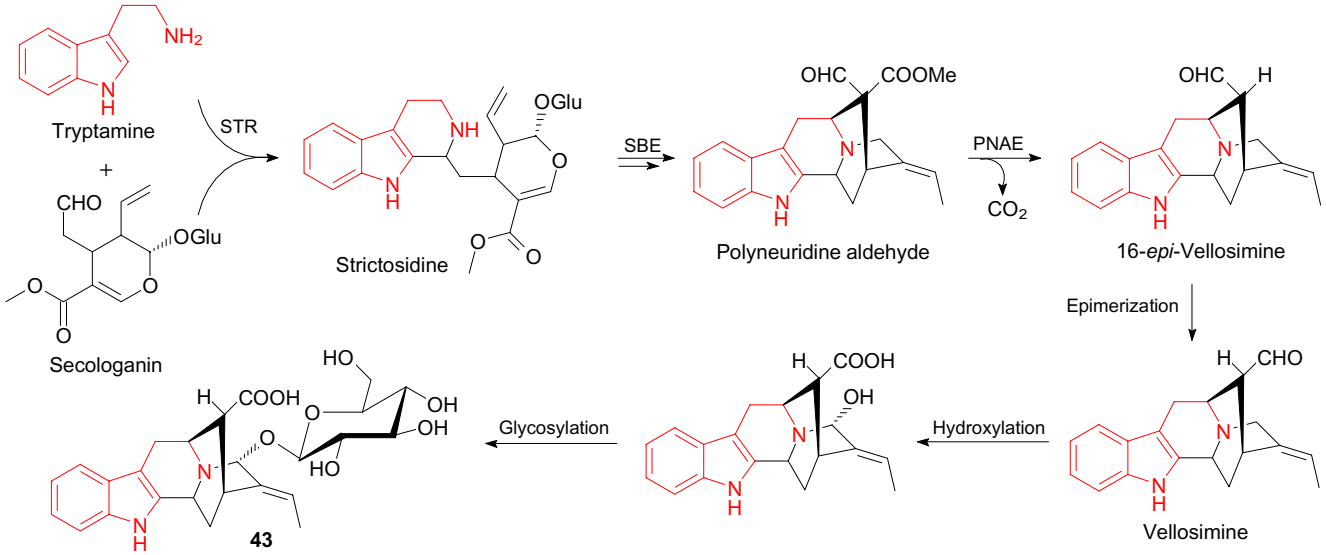
44

Figure 10. Atom numbering and stereochemical structure of strychnobaillonine (**44**).

3.1.3. Trimeric monoterpene indole alkaloids

To date, the isolation of only four trimeric monoterpene indole alkaloids has been reported, namely, strychnohexamine (**45**),[93] ervadivamines A (**46**) and B (**47**),[94] and bousigonine B (**48**).[95] Interpretation of the NMR spectral data of such large objects is an unprecedentedly complex structural problem, and a complex solution in this case can be achieved with much difficulty, mostly by using the methods of modern quantum chemistry.

The first representative of that family, trimeric indole alkaloid strychnohexamine (**45**), has the empirical formula $C_{59}H_{60}N_6O$ consisting of 66 second-raw atoms and 60 protons (Fig. 12). This unique molecule was subjected to the state-of-the-art high-level computation of its ^{1}H and ^{13}C chemical shifts of the configurational isomers at each of its 14 asymmetric centers.[96] Based on those calculations, several reassignments and corrections to the ^{1}H and ^{13}C NMR spectra of strychnohexamine were suggested.



STR is Strictosidine synthase, SBE is Sarpagan bridge enzyme, PNAE is Polyneuridine aldehyde esterase

Figure 9. Biogenetic pathways to the glucosyl sarpagan alkaloid **43**. Reproduced from Magalhães *et al.*[91] with the permission of Elsevier.

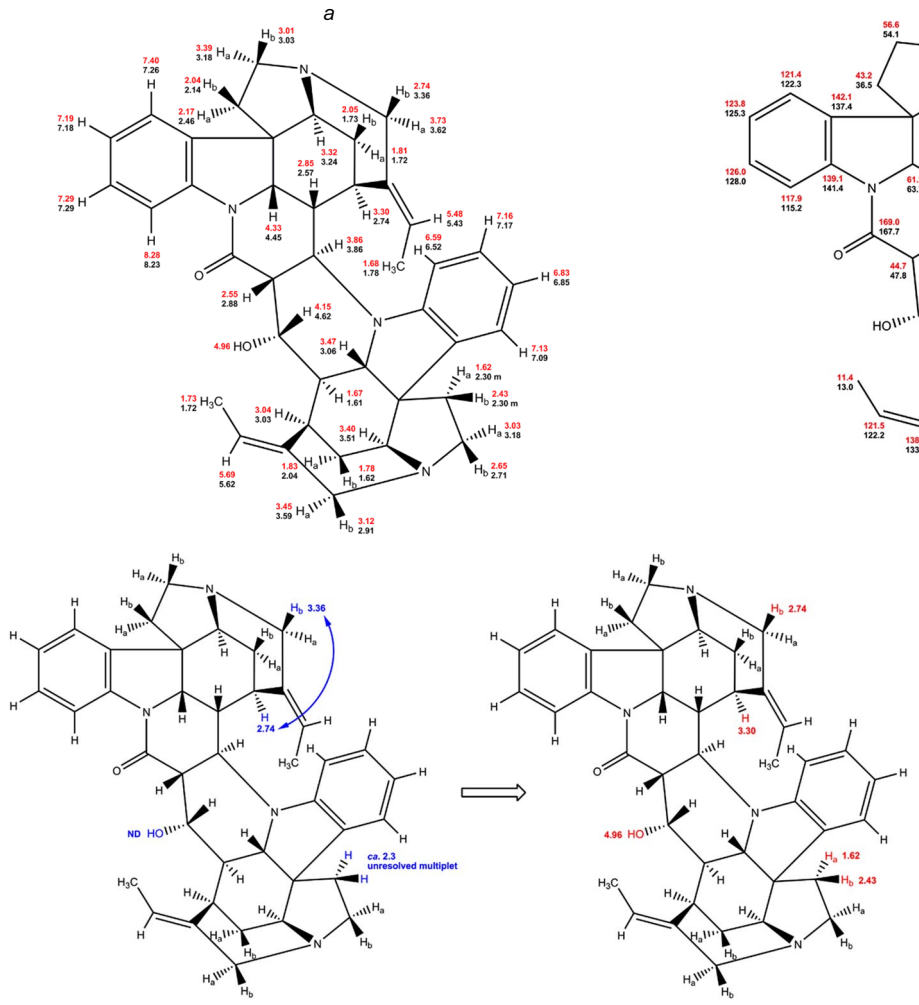


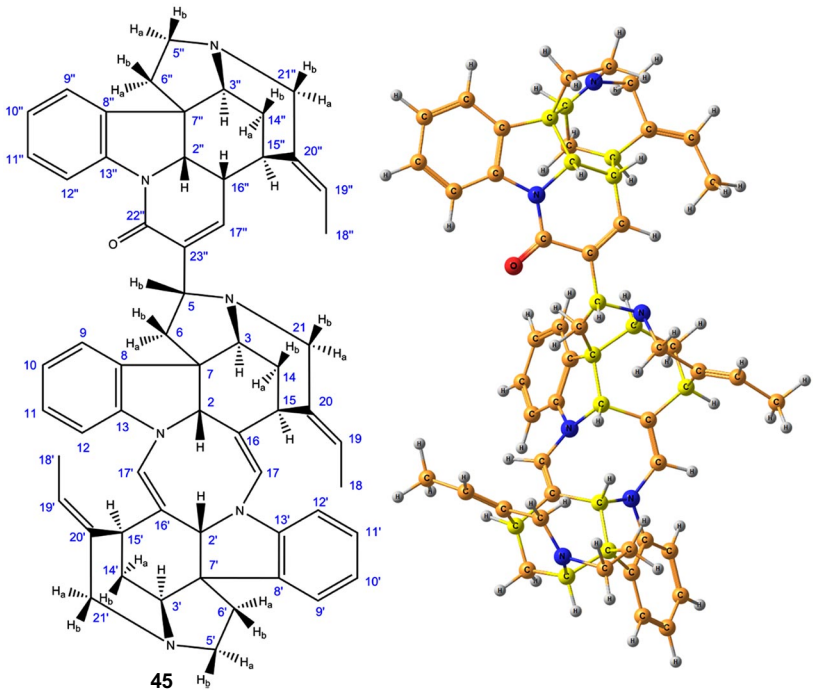
Figure 11. Calculated and experimental ^{1}H (marked in red, *a*) and ^{13}C (marked in black, *b*) NMR chemical shifts of strychnobaillonine **44**. Suggested reassignements in the NMR spectrum of **44** (*c*). Reproduced with minor editing privilege from Semenov and Krivdin [92] with the permission of Wiley.

Table 2. Statistical parameters of the calculated ^{1}H and ^{13}C NMR chemical shifts of strychnobailonine using different DFT functionals. Compiled from Semenov and Krivdin.[92]

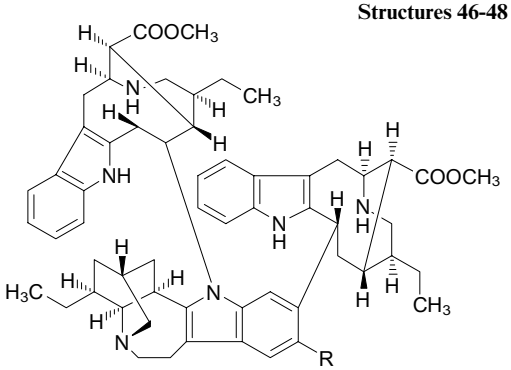
Functional	Range, ppm	Error range, ppm		Slope	Correlation coefficient	Relative error (%)	MAE, ppm
		from	to				
			^{1}H NMR chemical shifts				
KT2	1.40 – 8.50	−2.44	+0.76	0.9749	0.991	3.1	0.21
KT3	1.43 – 8.50	−2.42	+0.73	0.9756	0.993	2.7	0.18
OLYP	1.55 – 8.33	−0.62	+0.63	1.0169	0.992	2.6	0.17
PBE0	1.62 – 8.28	−0.56	+0.62	1.0542	0.994	2.2	0.14
			^{13}C NMR chemical shifts				
KT2	6.2 – 169.3	−8.9	+7.6	0.9424	0.995	2.3	3.6
KT3	7.6 – 169.3	−7.3	+6.7	0.9379	0.996	2.1	3.2
OLYP	8.6 – 167.8	−6.7	+6.0	0.9856	0.997	1.9	2.9
PBE0	11.4 – 169.0	−6.7	+5.0	1.0668	0.998	1.5	2.4

Additionally, the ^{1}H and ^{13}C NMR chemical shifts of as many as 14 configurational isomers at each asymmetric center together with 3 alternative geometrical isomers at three double bonds were calculated using the most effective DFT computational scheme, PBE0/pcSseg-2//pcseg-2.[96] Fig. 13 presents the calculated and experimental ^{1}H and ^{13}C NMR chemical shifts of strychnohexamine, while the calculated and experimental ^{1}H and ^{13}C NMR chemical shifts at chiral carbon centers of this compound are compiled in Table 3.

As a result, a number of NMR reassignments of the ^{1}H and ^{13}C NMR spectra of this alkaloid were suggested. In some particular cases, the reassignment of the individual resonances and the assignments of the experimentally unresolved signals (mostly those of protons) were performed (Fig. 14).

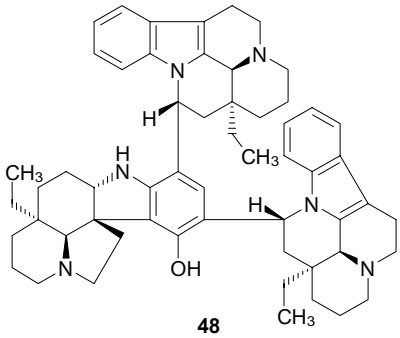


Structures 46-48



46, **47**

R = H (**46**), OCH_3 (**47**)



48

Figure 12. Atom numbering and stereochemical structure of strychnohexamine (**45**). Asymmetric carbons are shown in bright yellow. Reproduced with minor editing privilege from Semenov and Krivdin[96] with the permission of Wiley.

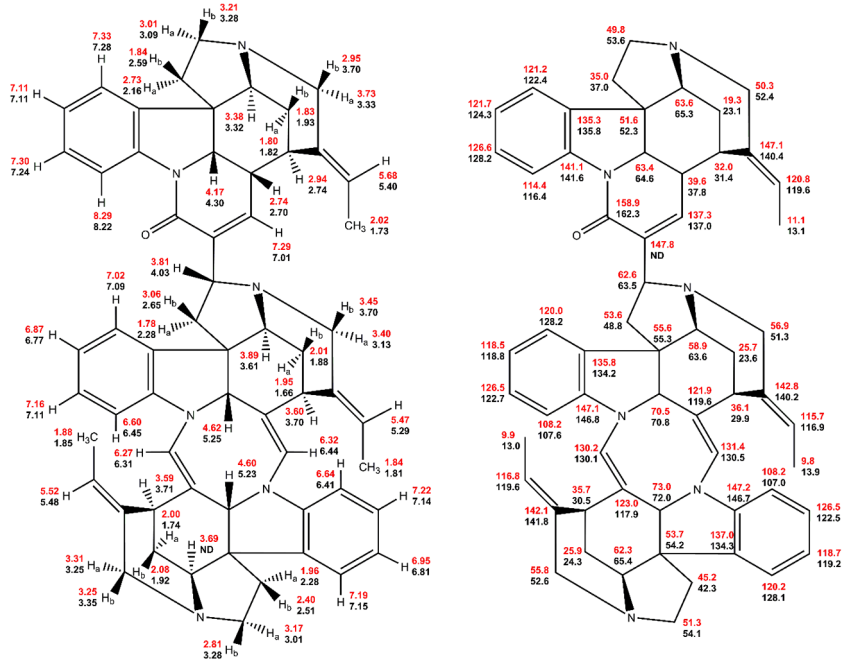


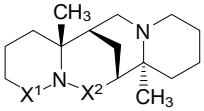
Figure 13. Calculated and experimental ^{1}H and ^{13}C NMR chemical shifts of strychnohexamine **45**. Erroneous and/or missing assignments are shown in red. Reproduced with minor editing privilege from Semenov and Krivdin[96] with the permission of Wiley.

Generally, the high potential of such calculations in the series of large natural products for the purposes of their structural elucidation, as exemplified with the trimeric indole alkaloid strychnohexamine, was demonstrated.[96]

3.2. Quinolizidine alkaloids

In the early paper by Galasso *et al.*,[97] physiologically active quinolizidine alkaloid sparteine (**49**) and all eleven oxo-derivatives involving the mostly known lupanine (**50**) and aphylline (**51**) were investigated within the DFT framework using the B3LYP functional. In that study, ^{13}C NMR

Structures 49 – 51



49 – 51

49: $X^1 = X^2 = CH_2$;
50: $X^1 = C(O)$, $X^2 = CH_2$;
51: $X^1 = CH_2$, $X^2 = C(O)$

Table 3. Calculated and experimental ^{1}H and ^{13}C NMR chemical shifts at the chiral carbon centers of strychnohexamine. Compiled from Semenov and Krivdin.[96]

Chiral center	^{13}C NMR, ppm			^{1}H NMR, ppm		
	calculation	experiment	established configuration	calculation	experiment	established configuration
C-2	68.8 (*R*)	70.8	*S*	4.75 (α)	5.25	*β*
	70.5 (*S*)			4.62 (*β*)		
C-3	99.1 (*R*)	63.6	*S*	3.89 (α)	3.61	α
	58.9 (*S*)			4.72 (*β*)		
C-5	61.8 (*S*)	63.5	*R*	4.39 (α)	4.03	*β*
	70.7 (*R*)			3.81 (*β*)		
C-7	55.6 (*R*)	55.3	*R*			
	68.4 (*S*)					
C-15	50.0 (*R*)	29.9	*S*	3.60 (α)	3.70	α
	36.1 (*S*)			3.45 (*β*)		
C-2′	77.5 (*R*)	72.0	*S*	4.47 (α)	5.23	*β*
	73.0 (*S*)			4.60 (*β*)		
C-3′	101.0 (*R*)	65.4	*S*	3.70 (α)	ND	α
	62.3 (*S*)			4.32 (*β*)		
C-7′	53.7 (*R*)	54.2	*R*			
	67.0 (*S*)					
C-15′	49.3 (*R*)	30.5	*S*	3.69 (α)	3.71	α
	35.7 (*S*)			2.97 (*β*)		
C-2″	61.8 (*R*)	64.6	*S*	3.78 (α)	4.30	*β*
	63.4 (*S*)			4.17 (*β*)		
C-3″	102.2 (*R*)	65.3	*S*	3.38 (α)	3.32	α
	63.6 (*S*)			4.10 (*β*)		
C-7″	51.6 (*R*)	52.3	*R*			
	71.8 (*S*)					
C-15′	32.0 (*R*)	31.4	*R*	2.95 (α)	2.74	α
	36.6 (*S*)			2.68 (*β*)		
C-16′	50.9 (*R*)	37.8	*S*	2.70 (α)	2.70	*β*
	39.6 (*S*)			2.74 (*β*)		

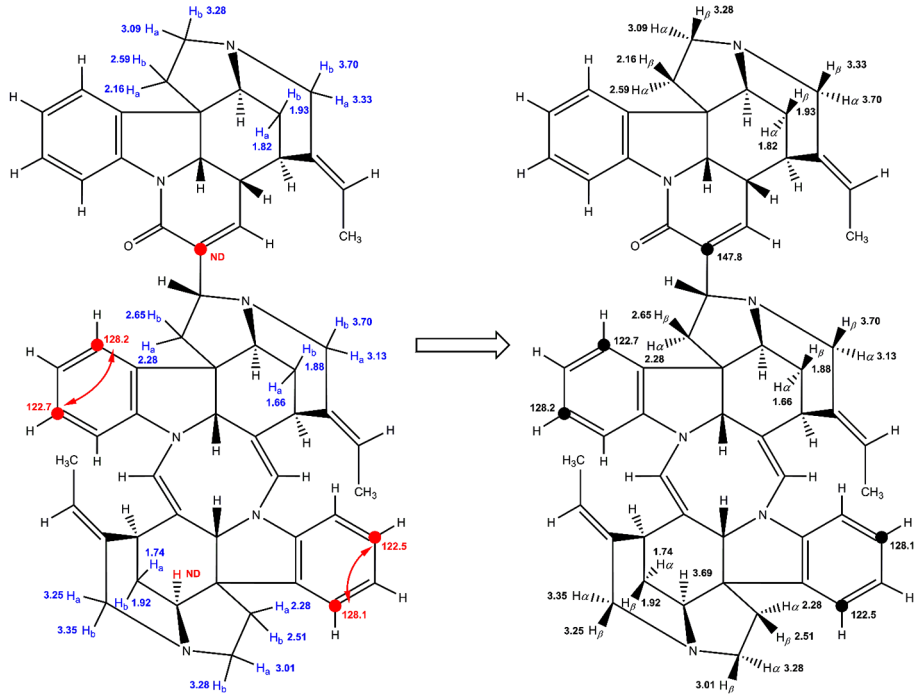


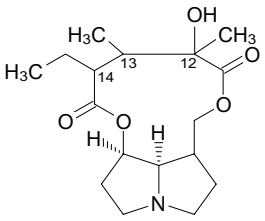
Figure 14. Selected reassigned ^{1}H and ^{13}C NMR chemical shifts of strychnohexamine **45**. Erroneous and/or missing assignments are shown in red. Reproduced with minor editing privilege from Semenov and Krivdin [96] with the permission of Wiley.

chemical shifts of those compounds were calculated at the B3LYP/6-311 + G(2d,p) level, while $^{n}J_{H,H}$ (n = 2, 3) and $^{n}J_{C,H}$ (n = 1–3) spin–spin coupling constants were evaluated with the same B3LYP functional and the double zeta DZP basis set in good agreement with available experiments.

3.3. Pyrrolizidine alkaloids

In a recent paper by Oliveira *et al.*,[98] the structure of a novel pyrrolizidine alkaloid, ethylcrotaline, was identified by combined NMR analysis and DFT calculations. The relative stereochemistry of this alkaloid was defined by comparing the calculated ^{1}H and ^{13}C NMR chemical shifts of the candidate diastereotopic structures with the experimental NMR spectrum. A quantum mechanical computational study of the relative configuration of that natural product demonstrated the power of the applied approach for stereochemical analysis. Thus, to determine which of the eight stereoisomers **52**–**59** was the true one, the DP4 statistical methodology was used to evaluate which one of the theoretical data sets fits the experimental ^{1}H and ^{13}C NMR chemical shifts better. The second step was to calculate NMR chemical shifts for the candidate structures at the B3LYP/6-31G(d,p) level of theory. Finally, the experimental carbon and hydrogen NMR chemical shifts were compared with their theoretical values calculated at the B3LYP/6-311 + G(2d,p)//M06-2X/6-31 + G(d,p) level. As a result, the complete stereochemical assignment of the novel natural alkaloid was performed, indicating the stereoisomer **52**.

Structures 52 – 59



52 – **59**

52: 12*R*, 13*S*, 14*R*;
53: 12*R*, 13*R*, 14*R*;
54: 12*R*, 13*S*, 14*S*;
55: 12*R*, 13*R*, 14*S*;
56: 12*S*, 13*S*, 14*S*;
57: 12*S*, 13*S*, 14*R*;
58: 12*S*, 13*R*, 14*S*;
59: 12*S*, 13*R*, 14*R*

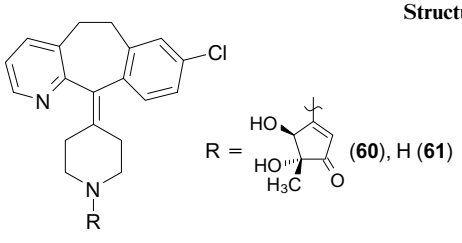
3.4. Piperidine alkaloids

Yu *et al.*[99] elucidated the structure of a novel degradant **60** formed between desloratadine (**61**) and a previously unidentified starch impurity based on the calculations of the ^{13}C NMR chemical shifts of all possible alternative structures of **60** at the B3LYP/6-311 + G(d,p) level on the B3LYP/6-31G(d) geometries. The smallest error between the predicted and experimental values for the ^{13}C NMR chemical shifts was found for structure **60** with RMSD = 5.4 ppm, which was more than three times lower than the errors for the alternative isomers (RMSD $\geqslant$ 17 ppm). Such a marked difference between the RMSD values conclusively showed that the new degradant should have structure **60**.

Smith and Goodman[100] revised a number of natural products, including those of nankakurine A (**62**), ottensinin (**63**), and cephalandole A (**65**), which were originally misassigned as structures **62a**, **64**, and **66**, respectively. These reassignments were based mainly on the DP4 calculations and B3LYP/631G(d,p) computations of their ^{1}H and ^{13}C NMR chemical shifts.

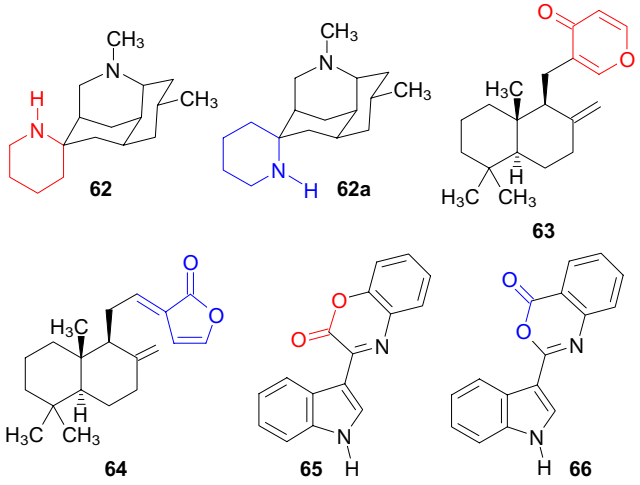
The general conclusion was that NMR shift calculation in combination with the DP4 probability method was a powerful tool for assigning the stereochemistry of natural products when only one set of experimental data was available. Furthermore, it was shown that the DP4 method was much more effective at making correct assignments with higher confidence. In the cases when the structures of natural products provided very similar spectra, the DP4 formalism was much more robust than other statistical approaches.

Structures 60, 61



60, **61**

Structures 62 – 66



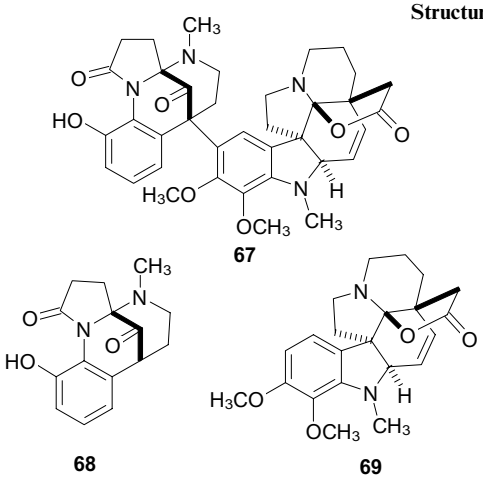
62 **62a** **63** **64** **65** **66**

3.5. Indolizidine alkaloids

Galasso[101] performed a DFT study of the structure and several spectroscopic properties, involving ^{13}C NMR chemical shifts, of haplophytine (**67**) and its 'half-molecules' components — unnamed moiety **68** made of a 2,8-diazabicyclo[3.3.1]skeleton, which included bridged ketone and two aminal functions, and, on the other hand, aspidophytine (**69**), both exhibiting unique structural skeletons and unusual spectroscopic features. These architecturally intriguing and synthetically challenging alkaloids were extracted from the dried leaves of the plant *Haplophyton cimicidum*, providing anticockroach insecticidal activity.

Based on the performed calculations, several stereochemical updates dealing with the resonances of the aryl

Structures 67 – 69



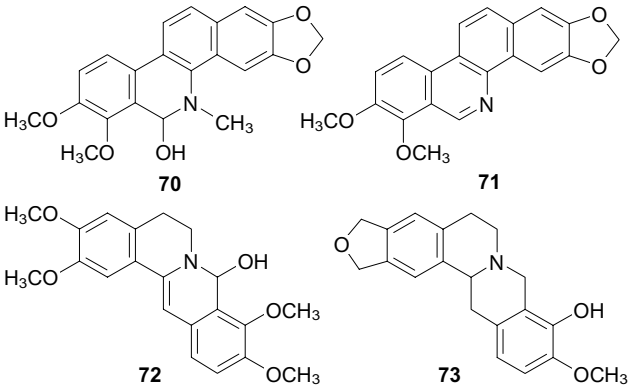
67 **68** **69**

and olefinic carbons were suggested for further clarification and/or revision.

3.6. Quinoline and isoquinoline alkaloids

Toušek *et al.*[102] discovered that the unusual lowfield ^{13}C NMR chemical shifts of a number of overcrowded natural products were not directly related to a different conjugation of the lone pair of electrons of the methoxy oxygen with the aromatic ring but rather were connected with the changes in the virtual molecular orbital space. The latter were found to be correlated with the predominant part of the contribution of the paramagnetic deshielding connected with the magnetic interactions of the bonding and antibonding orbitals involving the methoxy group. This effect was exemplified for two benzo[c]phenantridine alkaloids, 6-hydroxy-5,6-dihydrochelerythrine (**70**) and norchelerythrine (**71**), and two protoberberine alkaloids, 8-hydroxy-7,8-dihydropalmatine (**72**) and tetrahydroberrubine (**73**). In those calculations, the generalized gradient approximation exchange-correlation DFT functionals BLYP and BP86 as well as the hybrid functionals B3LYP, B3PW91, PBE0, and BHandHLYP were used for the calculations of ^{13}C NMR chemical shifts in combination with the 6-31G(d,p) basis set for the geometry optimization and 6-311G(d,p) for the calculation of NMR shielding constants.

Structures 70 – 73



Unusual lowfield ^{13}C NMR chemical shifts of ~62 ppm have been reported for methoxy groups attached to aromatic carbons. Those strong deshielding effects were typically observed for the molecules bearing bulky substituents in the neighborhood of the methoxy group; in contrast, in the absence of a bulky substituent, ^{13}C NMR chemical shifts of the methyl carbon were typically ~56 ppm, as illustrated in Fig. 15. The observed unusual lowfield resonances were shown to be not directly related to the conjugation of the lone pair of the methoxy oxygen with the aromatic ring, as has been known previously, but rather could be rationalized as reflecting the different orbital magnetic interactions between the occupied orbitals corresponding to the C–H bonds and the vacant antibonding C–O orbital.[102]

Thus, it was concluded that the interactions of the C–H bonding orbital with the C–O antibonding orbital, characterized by conformationally dependent delocalization, were mainly responsible for the stereochemical changes of the ^{13}C NMR chemical shift of the methoxy group in the natural products of that type.

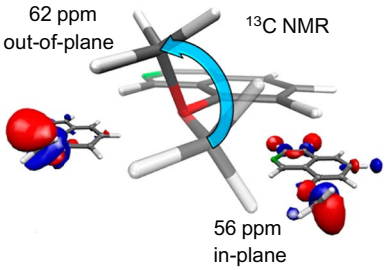
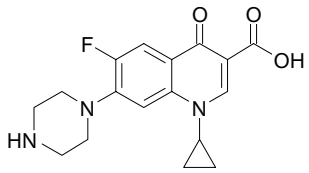


Figure 15. The spatial deshielding effect of a bulky substituent on the ^{13}C NMR chemical shift of the adjacent methoxy group. Reproduced from Toušek *et al.*[102] with the permission of the American Chemical Society.

Recently, Koch *et al.*[103] calculated ^{19}F – ^{13}C coupling constants in the molecule of ciprofloxacin (**74**), a widely known fluoroquinolone antibiotic. As a measure of its practical importance, a number of ciprofloxacin derivatives with novel benzamidomethyl substituents have been recently synthesized,[104] which showed much higher lipophilicity than the parent ciprofloxacin. Calculations on this prospective drug were performed with different DFT methods and a variety of basis sets.[103] In general, calculations of different ^{19}F – ^{13}C coupling constants ($^nJ_{F,C}$, n = 1 – 4) with the BHandH functional and 6-311++G(d,p), EPRII, and EPRIII basis sets demonstrated the best reproducibility of their experimental values. Interestingly, Dunning's aug-pVDZ and Jensen's pcJ-1, pcJ-2, and aug-pcJ-1 basis sets provided much less reliable results. It was also found that taking into account solvent effects did not show any improvement of the computational results in most cases.

Structure 74



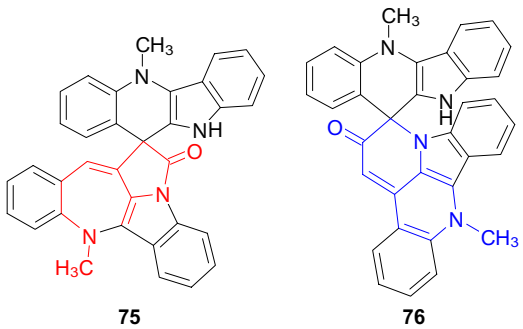
3.7. Indoloquinoline alkaloids

Saurí *et al.*[105] reinvestigated the structure of the plant alkaloid cryptospirolepine **75**[106] which led to the revision of the originally suggested formula to structure **76**. Thus, mainly the DFT calculations of its $^2J_{C,H}$ provided important information that allowed essential structural revision of this alkaloid.

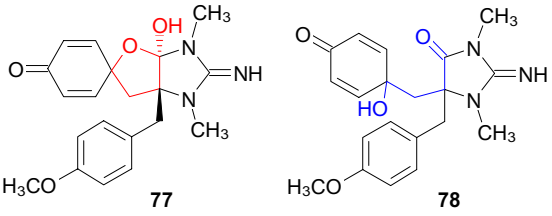
3.8. Guanidine alkaloids

Aberle *et al.*[107] performed DFT calculations to predict ^{13}C NMR chemical shifts of two possible alternative structures of the spirocyclic guanidine alkaloid spiroleucettadine,

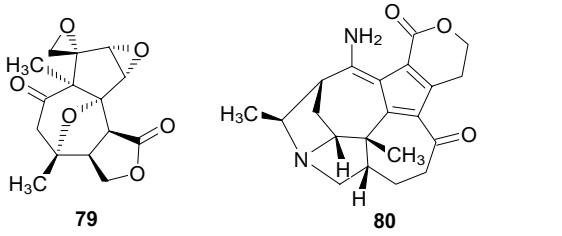
Structures 75, 76



Structures 77, 78



Structures 79, 80



extracted from the bright yellow *Leucetta* sponge. The reevaluation of the NMR data supported by the DFT calculations of the ^{13}C NMR chemical shifts of the two alternative structures **77** and **78** allowed the revision of the earlier proposed structure **77** to structure **78**. In those calculations, the hybrid functional MPW1PW91 was shown to perform particularly well, especially when employed with Pople's 6-311+G(2d,p) basis set.

4. Pseudoalkaloids

4.1. Terpenes

In one of the most recent publications by Kutateladze and Kuznetsov,[108] more than 90 natural sesquiterpenes possessing triquinane cores were studied with the help of the relatively new so-called 'Relativistic Force Field' (RFF) parametrization method (abbreviated as DU8+).[80] Note that the word 'relativistic' in this context has nothing in common with the phenomenon of relativism and/or relativistic effects. The structures of thirteen of those compounds, namely, hirsutanols B and D, hirsutenol E, cucumin B, antrodins C-E, chondroterpenes A and H, chondrosterins C and E, dichrocephone A, and pethybrene, were reestablished (Fig. 16).

Bagno *et al.*[77] performed DFT calculations of ^{1}H and ^{13}C NMR chemical shifts (together with ^{1}H–^{1}H spin–spin coupling constants in some particular cases) compared to experiments for a series of naturally occurring molecules involving corianlactone (**79**), daphnipaxinin (**80**), and the mostly exotic overcrowded compound boletunone B, originally reported as **81** and revised to **82**. Most calculations of NMR parameters were performed at the B3LYP/cc-pVTZ level on the B3LYP/6-31G(d,p) geometries by taking into account solvent effects within the IEF-PCM formalism.[49]

As mentioned by the authors, for natural products characterized by 'challenging' NMR spectra, there were four major problems: (i) these molecules possess a large and complex molecular backbone, often with unprecedented features; (ii) flexible molecules may exist in many conformations, thus greatly increasing the computational effort needed; (iii) their spectral assignment relies mostly on ^{1}H and ^{13}C NMR spectra, with most signals lying within very crowded regions; and (iv) ^{1}H chemical shifts are generally influenced by solvent effects. This is mostly illustrated by the case of boletunone B, which was revised from **81** to **82** based on a direct comparison of its calculated and experimental ^{13}C NMR spectra (Fig. 17).

Saielli *et al.*[109] reported the results of the DFT calculations of ^{13}C NMR chemical shifts and ^{1}H–^{1}H spin–spin coupling constants in a series of vannusals, which represent a class of natural products whose structures have been the subject of numerous earlier studies.[110–115] The originally assigned structure **83** and revised structure **83a** possess rather unusual molecular structures consisting of a complex molecular framework consisting of 30 carbons and including seven rings and thirteen asymmetric centers.

The calculations were performed at the M06/pcS-2 level on the B3LYP/6-31G(d,p) geometries. The availability of the experimental NMR spectra of vannusal B and all its stereoisomers, synthesized independently, allowed the authors to carry out a direct comparison of ^{13}C NMR chemical shifts and ^{1}H–^{1}H spin–spin coupling constants predicted from the DFT calculations with their experimental values. It was shown that all stereoisomers of vannusal B showed significant differences in their ^{13}C NMR spectra that could be exploited for their structural elucidation.

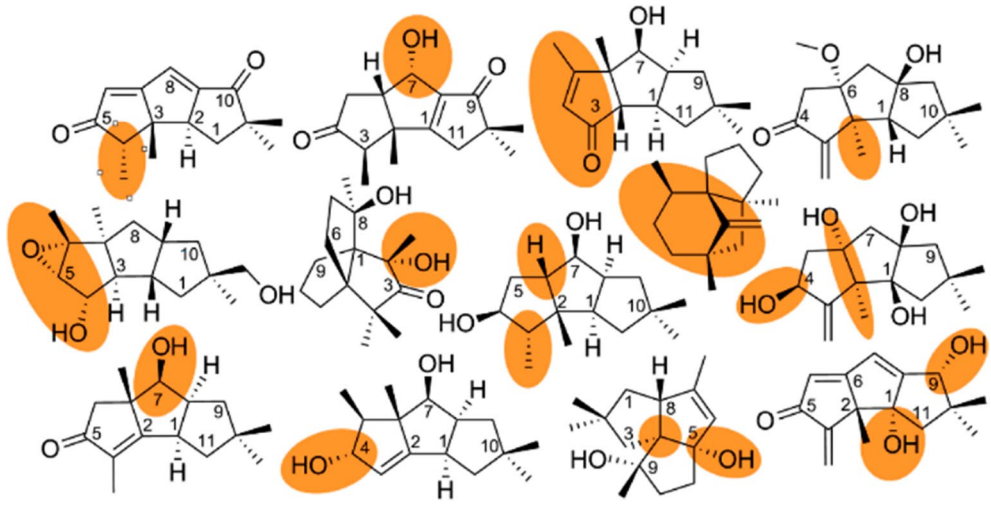


Figure 16. Structures of natural sesquiterpenes possessing triquinane cores, revised by means of the DU8+ calculations. Shown in colour are the reestablished molecular fragments. Reproduced from Kutateladze and Kuznetsov [108] with the permission of the American Chemical Society.

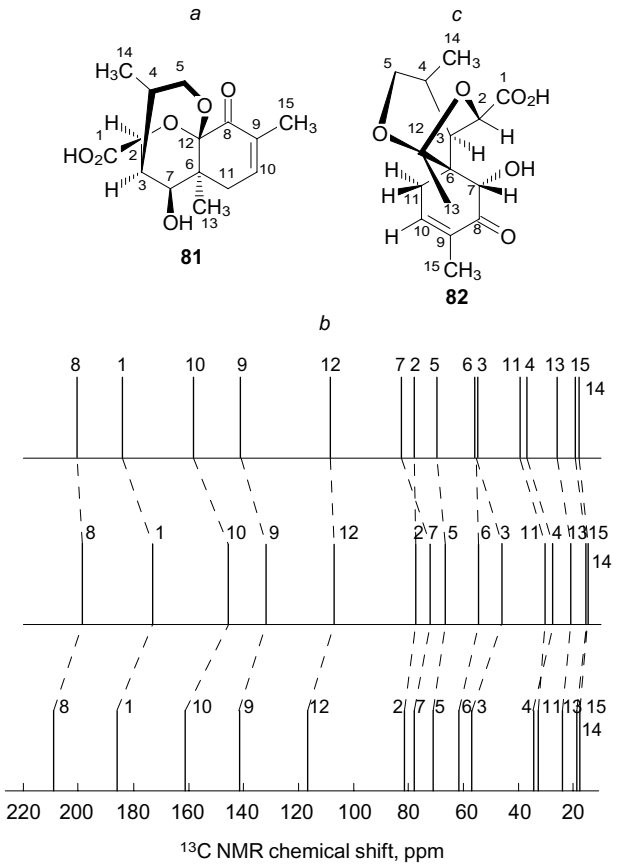
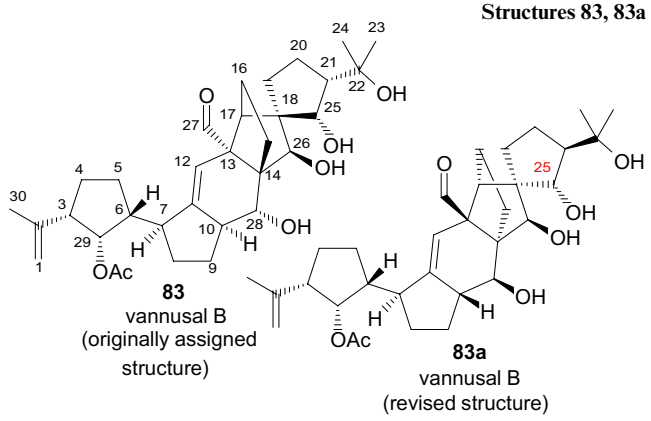


Figure 17. ^{13}C NMR spectra of boletunone B. Experimental (*b*); calculated for the original structure **81** (*a*) and for the revised structure **82** (*c*). Reproduced from Bagno *et al.*[77] with the permission of Wiley.

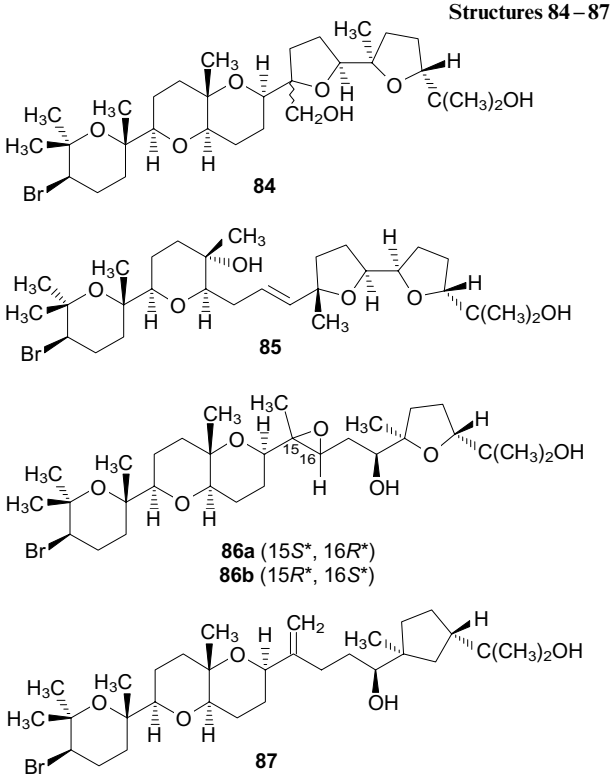
Structures 83, 83a



Cen-Pacheco *et al.*[116] reported isolation and a detailed experimental and computational NMR study of the four metabolites of the red alga *Laurencia viridis* new polyether triterpenoids: 28-hydroxysaiyacenol B (**84**), saiyacenol C (**85**), 15,16-epoxythyrsiferol A (**86a**), and 15,16-epoxythyrsiferol B (**86b**), derivatives of the parent dehydrothyrsiferol (**87**). All calculations were performed at the DFT level using the traditional B3LYP functional and allowed us to assign relative configurations for epoxythyrsiferols A and B.

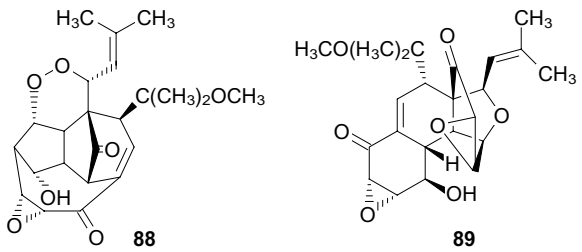
In 2002, Schlegel *et al.*[117] reported the isolation of hexacyclinol, a novel antibiotic from the basidiomycete

Structures 84 – 87



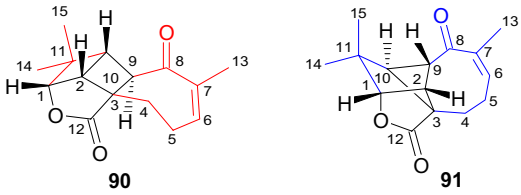
Panus rudis, and following its promising biological activity, a total synthesis of that molecule was realized in 2006 by La Clair.[118] Originally, the structure **88** was proposed for that alkaloid based on its detailed NMR study. However, an alternative structure **89** was suggested by Rychnovsky[119] on the basis of ^{13}C NMR chemical shifts, calculated at the mPW1PW91/6-31G(d,p) level using the HF/3-21G geometries. Examination of both structures with the aid of the computer-assisted structure elucidation (CASE) algorithm[120] and, on the other hand, by the in-depth NMR computational study[121] witnessed in favour of the revised structure **89**. Computation of ^{13}C NMR chemical shifts and $^{1}H-^{1}H$ spin–spin coupling constants of those structures was performed in the latter paper by Saielli and Bagno[121] at the B97-2/cc-pVTZ level on the B3LYP/6-31G(d,p) geometries.

Structures 88, 89



An interesting and very illustrative example of the structural revision of the carbon skeleton of a natural product was presented by Lodewyk *et al.*[122] who reestablished the structure of aquatolide primarily by means of the computation of its ^{1}H and ^{13}C NMR chemical shifts. Many of the computed chemical shifts for the original structure **90** did not match well with those reported for that natural

Structures 90, 91



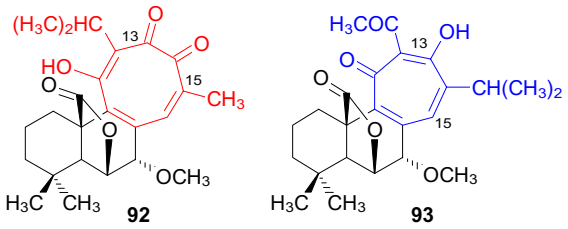
90 **91**

product. Significant deviations were found for many nuclei throughout the molecule, indicating that the core structure of aquatolide was most likely incorrect. Indeed, the ^{1}H and ^{13}C NMR chemical shifts were in much better agreement with the revised structure **91** derived in that study.

Table 4 shows the computed ^{1}H and ^{13}C NMR chemical shifts of aquatolide compared to their experimental values. Indeed, the corrected mean absolute deviation (CMAD) was found to be essentially smaller for the revised structure **91** compared to the originally proposed structure **90** (1.37 *vs* 7.23 ppm for ^{13}C NMR chemical shifts and 0.10 *vs* 0.35 ppm for ^{1}H NMR chemical shifts), which strongly favoured the former.

Yang *et al.*[123] performed MPW1PW91/6-31G(d,p) calculations of ^{13}C NMR chemical shifts in chloroform on HF/3-21G, B3LYP15/6-31G(d), and MPW1PW9116/6-31G(d,p) geometries of a natural product hassananes (**92**) isolated from *Salvia apiana* collected in the coastal range and valleys of southern California. The performed calculations were compared with those for the proposed alternative structure **93**. The original structure **92** possessing a new diterpenoid skeleton was established based on different spectroscopic data, mainly NMR spectra. A careful examination of both molecules resulted in a revision of that natural product to structure **93** based on the calculations of ^{13}C NMR chemical shifts. The most striking difference between the computed and experimental shifts was found for C-13 (21 ppm) and C-15 (34 ppm) atoms originating in their essentially different chemical environments.

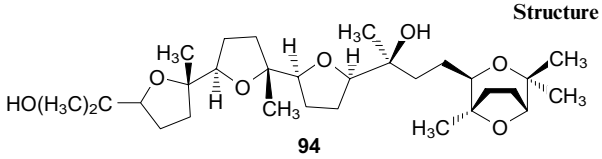
Structures 92, 93



92 **93**

Cen-Pacheco *et al.*[124] performed a state-of-the-art elucidation of a new polyether squalene derivative, nivariol (**94**), based mainly on DFT calculations. Calculations were performed on a series of model structures, which were optimized at the B3LYP/6-31G(d) and/or MP1WMP91/6-31G(d) levels (Fig. 18). The ^{13}C NMR chemical shifts of the nivariol models were calculated by using the MP1WMP91/6-31(d,p) functional in the IEF-PCM medium for chloroform according to their Boltzmann populations and compared to their experimental values.

Structure 94



94

Two additional examples are provided in the review paper by Tantillo.[36] The first example deals with plakotenin (**95**), a total synthesis of which led to an initially identified natural product, but Bihlmeier *et al.*[125] suggested that both the natural and synthetic species corresponded to the diastereomers of compound **95**. The second example was provided by Vaughan *et al.*[126] on the polycyclic, stereodense diterpene rhizathalene A (**96**), the structure of which was determined through extensive NMR experiments, supported by ^{1}H and ^{13}C NMR chemical shift calculations.

Garson *et al.*[127] reported the revision of the published structure of the fungal metabolite meroterpenoid acremine P (**97**), which actually had the structure **98**. The revision was mainly performed by using the DP4+ computational approach and discussed elsewhere in this review.

Table 4. Experimental and computed ^{1}H and ^{13}C NMR chemical shifts (ppm) of aquatolide. Compiled from Lodewyk *et al.*[122]

Carbon	**90**	**91**	Experiment	Hydrogen	**90**	**91**	Experiment
C-1	80.76	83.29	84.20	H-1	4.23	4.21	4.48
C-2	41.66	54.75	54.54	H-2	2.99	3.20	3.26
C-3	48.84	62.83	62.83				
C-4	31.23	22.46	22.15	H-4	1.99	2.48	2.52
					1.89	1.89	1.96
C-5	30.16	30.49	28.63	H-5	3.69	2.29	2.35
					2.32	2.08	2.03
C-6	143.61	135.22	131.10	H-6	6.36	5.94	5.85
C-7	139.04	138.11	135.08				
C-8	211.93	211.87	211.94				
C-9	55.53	54.76	54.45	H-9	3.22	2.78	2.92
C-10	38.24	63.89	62.59	H-10	2.97	2.49	2.64
C-11	44.89	44.57	41.86				
C-12	181.17	177.65	177.50				
C-13	21.98	23.19	22.22	H-13	1.89	1.84	1.87
C-14	16.72	21.09	22.62	H-14	0.99	0.98	1.05
C-15	25.21	20.80	22.84	H-15	1.17	1.09	1.19
CMAD	7.23	1.37			0.35	0.10	

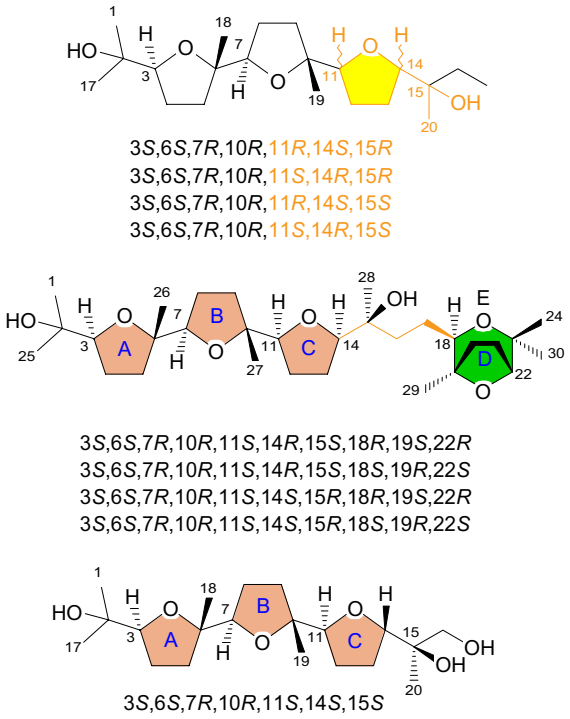
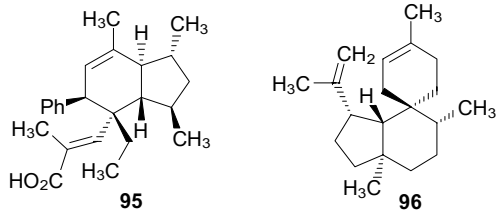


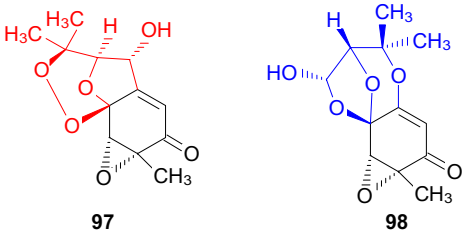
Figure 18. The DFT models of nivariol **94** with different configurations of its asymmetric centers (*a*); model structures of nivariol (*b*) and its synthetic intermediate (*c*). Reproduced with minor editing privilege from Cen-Pacheco *et al.*[124] with the permission of Wiley.

Structures 95, 96

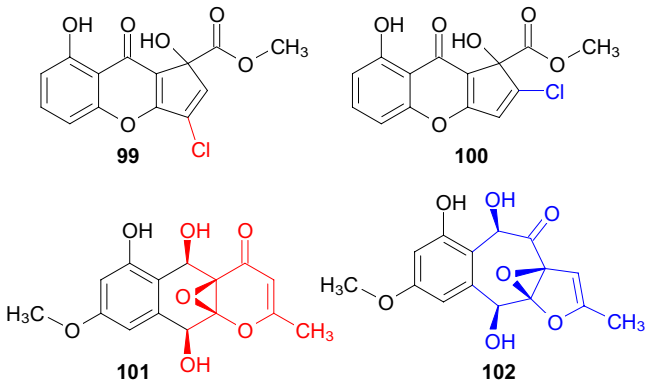


The CASE studies in combination with the DFT calculations of ^{13}C NMR chemical shifts were announced to be a straightforward tool for the structural revision of a number of challenging natural products.[128] The CASE expert systems were introduced in that publication. However, in some cases, empirical chemical shift prediction was incapable of distinguishing the correct structure. It was demonstrated for the first time that the combination of CASE and DFT methods for NMR chemical shift prediction allowed the determination of the correct structure even in the most difficult situations. This approach has been successfully tested for the structural elucidation of aquatolide (**91**), coniothyrione (**99**), and chiral epoxyroussoenone (**101**) against their alternative structures **90**, **100**, and **102**.

Structures 97, 98



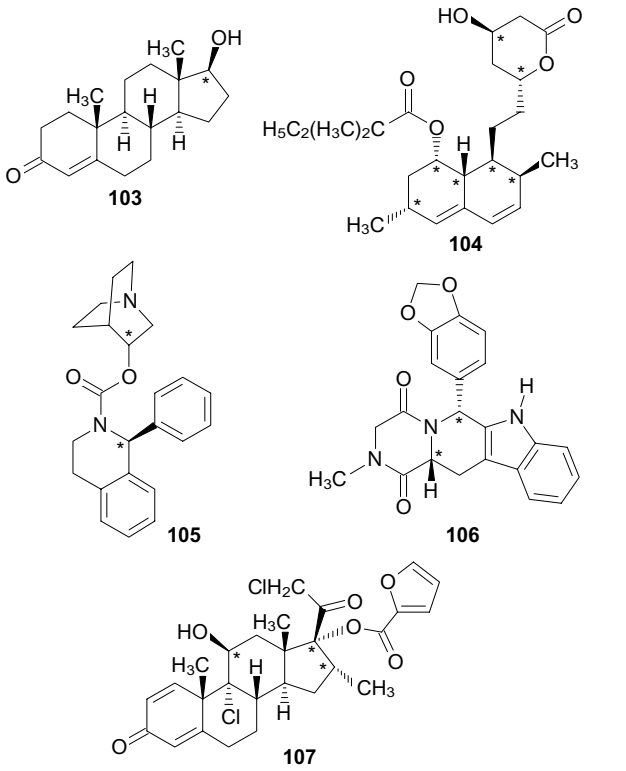
Structures 99 – 102



4.2. Steroids

Ermanis *et al.*[62] reported a novel and general approach to the automatic generation of diastereomers that was tested on ten representative natural products, including testosterone (**103**), simvastatin (**104**), solifenacin (**105**), tadalafil (**106**), and mometasone (**107**). The configurations at the asymmetric centers being varied are marked below with asterisks. As a result of that study, a full automation of the DP4 workflow procedure was carried out, reducing user interaction to a minimum (as stated by the authors). The verification or elucidation of the stereochemical structure of any natural product was announced to be done in as little as one hour in a fully automated mode.

Structures 103 – 107



5. Quinones

As an example of the structural elucidation of natural quinones, the structures of altersolanol P (**108**), a new member of the altersolanol family of compounds, and its derivative **109** were established based on the corresponding chemical shifts predicted by the DFT calculations.[129] The latter were performed with the MPW1PW91 functional and 6-31G(d,p) basis set on the B3LYP/6-31G(d) geometries.

Structures 108, 109

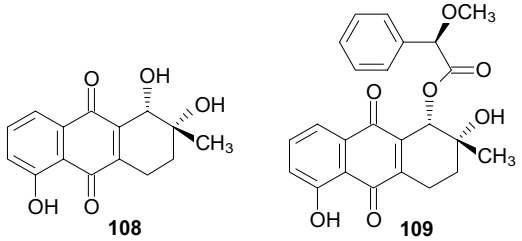


Fig. 19 illustrates the equilibrium between two conformations of altersolanol P, **108a**,**b** (hereinafter denoted as A and B, respectively). The ratio of those conformations was estimated from the analysis of the experimental $^{3}J_{H1',H2}$ and $^{3}J_{H1,H2'}$ coupling constants. Each of these couplings is the average value of J_A and J_B of conformations A and B. To calculate J_A and J_B, the uncontracted basis set was additionally tightened with the *s* and *d* functions to evaluate the Fermi contact contributions. The ratio of A and B conformers was estimated to be 65 : 35, in good agreement with the observed nuclear Overhauser effect (NOE) data. The discrepancy between the calculated and experimental proton chemical shifts of the C-4 hydroxyl was explained by that conformational equilibrium, which had in fact rather little effect on chemical shifts except for the C-4 hydroxyl. Thus, taking into consideration the 65 : 35 ratio of those conformations and the DFT-predicted ^{1}H NMR chemical shift for the second hydroxyl in A and B, 5.15 and 2.97 ppm, respectively, the average value was estimated to be 4.39 ppm, which coincided well with the experimentally observed value of 4.08 ppm.

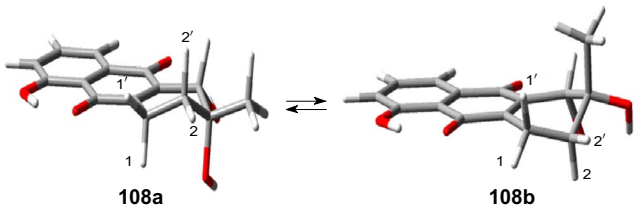
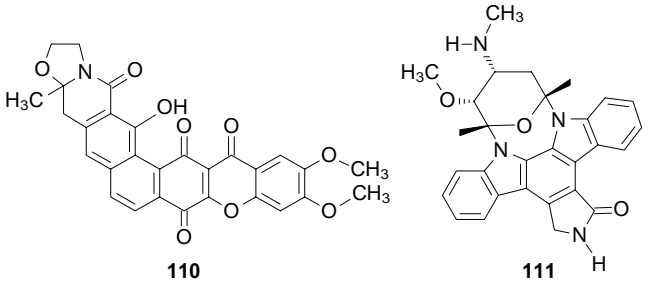


Figure 19. Conformational equilibrium of altersolanol P. Reproduced from Ondeyka *et al.*[129] with the permission of the American Chemical Society.

In three related publications,[82, 130, 131] an unambiguous structural elucidation of cervinomycin A_2 (**110**) and staurosporine (**111**) was performed based on the calculations of the long-range carbon-hydrogen couplings, $^{n}J_{C,H}$, in the framework of the CASE technique.

Structures 110, 111



6. Miscellaneous

6.1. Lactones

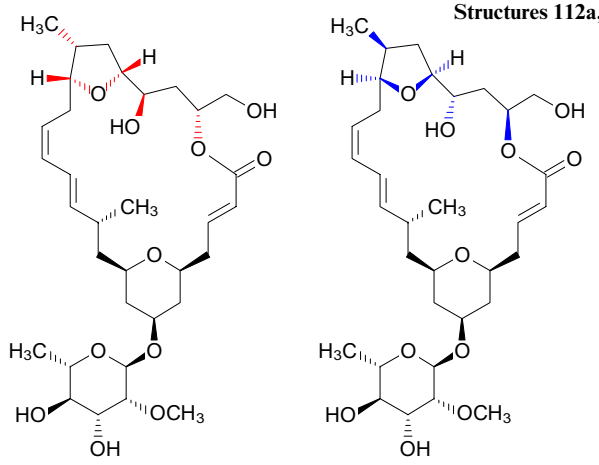
Sarotti[132] demonstrated that NMR chemical shift calculations coupled with the so-called trained 'Artificial Neural Networks' (ANN) provide a new strategy for simple and rapid detection of structural misassignments of natural products exemplified with 200 molecules, including a set of 26 natural products that had been incorrectly assigned along with their revised structures. The calculations were carried out using computationally inexpensive methods such as HF/3-21G and even semiempirical AM1 for geometry optimization and mPW1PW91/6-31G(d) for the calculation of NMR shielding constants. In other words, the main goal of that work was the development of a simple procedure to be used as a test for rapid and straightforward detection of structural misassignments of natural products. It has been generally demonstrated that NMR shift calculations using low theory levels in geometry optimization, which constitutes one of the most time-consuming steps, coupled with trained ANN represent a powerful test for the simple, rapid and reliable identification of structural misassignments.

In a follow-up study,[133] the ANN method was further enhanced by taking into account classification ability refined enough to detect slight errors typically found in regio- or stereochemical misassignments. To test that modification of the ANN method, 100 known compounds (for which the ^{1}H and ^{13}C NMR spectra were confidently assigned) were taken to ensure functional groups diversity and molecular complexity.

As an example of the performed survey, the case of the structural revision of mandelalide A (original structure **112a**, revised structure **112b**) was thoroughly analyzed by Zanardi and Sarotti.[133] The planar structure of mandelalide A was elucidated by extensive 1D and 2D NMR studies, whereas the relative configuration of its asymmetric centers was assigned based on ROESY NMR experiments.[134] However, the revised structure was published two years later by Lei *et al.*[135] The origin of the mistake in the original assignment was the stereochemistry of the upper side of the molecule, with all the corresponding stereocenters inverted.

Sun *et al.*[136] reported two new biscembranoid-like compounds, bissubvilides A (**113**) and B (**114**) (Fig. 20). Their structures and absolute configurations were assigned by spectroscopic analysis and DFT calculations. Structures **113** and **114** were optimized using the MPW1PW91 functional and the 6-31G(d) basis set, while their ^{1}H and ^{13}C NMR chemical shifts were evaluated using the same functional and 6-31G(d,p) basis set.

Structures 112a,b



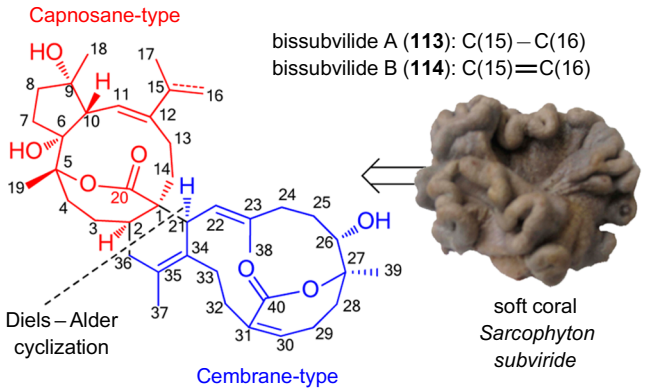
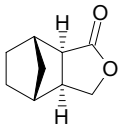


Figure 20. The structures of bissubvilides A and B isolated from the soft coral *Sarcophyton subviride*. Reproduced from Sun *et al.*[136] with the permission of the American Chemical Society.

Teixeira and Alvarenga [137] examined the bromination of **115**, providing two major products of unknown structure. Derivatives of phthalides are frequently found in naturally occurring substances and exhibit a broad spectrum of biological activities.

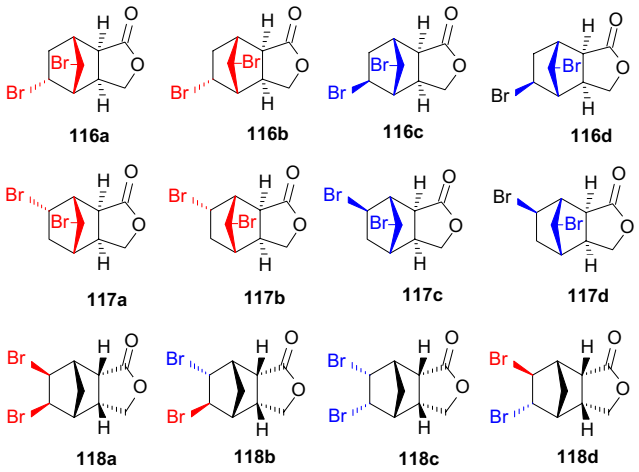
Structure 115



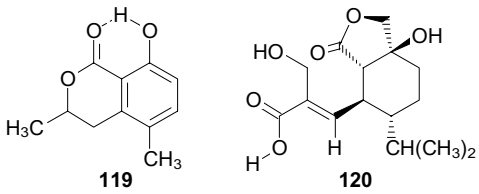
To identify these two products, twelve candidate compounds (**116a – d**, **117a – d** and **118a – d**) were tested using a variety of computational methods, resulting in structures **116b** and **118a**. Our concern addresses the fact that the authors did not discuss in any way the relativistic effect of the fourth-period bromine on the ^{1}H and ^{13}C NMR chemical shifts of the neighboring atoms. It should certainly be not neglected and, in our opinion, requires the implication of relativistic treatment.

Harper and co-workers [138] performed a systematic stereochemical study of the natural products 5-methylmellein (**119**) and hydroheptelidic acid (**120**) by means of the computation and experimental measurement of their $^{1}J_{C,C}$ constants. It was demonstrated that the combination of theoretical predictions and experimental measurements of $^{1}J_{C,C}$ values had the potential to solve challenging structural

Structures 116 – 118



Structures 119, 120



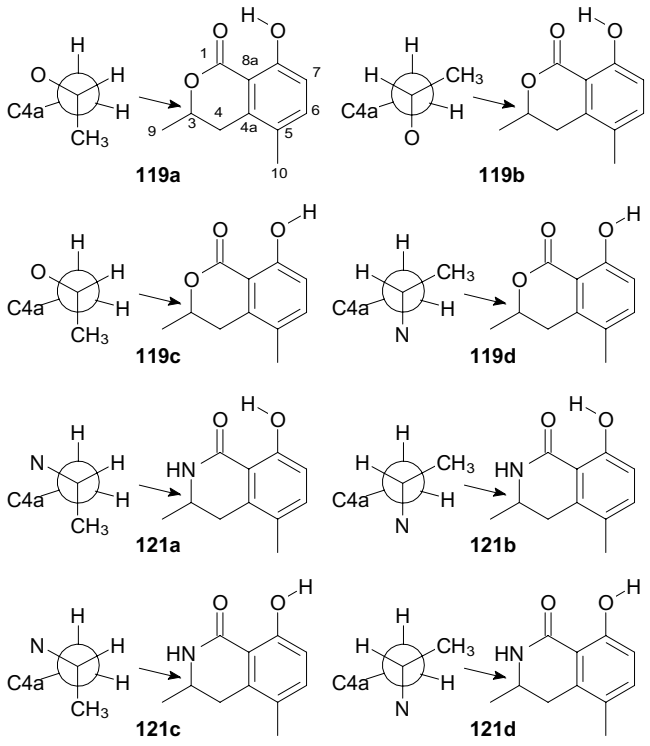


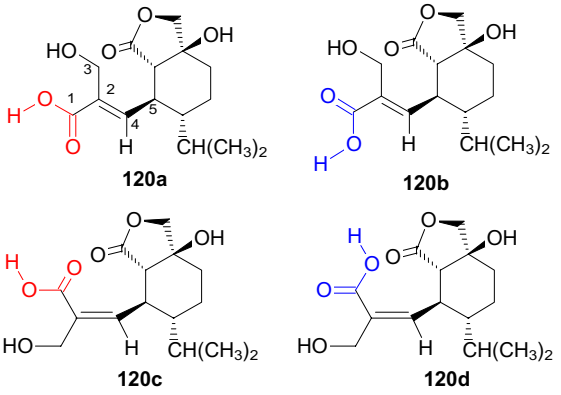
Figure 21. The Newman projections of the model structures of 5-methylmelleins (**119a – d** and **121a – d**) viewed along the C(3) – C(4) bond to illustrate the conformations of the C-9 methyl group. Reproduced from Harper and co-workers [138] with the permission of Wiley.

problems. Computation of the $^1J_{C,C}$ values of compounds **119** and **120** was performed at the B3LYP/EPRIII level, while geometry optimization was carried out within the B3LYP/D95(d,p) method.

Fig. 21 shows eight candidate structures of 5-methylmellein (**119a**–**d**) differing in the hydroxyl hydrogen orientation, conformation of the methyl group on the lactone ring, and the identity of the heteroatom in the lactone ring, with both oxygen and nitrogen atoms (**121a**–**d**) being considered.

On the other hand, hydroheptelidic acid represents a natural product that has been investigated by several groups and retains structural uncertainty at a few sites.[138] Four types of model structures **120a**–**d** were evaluated to assess the ability of $^1J_{C,C}$ data to resolve those questions. These models differed in the configuration at the C(2)–C(4) double bond and in conformations around the C(1)–C(2) bond.

Structures 120



Performed calculations of $^1J_{C,C}$ of the model structures **120a**–**d** compared to the Incredible Natural Abundance DoublE QUAntum Transfer Experiment (INADEQUATE) revealed the true structure **120b** existing in the mixture of three basis conformations A, B, and C (Fig. 22).[138] These structures differ only in conformation, and all have the *s-trans* conformation at the C(1)–C(2) bond and the *E* configuration at the C(2)–C(4) bond.

The stereochemistry of hemicalide (**122**), a cytotoxic polyketide isolated from the marine sponge *Hemimycale* sp. collected in the South Pacific, was computationally analyzed by using the DP4f NMR method, resulting in a structural reassignment at the C(18) asymmetric carbon.[139] Its complex planar structure, containing three separate

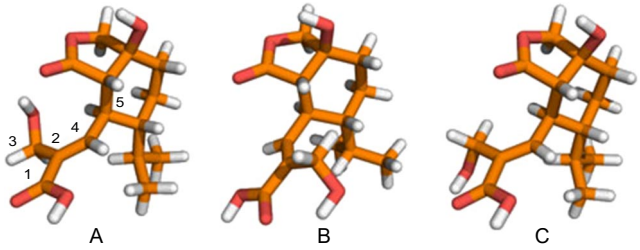
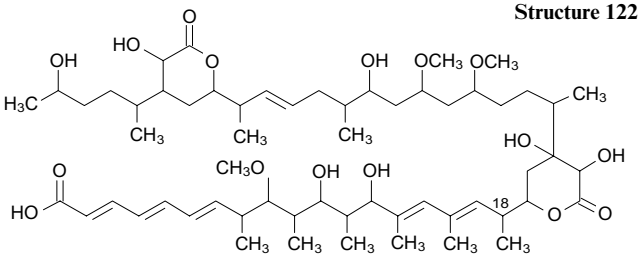


Figure 22. The three structures of hydroheptelidic acid **120** were found to be mostly compatible with the $^1J_{C,C}$ data. Reproduced from Harper and co-workers [138] with the permission of Wiley.

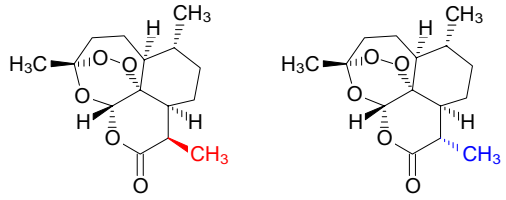
Structure 122



olefinic regions and two δ-lactone rings, was deduced using an extensive NMR spectroscopic analysis substantiated by a thorough theoretical study involving computation of ^{13}C NMR chemical shifts at the B3LYP/6-31G(d,p) level.

Ermanis *et al.*[64] conducted a large-scale systematic search of the best computational method for the elucidation of the relative stereochemistry of natural products at the

Structures 123



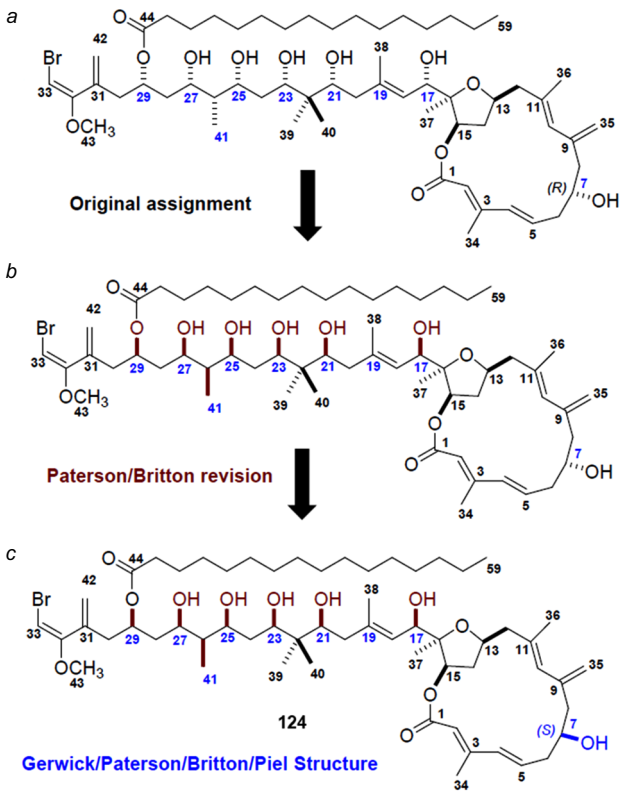


Figure 23. The stereochemical reassignment of phormidolide A (**124**): original incorrect structure (*a*), synthetic revision of the side chain (*b*), and fully revised structure following computational DP4 NMR analysis (*c*). Reproduced from Ndukwe *et al.*[140] with the permission of the Royal Society of Chemistry.

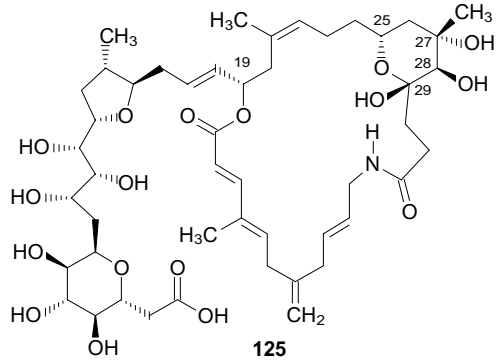
DFT level, resulting in a new version of the DP4 family of methods, DP4.2, which was able to identify the correct structure with a high realistic confidence level. This was illustrated on a number of natural products involving the most challenging molecules of artemisinin (**123a**) and epi-artemisinin (**123b**), with as many as 32 diastereomers being considered for each compound. DFT calculations of ^{13}C NMR chemical shifts were performed with B3LYP, mPW1PW91, WP0419, and M06-2X functionals in combination with Pople's 6-31G(d,p) and 6-311G(d,p) and Jensen's double zeta pcS-1 basis sets.

A paper by Ndukwe *et al.*[140] addresses a rigorous study of the configuration of phormidolide A (**124**). The initially large prediction errors were significantly reduced in the reassigned structure (Fig. 23). In this study, chemical shifts were evaluated at the mPW1PW9129/6-311 + G(2d,p)//M06-2X/6-31 + G(d,p) level, while spin-spin coupling constants were calculated within the B3LYP/6-31G(d)//M06-2X/6-31 + G(d,p) framework.

6.2. Lactams

Domínguez *et al.*[141] reported the isolation and identification of belizentrin (**125**), a novel large 25-membered polyketide-derived macrocycle that exhibited potent bioactivity in neuronal survival assays *in vitro*. The structure of **125** was primarily determined by multipulse NMR COSY, TOCSY, HSQC, and HSQC-TOCSY experiments in combination with computational methods.

Structure 125

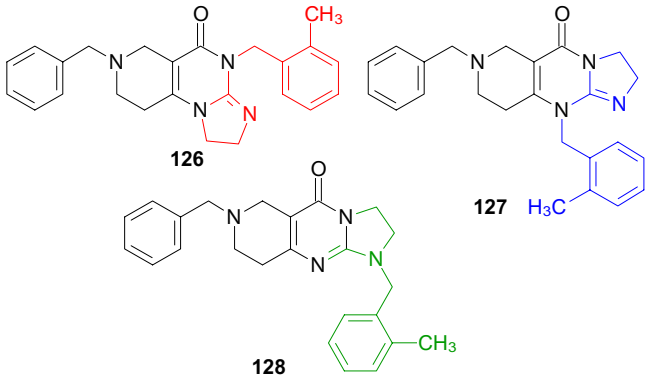


125

The quantum-chemical calculations of ^{13}C NMR chemical shifts were performed using the DP4 method, which proved to be an excellent tool for addressing the stereochemistry of this unique natural product. The calculations enabled us to assign the 19*S**, 25*R**, 27*S**, 28*R**, 29*S** configuration of belizentrin.

Xin *et al.*[142] reported a survey of the most popular density functionals and basis sets used in NMR chemical shift calculations. The combination of B3LYP/cc-pVDZ was declared the preferred choice for accuracy and computational efficiency. Corrections regarding both referencing and systematic errors for B3LYP/cc-pVDZ calculations were also presented, which altogether gave rise to an accurate approach with a reasonable computational cost. This was exemplified with the most convincing example of TIC-10. The active pharmaceutical ingredient TIC-10, having the structure **126**, was initially misassigned as **127** and later as its third isomer **128**. Comparison of the calculated ^{13}C NMR chemical shifts with those experimental for a genuine TIC-10 revealed the correct structure **126** (RMSD

Structures 126 – 128



2.80 ppm), compared to **127** (RMSD 3.14 ppm) and **128** (RMSD 5.57 ppm). However, the opinion of the authors of the present review is that a simple double zeta Dunning's basis set cc-pVDZ is too small for such calculations, so that the so-called 'fortuitous cancellation of errors' may be the reason for the profoundly good behaviour of that small basis set. In our practice, at least triple zeta basis sets are required for such calculations.

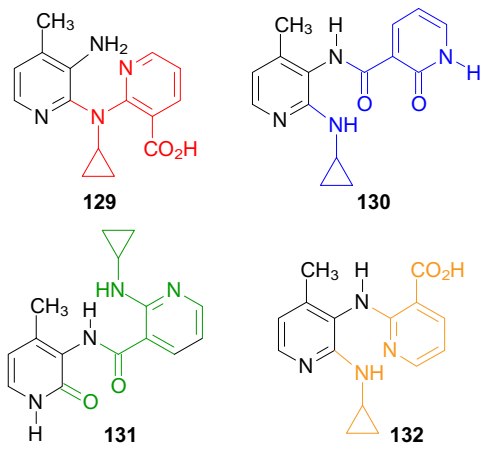
The second example taken from that publication [142] addresses a structural identification of a nevirapine hydrolysis product to ensure safety and efficacy in the drug development process. Nevirapine is a potent inhibitor of human immunodeficiency virus reverse transcriptase, which is required for early DNA synthesis. Because reverse transcriptase is a prime target for antiviral therapy against acquired immunodeficiency syndrome, inhibitors of this enzyme were developed for the treatment of virus infection.

Four possible isomers of the nevirapine hydrolysis product were proposed, resulting in structures **129** – **132**. Based on the performed calculations of ^{13}C NMR chemical shifts of those isomers as matched to experiment, the true structure **132** (RMSD 2.37 ppm) was revealed, compared to three alternative ones, namely **129** (RMSD 10.78 ppm), **130** (RMSD 6.16 ppm), and **131** (RMSD 5.70 ppm).

Based on these examples, a general methodology for assigning the correct structure of natural products has been formulated, as presented in the suggested self-explanatory procedure (Fig. 24).

White *et al.*[143] reported the revision of spiroleucettadine, a proton-deficient bicyclic sponge alkaloid. In addition, a

Structures 129 – 132



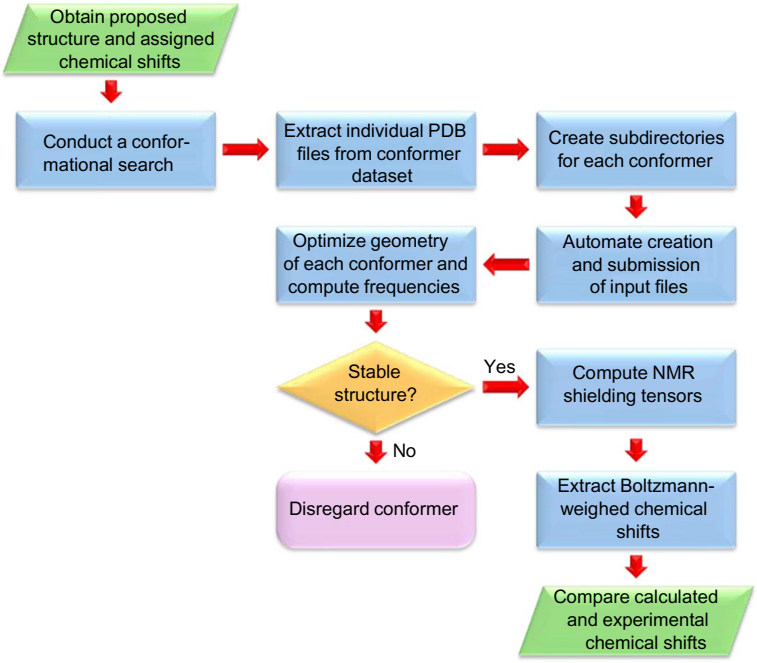
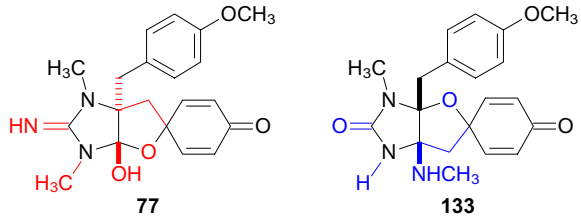


Figure 24. The flowchart depicting the methodology for calculating ^{1}H and ^{13}C NMR chemical shifts for the identification of a natural product of unknown (or ambiguous) structure. Reproduced from Xin *et al.*[142] with the permission of the American Chemical Society.

thorough systematic analysis of several candidate structures was performed *via* DFT calculations of their ^{13}C NMR chemical shifts; a favoured high scoring structure **133** was ultimately confirmed to be spiroleucettadine rather than the previously adopted structure **77**. All calculations of ^{13}C NMR chemical shifts were performed using a standard B3LYP/6-31G(d) method.

Structure 133



Wang *et al.*[144] reported the isolation of cytochalasins D1 (**134**) and C1 (**135**), which possess a unique eleven-membered macrocycle with an oxygen bridge and were extracted from the liquid fermentation of the fungus *Xylaria* cf. *curta*. Their structures and absolute configurations were determined by comprehensive experimental spectroscopic methods supported by calculations of ^{13}C NMR chemical shifts, which were performed at the ωB97x-D/6-31G(d)//B3LYP-D3(BJ)/TZVP level. The calculated chemical shifts matched the experimental ^{13}C NMR data quite well with an MAE of 1.3 ppm in the range of approximately 200 ppm, as illustrated in Fig. 25.

Howarth *et al.*[70] developed a robust system DP4-AI for the automatic processing and assignment of raw ^{13}C and ^{1}H NMR spectra integrated into the computational elucidation workflow (Fig. 26). This method achieved a 60-fold increase in processing speed, enabling structural elucidation of molecules, which was previously impossible, as exemplified by the structures **136** and **137** with the stereochemistry

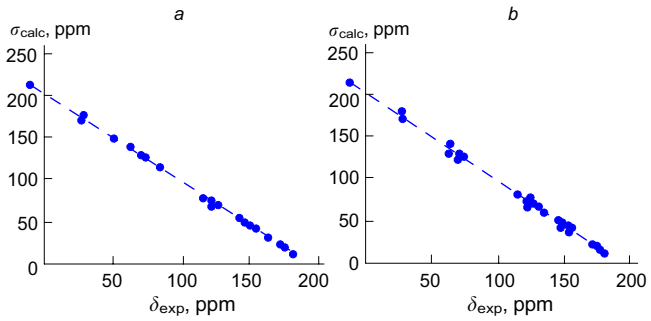
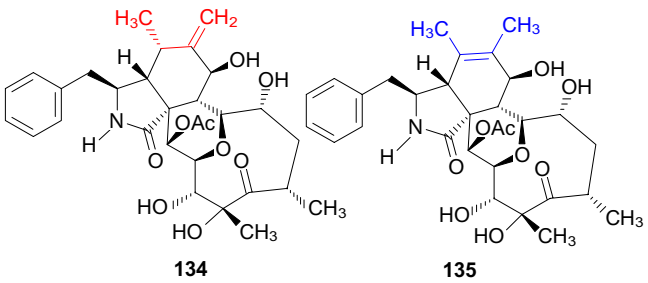
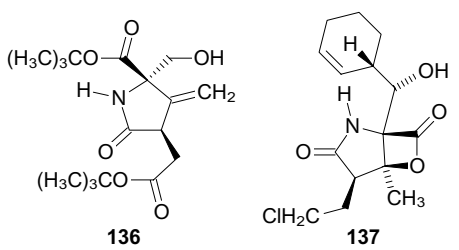


Figure 25. The linear regressions for the calculated shielding tensors of **134** (*a*) and **135** (*b*) compared to the experimental results. Reproduced from Wang *et al.*[144] with the permission of Elsevier.

Structures 134, 135



Structures 136, 137



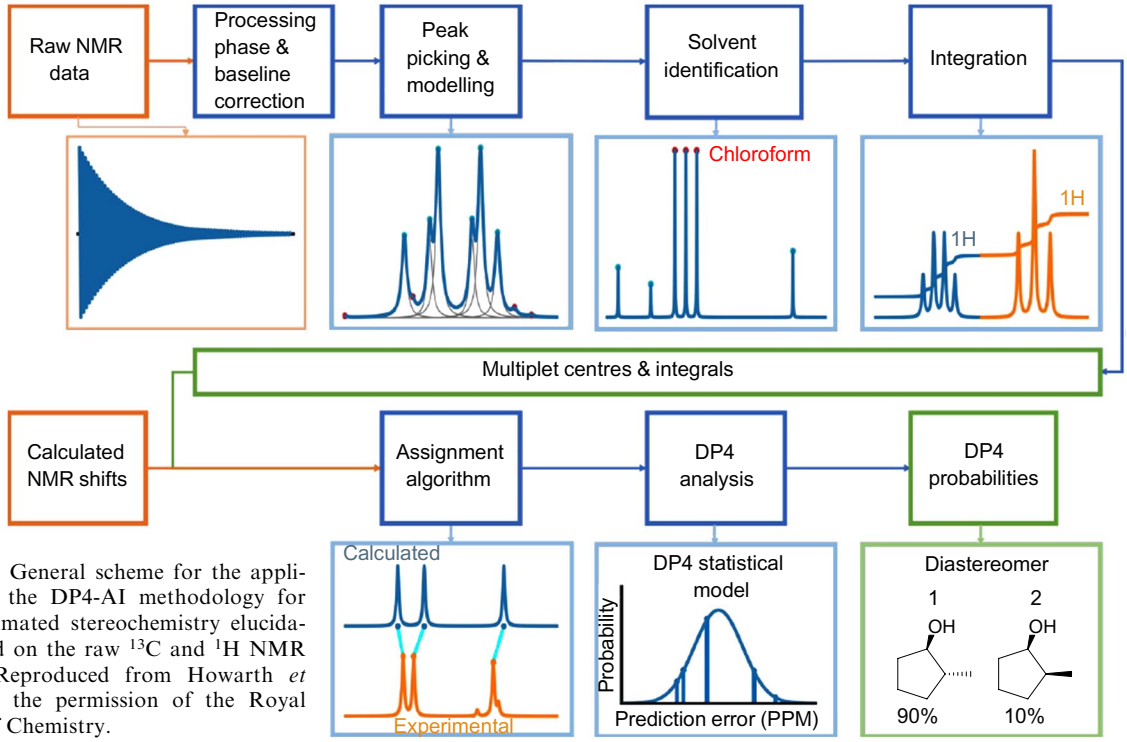


Figure 26. General scheme for the application of the DP4-AI methodology for fully automated stereochemistry elucidation based on the raw ^{13}C and ^{1}H NMR spectra. Reproduced from Howarth *et al.*[70] with the permission of the Royal Society of Chemistry.

predicted fully automatically by using the DP4-AI algorithm.

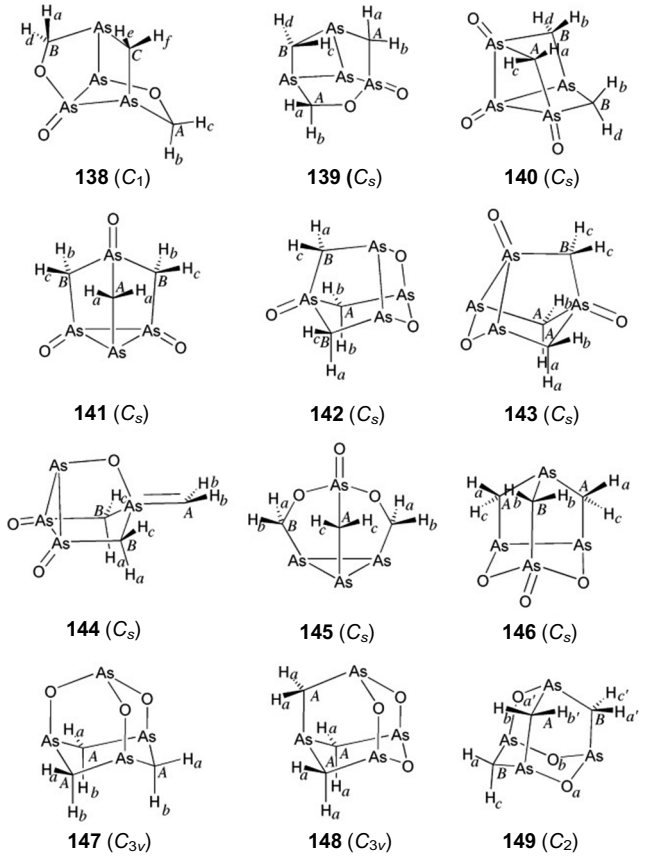
6.3. Organoelement natural products

Tähtinen *et al.*[145] reported the ^{1}H and ^{13}C NMR chemical shifts and coupling constants of a series of organoarsenic compounds calculated at the DFT level and compared them with available experimental data involving the natural polyarsenical arsenicin A isolated from the New Caledonian sponge *Echinochalina bargibanti*.[146] It was shown that non-relativistic methods successfully modelled NMR spectra of those molecules; relativistic spin-orbit effects were found to be small but appreciable for ^{13}C NMR chemical shifts, and their inclusion was 'beneficial'.[145]

Application of this approach to the intriguing natural polyarsenic compounds **138**–**149** allowed the viable alternative structures **138**–**148** to be ruled out after their thorough examination and thereby confirmed the previously suggested adamantane-like structure of arsenicin A as structure **149** with a C_2 symmetry point group.

The structures and energies of **138**–**149** were optimized at the B3LYP/6-311G(2d,2p) level, while their ^{1}H and ^{13}C NMR chemical shifts were calculated by taking into account spin-orbit relativistic corrections at the two-component zero-order regular approximation (so-ZORA) level using the Becke88-Perdew86 generalized gradient approximation (GGA) functional (known as 'BP') and a TZ2P basis set. This was done in view of the presence in the molecules under study the fourth-period arsenic. To the best of our knowledge, this is one of the very rare examples when a relativistic framework was adopted for the calculation of the ^{1}H and ^{13}C NMR chemical shifts of natural products.

Structures 138 – 149



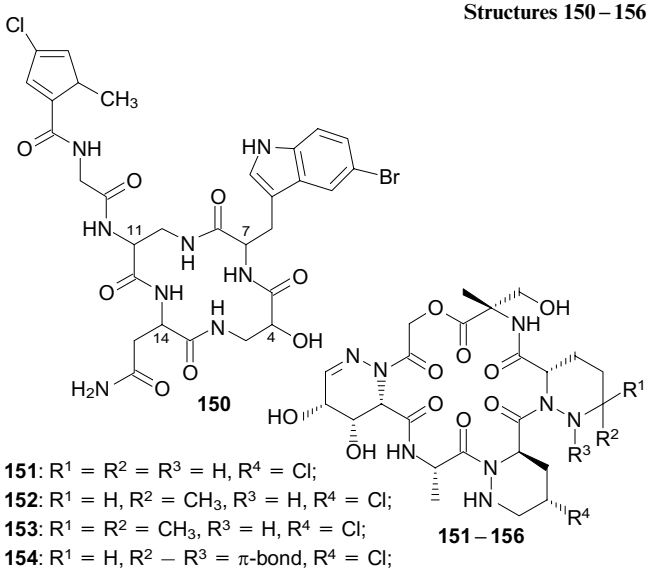
6.4. Peptides

Cooper *et al.*[147] established a structure of the natural product cyclocinamide A (**150**), a flexible cyclic peptide with four asymmetric stereocentres. The performed calculations led to the prediction of its natural stereochemistry as 4*S*,7*R*,11*R*,14*S*, which was confirmed by the total synthesis of cyclocinamide A. Geometry optimization of the candidate structures was carried out at the B3LYP/6-

311 + G(d,2p) level, while calculation of their ^{1}H and ^{13}C NMR chemical shifts was performed at the mPW1PW91/6-311 + G(3df,2p) level.

A representative paper by Dardić *et al.*[148] focuses on the structural characterization of six halogenated peptides termed svetamycins (**151** – **156**), which are characterized by the presence of a hydroxyl acetic acid and five amino acid moieties. The latter include a rare 4,5-dihydroxy-2,3,4,5-tetrahydropyridazine-3-carboxylic acid, a γ-halogenated piperazic acid, and a novel δ-methylated piperazic acid giving rise to the coexistence in one molecule of a whole series of different functional groups, such as hydroxyls, carbonyls, carboxyls, and their derivatives.

Structures 150 – 156



151: $R^1 = R^2 = R^3 = H$, $R^4 = Cl$;
152: $R^1 = H$, $R^2 = CH_3$, $R^3 = H$, $R^4 = Cl$;
153: $R^1 = R^2 = CH_3$, $R^3 = H$, $R^4 = Cl$;
154: $R^1 = H$, $R^2 - R^3 = \pi$-bond, $R^4 = Cl$;
155: $R^1 = R^2 = R^3 = H$, $R^4 = Cl$;
156: $R^1 = R^2 = CH_3$, $R^3 = H$, $R^4 = Cl$

The most well-known compound in this group is the parent svetamycin A (**151**). A combined computational/NMR approach to compare experimental and calculated ^{1}H and ^{13}C NMR chemical shifts was employed to corroborate the proposed configuration of that compound presented by eight possible diastereoisomers arising from the three optically active centers. To obtain information on the stereochemistry of svetamycin A, the ^{1}H and ^{13}C NMR chemical shifts were calculated at the M062X/6-31G(d,p) level for eight candidate structures (**a** – **h**). As shown in Fig. 27, isomer **g** among this series showed the lowest ^{1}H and ^{13}C CMAE values (0.21 and 1.60 ppm, respectively), suggesting the 2*S*,3*S*,4*R* absolute configuration.

In addition to the reported results, a careful analysis of the candidate structures revealed two main different conformers, *A* and *B*, as shown in Fig. 28. Interestingly, conformer *B* represented the main conformation of svetamicin A, while conformer *A*, which was not in agreement with the NMR data, represented the minor conformer. Taken together, the reported data supported the 2*S*,3*S*,4*R* structure as the most likely absolute configuration of svetamicin A.

In the paper by Ermanis *et al.*,[149] the effect of the quality of the optimized geometry on the computational NMR structure elucidation performance was reported. A number of semi-empirical, HF, and DFT methods used for the calculation of the conformer energies and ^{13}C NMR chemical shifts were explored. The B3LYP optimized geometries in combination with the mPW1PW91 and M06-2X functionals used for the evaluation of the NMR properties were found to be the best. The methodological steps of the computational NMR structure elucidation were formulated as follows: (i) conformational search; (ii) DFT structure optimization; (iii) DFT energy calculation; (iv) NMR shift calculation; and (v) statistical decision on which set of computed NMR shifts fit the experimental data best. These guidelines were illustrated on a wide series of natural products involving the most demanding case of lopinavir (**157**).

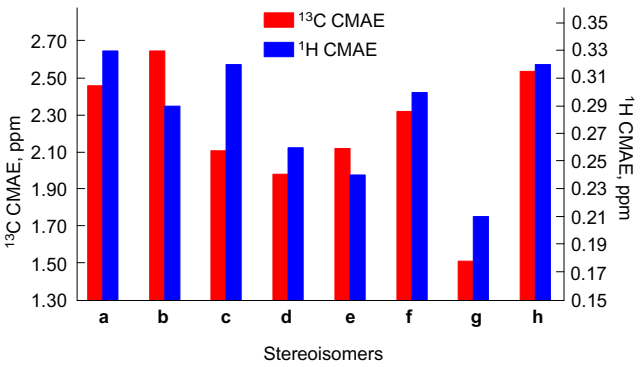


Figure 27. ^{13}C NMR (red bars) and ^{1}H NMR (blue bars) mean absolute error histograms related to the candidate diastereomers of svetamicin *A* (**151**) with the CMAEs of the most likely diastereomer shown in solid bars. Reproduced from Dardić *et al.*[148] with the permission of the American Chemical Society.

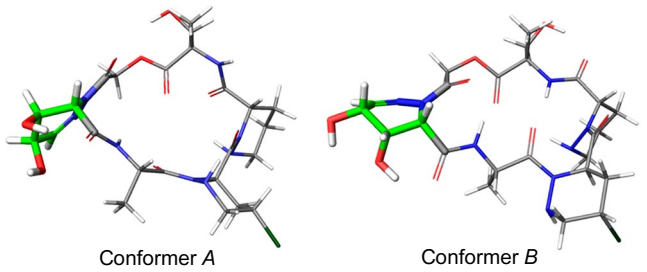
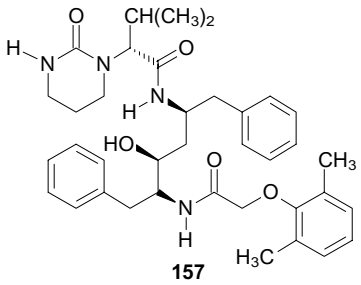


Figure 28. 3D representation of the most energetically favoured conformers of svetamicin A (**151**). Reproduced from Dardić *et al.*[148] with the permission of the American Chemical Society.

6.5. Mixed types

Sarotti and co-workers[63] introduced a modified probability method DP4+, whose main differences from the original DP4 version were the inclusion of the unscaled data and the use of the higher levels of theory for the NMR calculation

Structure 157



procedure, which resulted in a significant improvement in the overall performance of the DP4+ compared to the DP4 method. Implementation of DP4+ provided accurate and confident results in establishing the stereochemistry of approximately 90 challenging natural products exemplified here with structures **158**–**173**.

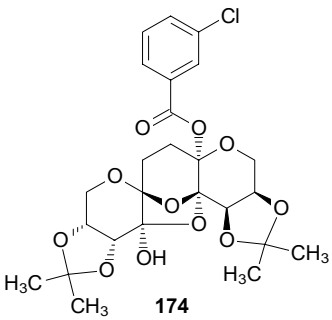
In the publication by Lorenc *et al.*,[150] it was reported that experimental data suggested a skeletal structure containing fused and spirocyclic rings for the synthetic spiroketal **174**, which was supported by the CASE (for CASE, see reviews [151, 152]) and the DFT calculations of its corresponding $^{2}J_{C,H}$ couplings.

Indeed, a powerful combination of CASE algorithms with DFT calculations enabled Buevich and Elyashberg[153] to perform unambiguous structural revision of a number of natural products, including cycloshermilamine D (**175**), a conformationally flexible chiral molecule of actinobenzoquinoline alkaloid (**176**), isolated from marine sediments; busseihydroquinone F (**177**), a polycyclic naphthalene; oroidin (**178**), a highly brominated natural product extracted from a marine *Pseudoalteromonas sp*. and tetrabromobenzofuropyrrole (**179**). Molecular geometries of **175**–**179** were optimized at the DFT level using the B3LYP functional in combination with Pople's 6-311+G(d,p) basis set, while calculation of ^{13}C NMR chemical shifts was performed with the mPW1PW91 functional and 6-311+G(2d,p) basis set. Again, it should be underlined that in the opinion of the authors of the present review, such calculations applied to molecules with heavy elements (such as bromine) should necessarily include relativistic treatment performed at either the two- or four-component level.

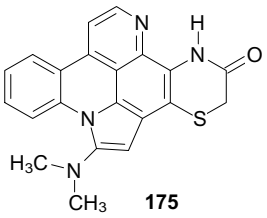
In the most comprehensive review by Grimblat and Sarotti,[35] a number of vivid examples were provided on how computational NMR could be used for the structural elucidation of a number of natural products. The benchmark natural products were exemplified in that publication with the most essential molecules of elatenyne (**180**, **181**), laurefurenynes A (**182a**) and B (**182b**), madeirolide A (**183a**,**b**), and gambierone (**184**) (Fig. 29).

The case of elatenyne from the family of 2,2 -bifuranyl-containing natural products is particularly interesting, as

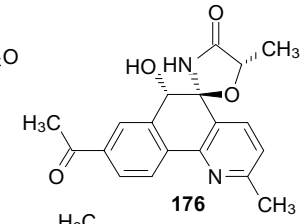
Structure 174 – 179



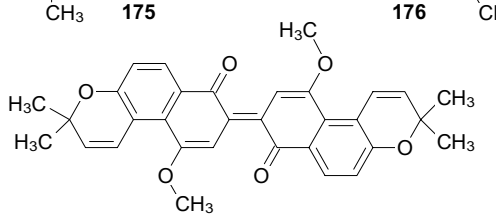
174



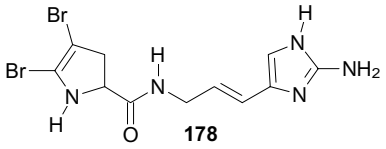
175



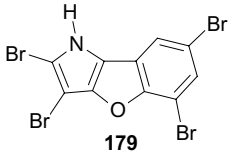
176



177

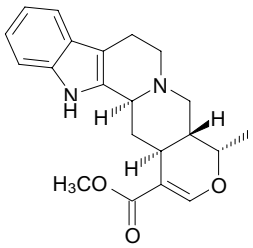


178

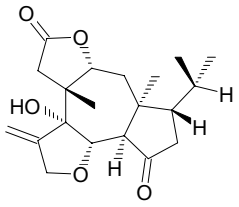


179

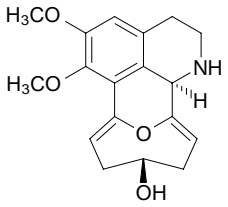
Structures 158 – 173



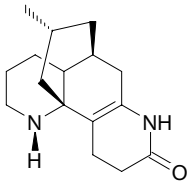
158



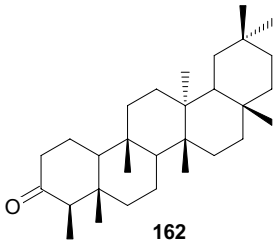
159



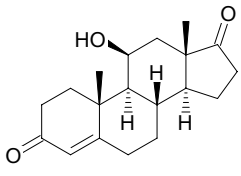
160



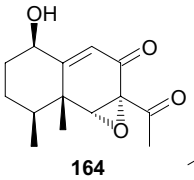
161



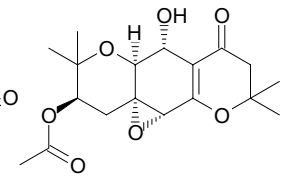
162



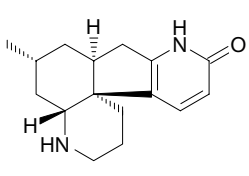
163



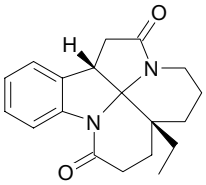
164



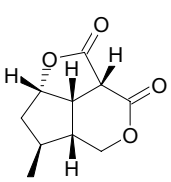
165



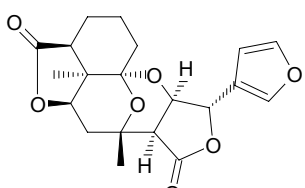
166



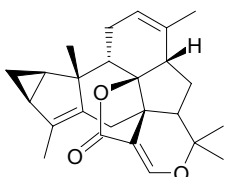
167



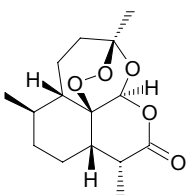
168



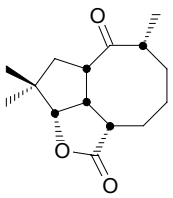
169



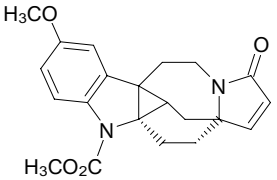
170



171



172



173

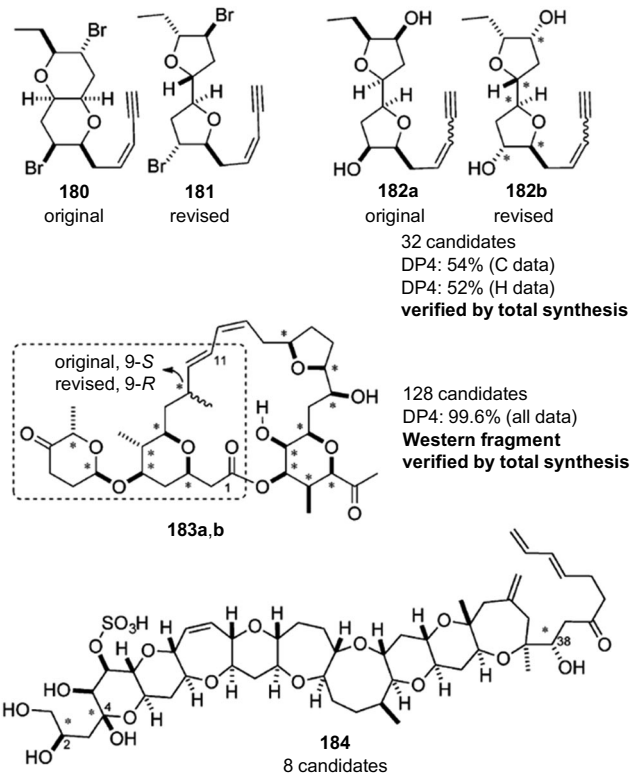


Figure 29. Original and revised structures of elatenyne (**180**, **181**), laurefurenynes A and B (**182a**,**b**), madeirolide A (**183a**,**b**), and gambierone (**184**). Reproduced from Grimblat and Sarotti[35] with the permission of Wiley.

for a long time, it was supposed to contain a pyrano[3,2-*b*]pyran system (see Fig. 29, unrevised structure **180**) in contrast to its computer-established stereostructure (see Fig. 29, revised structure **181**).[154]

The relative stereochemistry of laurefurenynes A and B (**182a**,**b**) was proposed on the basis of the NOESY experiments. The most likely stereostructures of laurefurenynes A and B were deduced based on the DP4 analysis including all plausible stereoisomers.

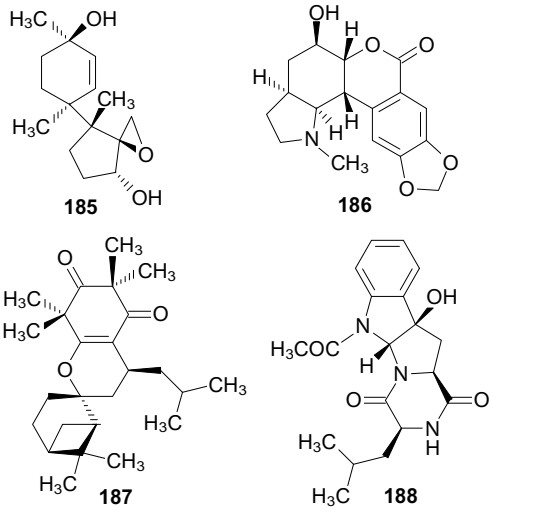
With the established stereochemistry of the reassigned madeirolide A, a successful synthesis of this natural product was conducted, providing a convincing homology for the ^{1}H and ^{13}C NMR data between the synthesized molecule and the isolated substance. The final assignment of madeirolide A was performed with the aid of DP4 analysis.

A unique and complex planar structure of gambierone **184** was deduced from extensive NMR analysis. However, those data were not conclusive for assigning the relative stereochemistry of that natural product. Only the DP4 probabilities computed from the ^{13}C NMR data strongly supported its 2*R**,4*R**,38*S** stereochemistry.

Some more structures established mostly by the DP4 computation include trichodiol (**185**), nobilisitine (**186**), nivariol **94** (see Section 4.1), ficifolidione (**187**), and protubonine A (**188**).[35]

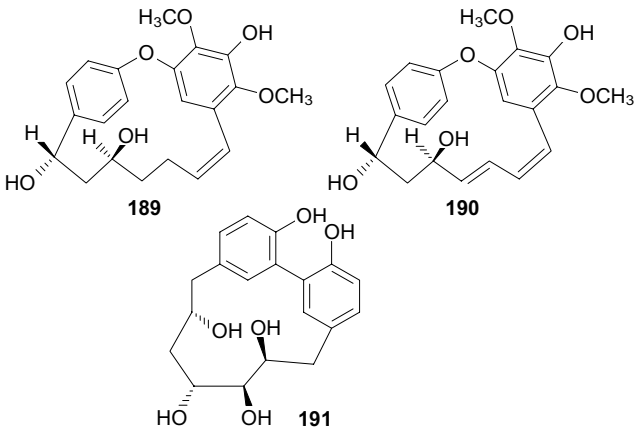
Masullo *et al.*[155] reported the isolation and identification of two new diaryl ether heptanoids, giffonins J (**189**) and K (**190**), along with five new diarylheptanoids, giffonins L-P, exemplified with compound **191**, which were extracted from the leaves of *Corylus avellana*. These compounds were identified as highly hydroxylated cyclized diarylheptanoids

Structures 185 – 188



using different NMR experiments supported by DFT calculations. The relative configurations of giffonins J-P were established by a direct comparison of the experimental ^{1}H and ^{13}C NMR chemical shifts, compared to their values calculated using the MPW1PW91 functional and Pople's 6-31G(d,p) basis set in methanol simulated within the IEF-PCM scheme.

Structures 189 – 191



Rodríguez *et al.*[156] reported the structural elucidation of lanesoic acid (**192**), which was obtained from DFT calculations performed using the B3LYP/6-31+G(d,p) method for geometry optimization and the MPW1PW91/6-311+G(2d,p) level for the calculation of ^{1}H and ^{13}C NMR chemical shifts (Fig. 30).

Domínguez *et al.*[157] performed DFT calculations of ^{13}C NMR chemical shifts of a rather complex natural product, okadaic acid (**193a**), as a structurally representative of a large group of marine toxins, using a standard computational protocol, B3LYP/6-31G+(d). A general conclusion of the performed study dealing with the computational procedure was that the use of the larger basis sets in those calculations was not needed and that inclusion of solvent effects slightly improved the quality of the results. Computational data were compared between the true structure of okadaic acid (**193a**) and that with inverted asymmetric

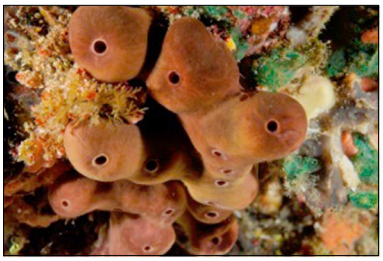
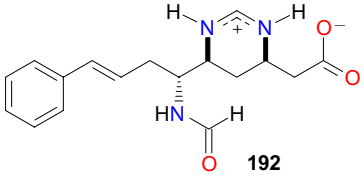
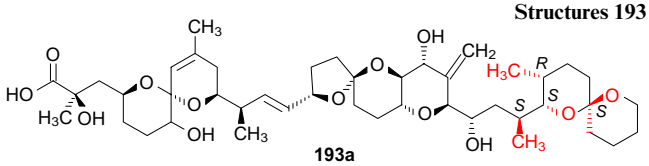


Figure 30. Lanesoic acid **192** isolated from *Theonella* sp. Reproduced from Rodríguez *et al.*[156] with the permission of the American Chemical Society.

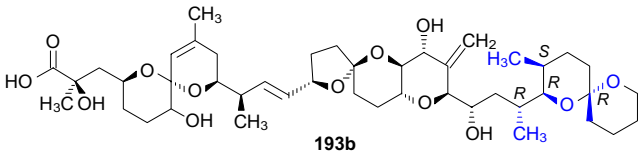


192

Structures 193



193a

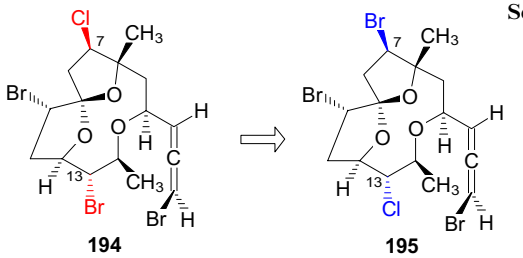


193b

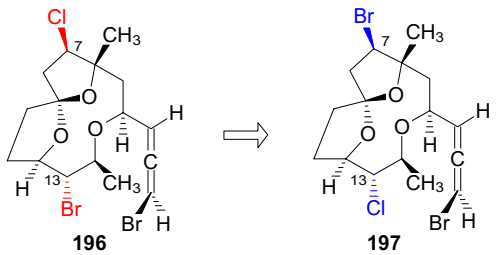
centers at four carbons (**193b**). When ^{1}H and ^{13}C NMR chemical shifts computed using both structures obtained from conformational searches were compared to each other, it turned out that in all circumstances, the correct stereoisomer was selected with 100% probability.

Braddock and Rzepa[158] reported the reassignment of obtusallenes V (**194**) and VI (**196**) isolated from the red seaweed *Laurencia obtusa* from the Turkish Mediterranean Sea and originally misassigned by Guella *et al.*,[159] to structures **195** and **197**, in which the halogens at C(7) and C(13) (bromine and chlorine) were transposed as shown below in Scheme 1. These reassignments were based on the computation of ^{13}C NMR chemical shifts with the mPW1PW91 functional and 6-31G(d,p) and/or aug-cc-pVDZ basis sets.

Scheme 1



194 **195**

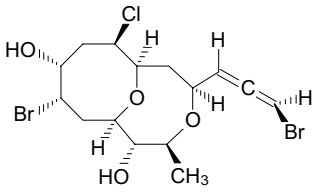


196 **197**

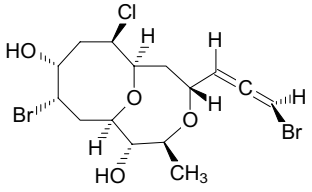
Grimblat *et al.*[65] performed stereo assignment of marilzabicycloallenes A (**198a**) and B (**198b**), two complex natural products possessing a flexible [5.5.1]bicyclotridecane ring. Using the standard DP4 treatment, the right structures were identified from the set of 128 different possible candidate stereoisomers based on the B3LYP/6-31G(d,p) calculations of their vicinal proton – proton spin – spin coupling constants ($^{3}J_{HH}$).

Additionally, the macrocyclic fragment of leiodermatolide (**199**) was thoroughly inspected. Restricting the conformational sampling with two and three experimental $^{3}J_{HH}$ values resulted in an 8- and 20-fold reduction in the number of conformations employed for further NMR calculations. Including up to seven additional couplings resulted in a minor effect on the resulting number of conformations to be considered.

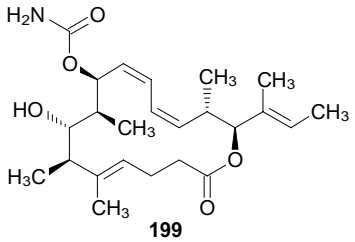
Structures 198, 199



198a



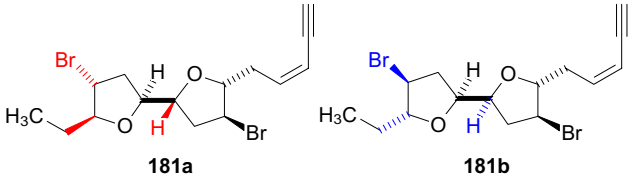
198b



199

Smith *et al.*[160] predicted the stereochemistry of the natural product elatenyne with the originally proposed structure **180** containing an octahydropyrano[3,2-*b*]pyran moiety, which was later revised to structure **181**, possessing a [2,2′]bifuranyl core (*vide supra*). Five-membered rings, such as the [2,2′]bifuranyl system, are highly flexible systems. Not only is there free rotation about the central bond, but each of the tetrahydrofurane rings can adopt many envelope and twist conformations. If there are substituents on the rings, as is the case of elatenyne, then the number of degrees of freedom is dramatically increased. The calculations revealed the two most likely stereochemical structures of elatenyne, **181a** and **181b**, with the former being the most preferable, as illustrated in Fig. 31. All calculations were performed using the combination B3LYP/6-31G(dp) with geometrical parameters optimized at the same level. For bromine, the LANL2DZ pseudopotential basis set was used throughout. No relativistic effects of heavy bromine on

Structures 181



181a **181b**

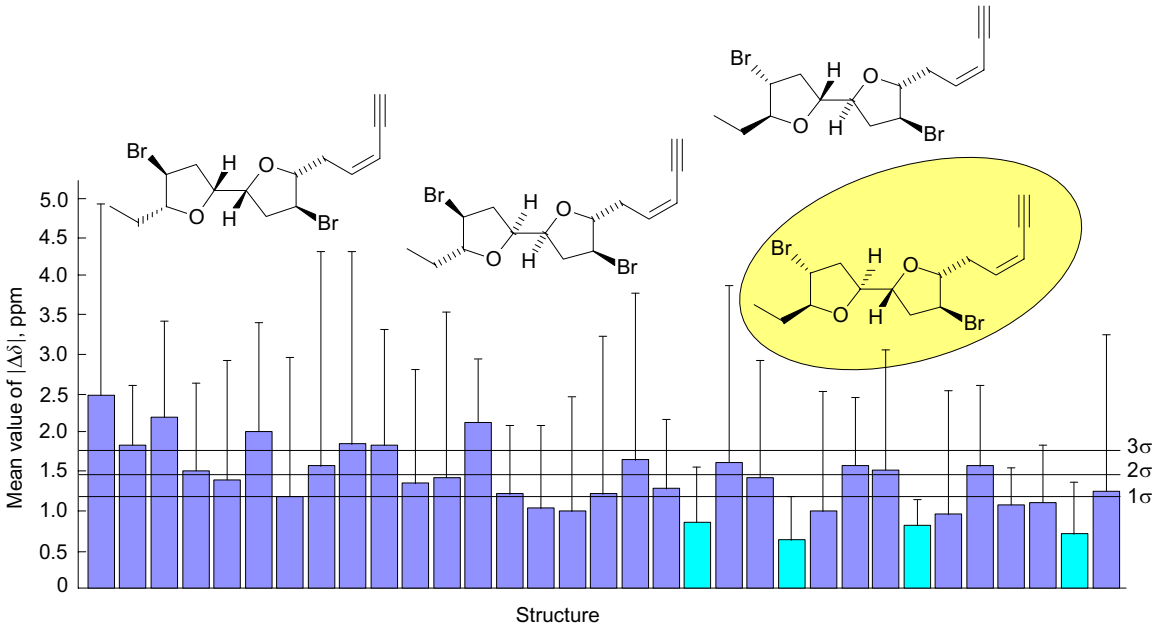


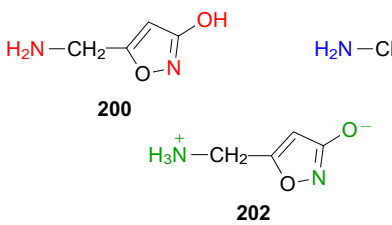
Figure 31. Mean (bars) and maximum (lines) values of $|\Delta\delta|$ for diastereomers of elatenyne **181**. The horizontal lines represent the values of the mean of $|\Delta\delta|$ that are one, two, and three standard deviations above the expectation value of the mean of $|\Delta\delta|$ for a correct structure. The smaller bars represent the best matches, and the top four matches are highlighted. Reproduced from Smith *et al.*[160] with the permission of the American Chemical Society.

^{13}C NMR chemical shifts were taken into account or even discussed.

Kupka and Wieczorek [161] reported a combined theoretical and experimental NMR study of muscimol (**200**), the bioactive alkaloid from the fly agaric mushroom *Amanita muscaria*. The assignment of the ^{1}H and ^{13}C NMR spectra of muscimol was supported by the DFT calculation of its proton and carbon shielding constants. The effect of solvent in theoretical calculations was included *via* the IEF-PCM model and the classical hybrid three-parameter B3LYP density functional in combination with Pople's 6-311++G(3df,2pd) basis set. The performed calculations enabled the authors to deduce the reliable structures of the non-ionized (neutral) molecule (**200**) and its NH (**201**) and zwitterionic (**202**) forms in the gas phase, chloroform, DMSO, and water. From the structural and energetic parameters obtained from the unconstrained geometry optimization in the gas phase and solution, the existence of equal amounts of the non-ionized and NH forms in polar solvents was deduced. The zwitterionic form was found to be significantly less stable than the non-ionized forms of muscimol.

In the paper by Martin *et al.*,[162] the structure of coniothyrione, a xanthone-derived antibiotic discovered recently by an antisense screening approach, was unambiguously reestablished by means of joint experimental and theoretical elucidation of carbon–carbon connectivity patterns resulting in structure **99** (see Section 4.1).

Structures 200 – 202



Calculations of $^{1}J_{C,C}$ were performed using the B3LYP and WC04 functionals in combination with Pople's 6-311+G(d,p) basis set compared to experiment to make choice between two alternative structures being two geometrical isomers with different position of chlorine atom (either at C(3) or at C(4) atom). Figure 32 shows that a very good correlation was observed between the calculated and experimental carbon–carbon couplings for both isomers, with only one marked deviation for $^{1}J_{C\text{-}2,C\text{-}3}$ of the unrevised isomer (red dot), which strongly supported the revised structure bearing a chlorine atom at C(4) rather than at C(3).

Hu *et al.*[163] reported the revision of the allenic structure **203** assigned to a principal component of the bark of *Brosimum acutifolium*. This component was shown to be a known nonallenic substance, mururin C (**204**), a natural product studied earlier by Takashima *et al.*[164] This reassignment was based on the GIAO-B3LYP/6-31G (2d,2p)//B3LYP/6-31G (2d,2p) calculations of ^{13}C NMR chemical shifts, providing no evidence for the existence of the allenic moiety.

One of the most important and ubiquitous classes of natural products in the plant and animal kingdoms are flavonoids, which include flavonols, flavones, flavanols,

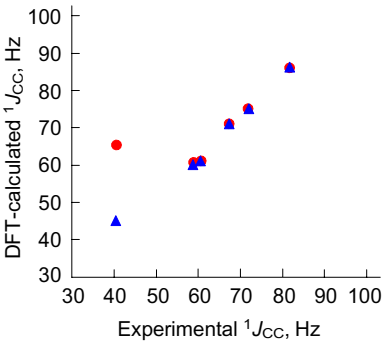


Figure 32. Plot of the DFT-calculated versus experimental $^{1}J_{C,C}$ coupling constants for two alternative structures of coniothyrione **99**: unrevised structure (red dots), revised structure (blue triangles). Reproduced from Martin *et al.*[162] with the permission of Wiley.

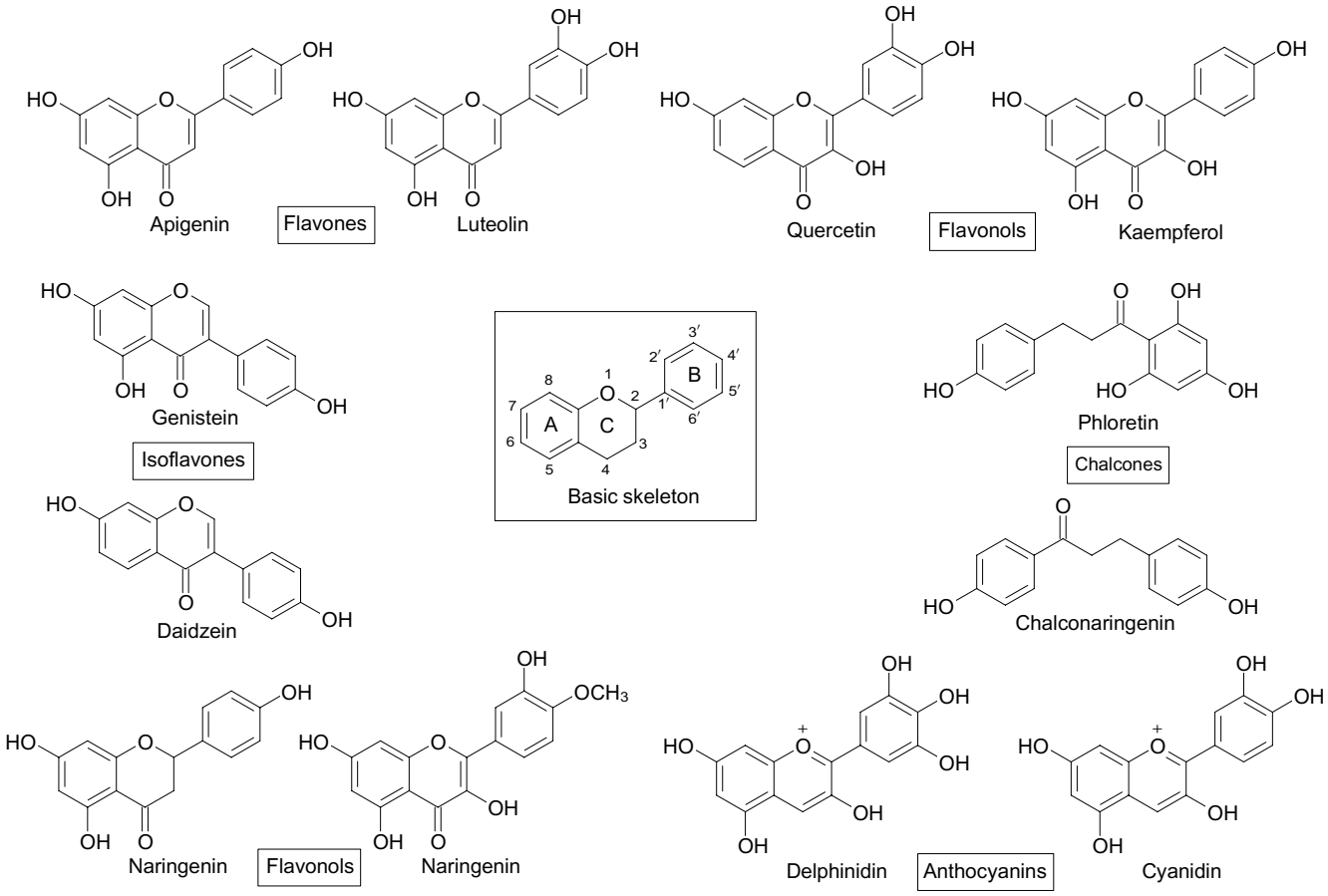
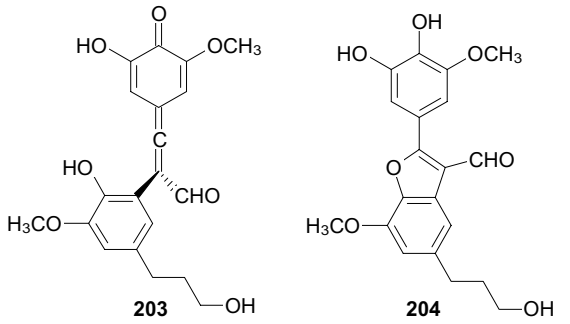


Figure 33. Basic skeleton structure and diversity of flavonoids and their classes. Reproduced from Panche *et al.*[165] under the Creative Commons Attribution 4.0 International Public License.

Structures 203, 204



flavanones, isoflavones, and anthocyanidins (Fig. 33).[165] Subdivision of flavonoids is presented in more detail in Fig. 34.[165]

7. Conclusion

Computational NMR of natural products is rapidly developing in parallel with the growing computational facilities becoming available in leading chemical and biochemical research centers and universities worldwide. We are now witnessing unprecedented progress in this field, and marked achievements in computational approaches to the structural elucidation of natural products together with other important biologically active compounds are on the cutting edge of modern chemical science.

A vast number of studies over the past several years have been devoted to the revision of the structure and configurations of numerous natural products together with the reassignment of their NMR spectra. Among these are the most impressive representatives of true alkaloids, including indole alkaloids (monoterpene, dimeric monoterpene, and trimeric monoterpene indole alkaloids), quinolizidine, pyrrolizidine, piperidine, indolizidine, quinoline and isoquinoline alkaloids, indoloquinoline, and guanidine alkaloids. Also discussed in this survey are pseudoalkaloids (terpenes and steroids) and quinones together with a number of miscellaneous alkaloids, including lactones, lactams, organoelement natural products, and peptides.

In the DFT calculations of ^{1}H and ^{13}C NMR chemical shifts and spin–spin coupling constants involving those nuclei of natural products, a vast amount of functionals and basis sets are currently used involving the most prospective B3LYP, B3PW91, PBE0, KT*n*, and mPW1PW91 functionals. The latter are used in combination with Pople s 6-31G and 6-311G, Dunning s cc-pV*n*Z (n = D, T, Q, 5) correlation-consistent basis sets and their augmented (diffuse) versions (aug-cc-pV*n*Z), Jensen s pcS-*n* and their augmented versions (aug-pcS-*n*).

In some specific cases, calculations of the ^{1}H and ^{13}C NMR parameters of natural products are performed at higher non-empirical levels, which are now realized, for example, in Gaussian and Dalton packages. However, these calculations are very resource demanding and time consuming, so at present they are still very far from practical (routine) applications.

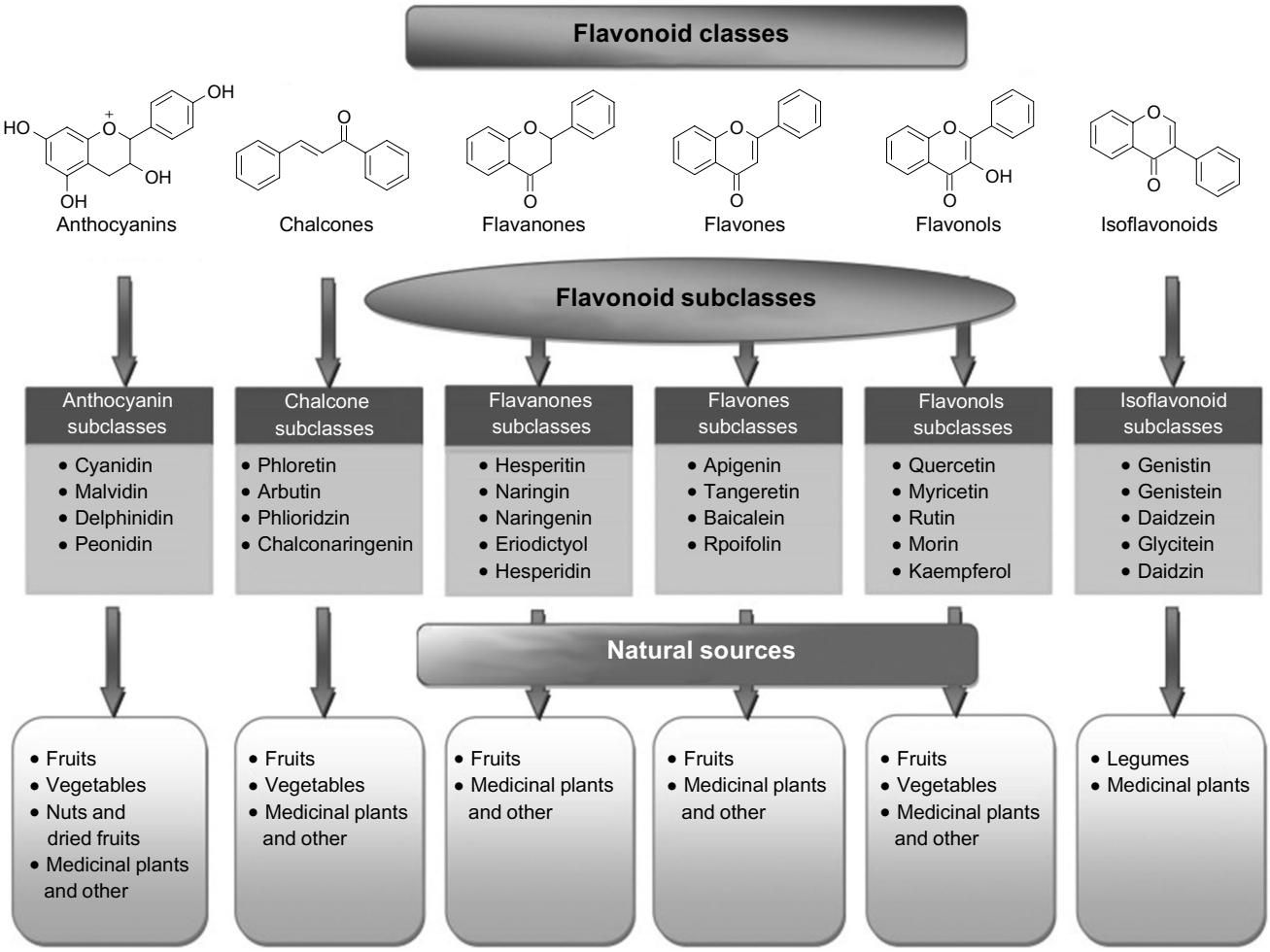


Figure 34. Flavonoid classes, subclasses and natural sources. Reproduced from Panche *et al.*[165] under the Creative Commons Attribution 4.0 International Public License.

8. List of acronyms and designations

ADEQUATE — adequate sensitivity double-quantum spectroscopy;
ANN — artificial neural network;
CASE — computer-assisted structure elucidation;
CBS — complete basis set;
CC3 — coupled cluster singles, doubles, and triples model;
CCSD — coupled cluster singles and doubles excitation model;
CCSD(T) — coupled cluster single and double excitation model with perturbative triples corrections;
CMAE — corrected mean absolute error;
COSMO — conductor-like screening model;
DNA — deoxyribonucleic acid;
DSO — diamagnetic spin-orbital (contribution);
FC — Fermi contact (contribution);
GGA — generalized gradient approximation;
GIAO — gauge-including atomic orbitals;
HALA — heavy-atom effect on the light-atom shielding;
HMBC — heteronuclear multiple bond correlation;
HSQC — heteronuclear single quantum correlation;
IEF-PCM — integral equation formalism polarizable continuum model;
LDBS — locally dense basis set;
MP2 — second-order Møller-Plesset perturbation theory;
NOE — nuclear Overhauser effect;
PBE — Perdew-Burke-Ernzerhof (functional);
PCM — polarizable continuum model;
PSO — paramagnetic spin-orbital (contribution);
RFF — relativistic force field;
RHF — restricted Hartree-Fock;
RMSD — root mean square deviation;
ROESY — rotating frame Overhauser effect spectroscopy;
RPA — random phase approximation;
SD — spin dipolar (contribution);
SC — scalar;
SO — spin-orbit;
SOPPA — second-order polarization propagator approach;
TO — total (sum of all coupling contributions);
ZORA — zero-order regular approximation;
ZPVC — zero-point vibrational correction.

9. References

1. S.P.A.Sauer. In *Molecular Electromagnetism. A Computational Chemistry Approach*. (Oxford: University Press, 2012); ISBN: 9780199575398
2. T.Helgaker, M.Jaszuński, K.Ruud. *Chem. Rev.*, **99**, 293 (1999); https://doi.org/10.1021/cr960017t

3. T.Helgaker, M.Jaszuński, M.Pecul. *Prog. NMR Spectrosc.*, **53**, 249 (2008); https://doi.org/10.1016/j.pnmrs.2008.02.002
4. T.Helgaker, S.Coriani, P.Jørgensen, K.Kristensen, J.Olsen, K.Ruud. *Chem. Rev.*, **112**, 543 (2012); https://doi.org/10.1021/cr2002239
5. D.Cremer, J.Grafenstein. *Phys. Chem. Chem. Phys.*, **9**, 2791 (2007); https://doi.org/10.1039/B700737J
6. J.Vaara. *Phys. Chem. Chem. Phys.*, **9**, 5399 (2007); https://doi.org/10.1039/B706135H
7. G.A.Aucar, R.H.Romero, A.F.Maldonado. *Int. Rev. Phys. Chem.*, **29**, 1 (2010); https://doi.org/10.1080/01442350903432865
8. M.Bühl, T.Mourik. *WIREs Comput. Mol. Sci.*, **1**, 634 (2011); https://doi.org/10.1002/wcms.63
9. *High Resolution NMR Spectroscopy: Understanding Molecules and their Electronic Structures*. (Ed. R.H.Contreras). (Elsevier, 2013); ISBN: 978-0444594112
10. Y.Y.Rusakov, L.B.Krivdin. *Russ. Chem. Rev.*, **82**, 99 (2013); https://doi.org/10.1070/RC2013v082n02ABEH004350
11. F.A.A.Mulder, M.Filatov. *Chem. Soc. Rev.*, **39**, 578 (2010); https://doi.org/10.1039/B811366C
12. T.Kupka. *Nucl. Magn. Reson.*, **46**, 1 (2021); https://doi.org/10.1039/9781788010665-00001
13. L.B.Krivdin, R.H.Contreras. *Ann. Rep. NMR Spectrosc.*, **61**, 133 (2007); ISBN: 9780123739186
14. L.B.Krivdin, Y.Y.Rusakov. *Encycl. Magn. Reson.*, **3**, 87 (2014); ISBN: 0471958395
15. Y.Xiao, W.Liu, J.Autschbach. In *Handbook of Relativistic Quantum Chemistry*. (Ed. W.Liu). (Berlin: Springer, 2017). P. 1; https://doi.org/10.1007/978-3-642-41611-8_17-1
16. J.Autschbach. *Phyl. Trans. Royal Soc. A*, **372**, 1 (2014); https://doi.org/10.1098/rsta.2012.0489
17. M.Repisky, S.Komorovsky, R.Bast, K.Ruud. In *Gas phase NMR*. (Eds K.Jackowski, M.Jaszunski). (Cambridge: The Royal Society of Chemistry, 2016). P. 267; https://doi.org/10.1039/9781782623816
18. I.L.Rusakova, Y.Y.Rusakov, L.B.Krivdin. *Russ. Chem. Rev.*, **85**, 356 (2016); https://doi.org/10.1070/RCR4561
19. I.L.Rusakova, L.B.Krivdin. *Mendeleev Commun.*, **28**, 1 (2018); https://doi.org/10.1016/j.mencom.2020.07.023
20. L.B.Krivdin. *Magn. Reson. Chem.*, **57**, 897 (2019); https://doi.org/10.1002/mrc.4873
21. L.B.Krivdin. *Magn. Reson. Chem.*, **58**, 5 (2020); https://doi.org/10.1002/mrc.4896
22. L.B.Krivdin. *Magn. Reson. Chem.*, **58**, 15 (2020); https://doi.org/10.1002/mrc.4895
23. L.B.Krivdin. *Prog. NMR Spectrosc.*, **108**, 17 (2018); https://doi.org/10.1016/j.pnmrs.2018.10.002
24. L.B.Krivdin. *Prog. NMR Spectrosc.*, **112** – **113**, 103 (2019); https://doi.org/10.1016/j.pnmrs.2019.05.004
25. L.B.Krivdin. *Prog. NMR Spectrosc.*, **102** – **103**, 98 (2017); https://doi.org/10.1016/j.pnmrs.2017.08.001
26. L.B.Krivdin. *Prog. NMR Spectrosc.*, **105**, 54 (2018); https://doi.org/10.1016/j.pnmrs.2018.03.001
27. L.B.Krivdin. *Russ. Chem. Rev.*, **89**, 449 (2020); https://doi.org/10.1070/RCR4927
28. L.B.Krivdin. *Russ. Chem. Rev.*, **89**, 1040 (2020); https://doi.org/10.1070/RCR4948
29. L.B.Krivdin. *Russ. Chem. Rev.*, **90**, 265 (2020); https://doi.org/10.1070/RCR44960
30. L.B.Krivdin. *Magn. Reson. Chem.*, **58**, 478 (2020); https://doi.org/10.1002/mrc.4965
31. L.B.Krivdin. *Magn. Reson. Chem.*, **58**, 500 (2020); https://doi.org/10.1002/mrc.4973
32. A.Bagno, G.Saielli. *WIREs Comput. Mol. Sci.*, **5**, 228 (2014); https://doi.org/10.1002/wcms.1214
33. A.Navarro-Vázquez. *Magn. Reson. Chem.*, **55**, 29 (2017); https://doi.org/10.1002/mrc.4502
34. M.W.Lodewyk, M.R.Siebert, D.J.Tantillo. *Chem. Rev.*, **112**, 1839 (2012); https://doi.org/10.1021/cr200106v
35. N.Grimblat, A.M.Sarotti. *Chem. – Eur. J.*, **22**, 12246 (2016); https://doi.org/10.1002/chem.201601150
36. D.J.Tantillo. *Nat. Prod. Rep.*, **30**, 1079 (2013); https://doi.org/10.1039/C3NP70028C
37. F.V.Toukach, V.P. Ananikov. *Chem. Soc. Rev.* **42**, 8376 (2013); https://doi.org/10.1039/C3CS60073D
38. W.Kohn, L.J.Sham. *Phys. Rev. A*, **140**, A1133 (1965); https://doi.org/10.1103/PhysRev.140.A1133
39. A.D.Becke. *J. Chem. Phys.*, **98**, 5648 (1993); https://doi.org/10.1063/1.464913
40. J.P.Perdew, in *Electronic Structure of Solids 91*. (Eds P.Ziesche and H.Eschrig). (Berlin: Akademie Verlag, 1991)
41. C.Adamo, V.Barone. *J. Chem. Phys.*, **108**, 664 (1998); https://doi.org/10.1063/1.475428
42. J.P.Perdew, K.Burke, M.Ernzerhof. *Phys. Rev. Lett.*, **77**, 3865 (1996); https://doi.org/10.1103/PhysRevLett.78.1396
43. J-D.Chai, M.Head-Gordon. *Phys. Chem. Chem. Phys.*, **10**, 6615 (2008); https://doi.org/10.1039/b810189b
44. M.R.Nyden, G.A.Petersson. *J. Chem. Phys.*, **75**, 1843 (1981); https://doi.org/10.1063/1.442208
45. F.Jensen. *J. Chem. Theory Comput.*, **4**, 719 (2008); https://doi.org/10.1021/ct800013z
46. W.J. Hehre, R.Ditchfield, J.A.Pople. *J. Chem. Phys.*, **56**, 2257 (1972); https://doi.org/10.1063/1.1677527
47. R.Krishnan, J.S.Binkley, R.Seeger, J.A.Pople. *J. Chem. Phys.*, **72**, 650 (1980); https://doi.org/10.1063/1.438955
48. D.B.Chesnut, K.D.Moore. *J. Comput. Chem.*, **10**, 648 (1989); https://doi.org/10.1002/jcc.540100507
49. B.Mennucci, E.Cancés, J.Tomasi. *J. Phys. Chem. B*, **101**, 10506 (1997); https://doi.org/10.1021/jp971959k
50. R.Ditchfield. *Chem. Phys.*, **63**, 185 (1981); https://doi.org/10.1016/0301-0104(81)80320-5
51. B.C.Mort. *Zero-Point and Temperature Dependent Vibrational Averaging of Molecular Properties*. (Buffalo, NY: State University of New York, 2007)
52. J.Vícha, J.Novotný, S.Komorovsky, M.Straka, M.Kaupp, R.Marek. *Chem. Rev.*, **120**, 7065 (2020); https://doi.org/10.1021/acs.chemrev.9b00785
53. A.F.Maldonado, G.A.Aucar. *Phys. Chem. Chem. Phys.*, **11**, 5615 (2009); https://doi.org/10.1039/B820609K
54. D.O.Samultsev, Yu.Yu.Rusakov, L.B.Krivdin. *Magn. Reson. Chem.*, **54**, 787, (2016); https://doi.org/10.1002/mrc.4452
55. P.A.M. Dirac. *Proc. R. Soc. Lond. A,* **117**, 610 (1928); https://doi.org/10.1098/rspa.1928.0023
56. E.van Lenthe, J.G.Snijders, E.J.Baerends. *J. Chem. Phys.*, **105**, 6505 (1996); https://doi.org/10.1063/1.472460
57. S.K.Wolff, T.Ziegler, E.van Lenthe, E.J.Baerends. *J. Chem. Phys.*, **110**, 7689 (1999); https://doi.org/10.1063/1.478680
58. B.A.Hess. *Phys. Rev. A*, **33**, 3742 (1986); https://doi.org/10.1103/PhysRevA.33.3742
59. M.Reiher, A.Wolf, *Relativistic Quantum Chemistry. The Fundamental Theory of Molecular Science. Second Edition*. (Weinheim: Wiley-VCH Verlag Co. KGaA, 2015)
60. S.G.Smith, J.M.Goodman. *J. Org. Chem.,* **74**, 4597 (2009); https://doi.org/10.1021/jo900408d
61. S.G.Smith, J.M.Goodman. *J. Am. Chem. Soc.,* **132**, 12946 (2010); https://doi.org/10.1021/ja105035r
62. K.Ermanis, K.E.B.Parkes, T.Agback, J.M.Goodman. *Org. Biomol. Chem.*, **14**, 3943 (2016); https://doi.org/10.1039/C6OB00015K
63. N.Grimblat, M.M.Zanardi, A.M.Sarotti. *J. Org. Chem.*, **80**, 12526 (2015); https://doi.org/10.1021/acs.joc.5b02396
64. K.Ermanis, K.E.B.Parkes, T.Agback, J.M.Goodman. *Org. Biomol. Chem.*, **15**, 8998 (2017); https://doi.org/10.1039/c7ob01379e
65. N.Grimblat, J.A.Gavín, A.H.Daranas, A.M.Sarotti. *Org. Lett.*, **21**, 4003 (2019); https://doi.org/10.1021/acs.orglett.9b01193
66. D.Xin, P.J.Jones, N.C.Gonnella. *J. Org. Chem.*, **83**, 5035 (2018); https://doi.org/10.1021/acs.joc.8b00338

67. P.Gao, J.Zhang, Q.Peng, J.Zhang, V-A.Glezakou. *J. Chem. Inf. Model.*, **60**, 3746 (2020); https://doi.org/10.1021/acs.jcim.0c00388
68. A.M.Sarotti. *Org. Biomol. Chem.*, **11**, 4847 (2013); https://doi.org/10.1039/c3ob40843d
69. D.-B.Pu, B.-W.Du, W.Chen, J.-B.Gao, K.Hu, N.Shi, Y.-M.Li, X.-J.Zhang, R.-H.Zhang, X.-N.Li, H.-B.Zhang, F.Wang, W.-L.Xiao. *Org. Lett.*, **20**, 6314 (2018)
70. A.Howarth, K.Ermanis, J.M.Goodman. *Chem. Sci.*, **11**, 4351 (2020); https://doi.org/10.1039/D0SC00442A
71. A.G.Kutateladze, O.A.Mukhina. *J. Org. Chem.*, **80**, 5218 (2015); https://doi.org/10.1021/acs.joc.5b00619
72. W.Hehre, P.Klunzinger, B.Deppmeier, A.Driessen, N.Uchida, M.Hashimoto, E.Fukushi, Y.Takata. *J. Nat. Prod.*, **82**, 2299 (2019); https://doi.org/10.1021/acs.jnatprod.9b00603
73. T.D.Tran, L.K.Cartner, H.R.Bokesch, C.J.Henrich, X.W.Wang, C.Mahidol, S.Ruchirawat, P.Kittakoop, B.R.O'Keefe, K.R.Gustafson. *Magn. Reson. Chem.*, **58**, (2020); https://doi.org/10.1002/MRC.4932
74. G.Casella, A.Bagno, S.Komorovsky, M.Repisky, G.Saielli. *Chem. – Eur. J.*, **21**, 18834 (2015); https://doi.org/10.1002/chem.201502252
75. A.M.A.Adam, M.S.Refat, H.A.Saad, M.S.Hegab. *J. Mol. Struct.*, **1102**, 170 (2015); https://doi.org/10.1016/j.molstruc.2015.08.065
76. V.A.Semenov, L.B.Krivdin. *Magn. Reson. Chem.*, **58**, 56 (2020); https://doi.org/10.1002/mrc.4922
77. A.Bagno, F.Rastrelli, G.Saielli. *Chem. – Eur. J.*, **12**, 5514 (2006); https://doi.org/10.1002/chem.200501583
78. R.T.Williamson, A.V.Buevich, G.E.Martin. *Org. Lett.*, **14**, 5098 (2012); https://doi.org/10.1021/ol302366s
79. G.Bifulco, R.Riccio, G.E.Martin, A.V.Buevich, R.T.Williamson. *Org. Lett.*, **15**, 654 (2013); https://doi.org/10.1021/ol3034803
80. A.G.Kutateladze, O.A.Mukhina. *J. Org. Chem.*, **80**, 10838 (2015); https://doi.org/10.1021/acs.joc.5b02001
81. T.Helgaker, M.Jaszuński, P.Świder. *J. Org. Chem.*, **81**, 11496 (2016); https://doi.org/10.1021/acs.joc.6b02157
82. A.V.Buevich, R.T.Williamson, G.E.Martin. *J. Nat. Prod.*, **77**, 1942 (2014); https://doi.org/10.1021/np500445s
83. M.Frédérich, Y.H.Choi, R.Verpoorte. *Planta Medica*, **69**, 1169 (2003); https://doi.org/10.1055/s-2003-818014
84. R.Verpoorte. *J. Pharm. Sci.*, **69**, 865 (1980); https://doi.org/10.1002/jps.2600690737
85. R.Verpoorte, T.A.Beek, R.L.M.Riegman, P.J.Hylands, N.G.Bisset. *Org. Magn. Reson.*, **22**, 345 (1984); https://doi.org/10.1002/mrc.1270220514
86. R.Verpoorte, P.J.Hylands, N.G.Bisset. *Org. Magn. Reson.*, **9**, 567 (1977); https://doi.org/10.1002/mrc.1270091004
87. S.P.Singh, V.I.Stenberg, S.S.Parmar, S.A.Farnum. *J. Pharm. Sci.*, **68**, 89 (1979); https://doi.org/10.1002/jps.2600680128
88. V.A.Semenov, D.O.Samultsev, L.B.Krivdin. *Magn. Reson. Chem.*, **58**, 532 (2020); https://doi.org/10.1002/mrc.4948
89. V.A.Semenov, D.O.Samultsev, L.B.Krivdin. *Int. J. Quant. Chem.*, **120**, e26348 (2020); https://doi.org/10.1002/qua.26348
90. S.Sauri, S.T.S.Chan, A.V.Buevich, K.R.Gustafson, R.T.Williamson, G.E.Martin. In *American Society of Pharmacognosy Annual Meeting*. (PQ32: Planta Medica, 2015); https://doi.org/10.1055/s-0035-1556366
91. H.S.Magalhães, A.B.da Silva, N.R.F.Nascimento, L.G.F. de Sousa, M.J.S.da Fonseca, M.I.B.Loiola, N.K.V.Monteiro, F.W.Q.A.Neto, K.M.Canuto, O.D.L.Pessoa. *Fitoterapia*, **143**, 104545 (2020); https://doi.org/10.1016/j.fitote.2020.104545
92. V.A.Semenov, L.B.Krivdin. *Magn. Reson. Chem.*, **59**, 108 (2021); https://doi.org/10.1002/mrc.5088
93. G.Philippe, E.Prost, J.-M.Nuzillard, M.Zèches-Hanrot, M.Tits, L.Angenot, M.Frédérich. *Tetrahedron Lett.*, **43**, 3387 (2002); https://doi.org/10.1016/S0040-4039(02)00476-8
94. Z.-W.Liu, J.Zhang, S.-T.Li, M.-Q.Liu, X.-J.Huang, Y.-L.Ao, C.-L.Fan, D.-M.Zhang, Q.-W.Zhang, W.-C.Ye, X.-Q.Zhang. *J. Org. Chem.*, **83**, 10613 (2018); https://doi.org/10.1021/acs.joc.8b01371
95. Y.-L.Wang, C.-R.Guo, Y.Mub, Y.-L.Lin, H.-J.Yan, Z.-W.Wang, X.-J.Wang. *Tetrahedron Lett.*, **60**, 151042 (2019); https://doi.org/10.1016/j.tetlet.2019.151042
96. V.A.Semenov, L.B.Krivdin. *Magn. Reson. Chem.*, **59**, 691 (2021); https://doi.org/10.1002/mrc.5129
97. V.Galasso, F.Asaro, F.Berti, I.Habuš, B.Kovač, C.D.Risi. *Chem. Phys.*, **301**, 33 (2004); https://doi.org/10.1016/j.chemphys.2004.03.003
98. R.P.Oliveira, A.J.Demuner, E.S.Alvarenga, L.C.A.Barbosa, T. de Melo Silva. *J. Mol. Struct.*, **1152**, 337 (2018); https://doi.org/10.1016/j.molstruc.2017.09.065
99. X.Yu, A.V.Buevich, M.Li, X.Wang, A.M.Rustum. *J. Pharm. Sci.*, **102**, 717 (2013); https://doi.org/10.1002/jps.23416
100. S.G.Smith, J.M.Goodman. *J. Am. Chem. Soc.*, **132**, 12946 (2010); https://doi.org/10.1021/ja105035r
101. V.Galasso. *Chem. Phys. Lett.*, **487**, 32 (2010); https://doi.org/10.1016/j.cplett.2010.01.008
102. J.Toušek, M.Straka, V.Sklenář, R.Marek. *J. Phys. Chem. A*, **117**, 661 (2013); https://doi.org/10.1021/jp310470f
103. A.Koch, B.Stamboliyska, B.Mikhova, P.Breznica-Selmani, K.Mladenovska, E.Popovski. *Magn. Reson. Chem.*, **57**, S75 (2019); https://doi.org/10.1002/mrc.4827
104. P.Breznica-Selmani, K.Mladenovska, G.Dräger, B.Mikhova, N.Panovski, A.Kaftandzieva, Z.Kavrakovski, A.Hoxha, N.Sheqerxhiu, M.J.Pavlova, E.Popovski, *Maced. J. Chem. Chem. Eng.*, **35**, 179 (2016); https://doi.org/10.20450/mjcce.2016.919
105. J.Saurí, W.Bermel, A.V.Buevich, E.C.Sherer, L.A.Joyce, M.H.M.Sharaf, P.L.Schiff, T.Parella, R.T.Williamson, G.E.Martin. *Angew. Chem., Int. Ed.*, **54**, 10160 (2015); https://doi.org/10.1002/anie.201502540
106. A.N.Tackie, G.L.Boye, M.H.M.Sharaf, P.L.Schiff, T.D.Spitzer, R.L.Johnson, J.Dunn, D.Minick, G.E.Martin. *J. Nat. Prod.*, **56**, 653 (1993); https://doi.org/10.1021/np50095a001
107. N.Aberle, S.P.B.Ovenden, G.Lessene, K.G.Watsona, B.J.Smith. *Tetrahedron Lett.*, **48**, 2199 (2007); https://doi.org/10.1016/j.tetlet.2007.01.088
108. A.G.Kutateladze, D.M.Kuznetsov. *J. Org. Chem.*, **82**, 10795 (2017); https://doi.org/10.1021/acs.joc.7b02018
109. G.Saielli, K.C.Nicolaou, A.Ortiz, H.Zhang, A.Bagno. *J. Am. Chem. Soc.*, **133**, 6072 (2011); https://doi.org/10.1021/ja201108a
110. G.Guella, E.Callone, D.Giuseppe, R.Frassanito, F.P.Frontini, I.Mancini, F.Dini. *Eur. J. Org. Chem.*, **2007**, 5226 (2007); https://doi.org/10.1002/ejoc.200700455
111. K.C.Nicolaou, H.Zhang, A.Ortiz, P.Dagneau. *Angew. Chem., Int. Ed.*, **47**, 8605 (2008); https://doi.org/10.1002/anie.200804228
112. K.C.Nicolaou, H.Zhang, A.Ortiz. *Angew. Chem., Int. Ed.*, **48**, 5642 (2009); https://doi.org/10.1002/anie.200902028
113. K.C.Nicolaou, H.Zhang, A.Ortiz. *Angew. Chem., Int. Ed.*, **48**, 5648 (2009); https://doi.org/10.1002/anie.200902029
114. K.C.Nicolaou, A.Ortiz, H.Zhang, P.Dagneau, A.Lanver, M.P.Jennings, S.Arseniyadis, R.Faraoni, D.E.Lizos. *J. Am. Chem. Soc.*, **132**, 7138 (2010); https://doi.org/10.1021/ja100740t
115. K.C.Nicolaou, A.Ortiz, H.Zhang, G.Guella. *J. Am. Chem. Soc.*, **132**, 7153 (2010); https://doi.org/10.1021/ja100742b
116. F.Cen-Pacheco, A.J.Santiago-Benítez, C.García, S.J.Álvarez-Méndez, A.J.Martín-Rodríguez, M.Norte, V.S.Martín, J.A.Gavín, J.J.Fernańdez, A.H.Daranas. *J. Nat. Prod.*, **78**, 712 (2015); https://doi.org/10.1021/np5008922
117. B.Schlegel, A.Härtl, H.M.Dahse, F.A.Gollmick, U.Gräfe, H.Dörfelt, B.Kappes. *J. Antibiot.*, **55**, 814 (2002); ISSN 1881-146.
118. J.J.La Clair. *Angew. Chem., Int. Ed.*, **45**, 2769 (2006); https://doi.org/10.1002/anie.200504033
119. S.D.Rychnovsky. *Org. Lett.*, **8**, 2895 (2006); https://doi.org/10.1021/ol0611346

120. A.J.Williams, M.E.Elyashberg, K.A.Blinov, D.C.Lankin, G.E.Martin, W.F.Reynolds, J.A.Porco, C.A.Singleton, S.Su. *J. Nat. Prod.*, **71**, 581 (2008); https://doi.org/10.1021/np070557t
121. G.Saielli, A.Bagno. *Org. Lett.*, **11**, 1409 (2009); https://doi.org/10.1021/ol900164a
122. M.W.Lodewyk, C.Soldi, P.B.Jones, M.M.Olmstead, J.Rita, J.T.Shaw, D.J.Tantillo. *J. Am. Chem. Soc.*, **134**, 18550 (2012); https://doi.org/10.1021/ja3089394
123. J.Yang, S.-X.Huang, Q.-S.Zhao. *J. Phys. Chem. A*, **112**, 12132 (2008); https://doi.org/10.1021/jp8072415
124. F.Cen-Pacheco, J.Rodríguez, M.Norte, J.J.Fernández, A.H.Daranas. *Chem. – Eur. J.*, **19**, 8525 (2013); https://doi.org/10.1002/chem.201204272
125. A.Bihlmeier, E.Bourcet, S.Arzt, T.Muller, S.Bräse, W.Klopper. *J. Am. Chem. Soc.*, **134**, 2154 (2012); https://doi.org/10.1021/ja2087097
126. M.M.Vaughan, Q.Wang, F.X.Webster, D.Kiemle, Y.J.Hong, D.J.Tantillo, R.M.Coates, A.T.Wray, W.Askew, C.O Donnell, J.G.Tokuhisa, D.Tholl. *The Plant Cell*, **25**, 1108 (2013); https://doi.org/10.1105/tpc.112.100057
127. M.J.Garson, W.Hehre, G.K.Pierens, Suciati. *Molecules*, **22**, 521 (2017); https://doi.org/10.3390/molecules22040521
128. A.V.Buevich, M.E.Elyashberg. *J. Nat. Prod.*, **79**, 3105 (2016); https://doi.org/10.1021/acs.jnatprod.6b00799
129. J.Ondeyka, A.V.Buevich, R.T.Williamson, D.L.Zink, J.D.Polishook, J.Occi, F.Vicente, A.Basilio, G.F.Bills, R.G.K.Donald, J.W.Phillips, M.A.Goetz, S.B.Singh. *J. Nat. Prod.*, **77**, 497 (2014); https://doi.org/10.1021/np400759f
130. K.A.Blinov, A.V.Buevich, R.T.Williamson, G.E.Martin. *Org. Biomol. Chem.*, **12**, 9505 (2014); https://doi.org/10.1039/C4OB01418A
131. R.T.Williamson, A.V.Buevich, G.E.Martin, T.Parella. *J. Org. Chem.*, **79**, 3887 (2014); https://doi.org/10.1021/jo500333u
132. A.M.Sarotti. *Org. Biomol. Chem.*, **11**, 4847 (2013); https://doi.org/10.1039/C3OB40843D
133. M.M.Zanardi, A.M.Sarotti. *J. Org. Chem.*, **80**, 9371 (2015); https://doi.org/10.1021/acs.joc.5b01663
134. J.Sikorska, A.M.Hau, C.Anklin, S.Parker-Nance, M.T.Davies-Coleman, J.E.Ishmael, K.L.McPhail. *J. Org. Chem.*, **77**, 6066 (2012); https://doi.org/10.1021/jo3008622
135. H.Lei, J.Yan, J.Yu, Y.Liu, Z.Wang, Z.Xu, T.Ye. *Angew. Chem., Int. Ed.*, **53**, 6533 (2014); https://doi.org/10.1002/anie.201403542
136. P.Sun, Q.Yu, J.Li, R.Riccio, G.Lauro, G.Bifulco, T.Kurtán, A.Mándi, H.Tang, T.-J.Li, C.-L.Zhuang, W.H.Gerwick, W.Zhang. *J. Nat. Prod.*, **79**, 2552 (2016); https://doi.org/10.1021/acs.jnatprod.6b00453
137. M.G.Teixeira, E.S.Alvarenga. *Magn. Reson. Chem.*, **54**, 623 (2016); https://doi.org/10.1002/mrc.4411
138. J.Powell, D.Valenti, H.Bobnar, E.Drain, B.Elliott, S.Frank, T.McCullough, S.Moore, A.Kettring, R.Iuliucci, J.K.Harper. *Magn. Reson. Chem.*, **55**, 979 (2017); https://doi.org/10.1002/mrc.4616
139. C.I.MacGregor, B.Y.Han, J.M.Goodman, I.Paterson. *Chem. Commun.*, **52**, 4632 (2016); https://doi.org/10.1039/C6CC01074A
140. I.E.Ndukwe, X.Wang, N.Y.S.Lam, K.Ermanis, K.L.Alexander, M.Bertin, G.E.Martin, G.Muir, I.Paterson, R.Britton, J.M.Goodman, E.J.N.Helfrich, J.Piel, W.H.Gerwick, R.T.Williamson. *Chem. Commun.*, **56**, 7565 (2020); https://doi.org/10.1039/D0CC03055D
141. H.J.Domínguez, J.G.Napolitano, M.T.Fernández-Sánchez, D.Cabrera-García, A.Novelli, M.Norte, J.J.Fernández, A.H.Daranas. *Org. Lett.*, **16**, 4546 (2014); https://doi.org/10.1021/ol502102f
142. D.Xin, C.A.Sader, O.Chaudhary, P.-J.Jones, K.Wagner, C.S.Tautermann, Z.Yang, C.A.Busacca, R.A.Saraceno, K.R.Fandrick, N.C.Gonnella, K.Horspool, G.Hansen, C.H.Senanayake. *J. Org. Chem.*, **82**, 5135 (2017); https://doi.org/10.1021/acs.joc.7b00321
143. K.N.White, T.Amagata, A.G.Oliver, K.Tenney, P.J.Wenzel, P.Crews. *J. Org. Chem.*, **73**, 8719 (2008); https://doi.org/10.1021/jo800960w
144. W.-X.Wang, T.Feng, Z.-H.Li, J.Li, H.-L.Ai, J.-K.Liu. *Tetrahedron Lett.*, **60**, 150952 (2019); https://doi.org/10.1016/j.tetlet.2019.150952
145. P.Tähtinen, G.Saielli, G.Guella, I.Mancini, A.Bagno. *Chem. – Eur. J.*, **14**, 10445 (2008); https://doi.org/10.1002/chem.200801272
146. I.Mancini, G.Guella, M.Frostin, E.Hnawia, D.Laurent, C.Debitus, F.Pietra. *Chem. – Eur. J.*, **12**, 8989 (2006); https://doi.org/10.1002/chem.200600783
147. J.K.Cooper, K.Li, J.Aubé, D.Coppage, J.P.Konopelski. *Org. Lett.*, **20**, 4314 (2018); https://doi.org/10.1021/acs.orglett.8b01756
148. D.Dardić, G.Lauro, G.Bifulco, P.Laboudie, P.Sakhaii, A.Bauer, A.Vilcinskas, P.E.Hammann, A.Plaza. *J. Org. Chem.*, **82**, 6032 (2017); https://doi.org/10.1021/acs.joc.7b00228
149. K.Ermanis, K.E.B.Parkes, T.Agback, J.M.Goodman. *Org. Biomol. Chem.*, **17**, 5886 (2019); https://doi.org/10.1039/C9OB00840C
150. C.Lorenc, J.Saurí, A.Moser, A.V.Buevich, A.J.Williams, R.T.Williamson, G.E.Martin, M.W.Peczuh. *ChemistryOpen*, **4**, 577 (2015); https://doi.org/10.1002/open.201500122
151. M.Elyashberg, A.Williams, K.Blinov. *Contemporary Computer-Assisted Approaches to Molecular Structure Elucidation*. (Cambridge: RSC Publishing, 2012); https://doi.org/10.1039/9781849734578
152. M.E.Elyasberg, A.J.Williams, G.E.Martin. *Prog. NMR Spectrosc.*, **53**, 1 (2008); https://doi.org/10.1016/j.pnmrs.2007.04.003
153. A.V.Buevich, M.E.Elyashberg. *Magn. Reson. Chem.*, **56**, 493 (2017); https://doi.org/10.1002/mrc.4645
154. B.S.Dyson, J.W.Burton, T.-I.Sohn, B.Kim, H.Bae, D.Kim. *J. Am. Chem. Soc.*, **134**, 11781 (2012); https://doi.org/10.1021/ja304554e
155. M.Masullo, V.Cantone, A.Cerulli, G.Lauro, F.Messano, G.L.Russo, C.Pizza, G.Bifulco, S. Piacente. *J. Nat. Prod.*, **78**, 2975 (2015); https://doi.org/0.1021/acs.jnatprod.5b00695
156. J.Rodríguez, C.Jiménez, M.Blanco, G.Tarazona, R.Fernández, C.Cuevas. *Org. Lett.*, **18**, 5832 (2016); https://doi.org/10.1021/acs.orglett.6b02832
157. H.J.Domínguez, G.D.Crespín, A.J.Santiago-Benítez, J.A.Gavín, M.Norte, J.J.Fernández, A.H.Daranas. *Marine Drugs*, **12**, 176 (2014); https://doi.org/10.3390/md12010176
158. D.C.Braddock, H.S.Rzepa. *J. Nat. Prod.*, **71**, 728 (2008); https://doi.org/10.1021/np0705918
159. G.Guella, I.Mancini, A.Öztunç, F.Pietra. *Helv. Chim. Acta*, **83**, 336 (2000); https://doi.org/10.1002/(SICI)1522-2675(20000216)83:2<336::AID-HLCA336>3.0.CO;2-R
160. S.G.Smith, R.S.Paton, J.W.Burton, J.M.Goodman. *J. Org. Chem.*, **73**, 4053 (2008); https://doi.org/10.1021/jo8003138
161. T.Kupka, P.P.Wieczorek. *Spectrochim. Acta*, **153**, 216 (2016); https://doi.org/10.1016/j.saa.2015.08.026
162. G.E.Martin, A.V.Buevich, M.Reibarkh, S.B.Singh, J.G.Ondeyka, R.T.Williamson. *Magn. Reson. Chem.*, **51**, 383 (2013); https://doi.org/10.1002/mrc.3952
163. G.Hu, K.Liu, L.J.Williams. *Org. Lett.*, **10**, 5493 (2008); https://doi.org/10.1021/ol802338z
164. J.Takashima, S.Asano, A.Ohsaki. *Planta Med.*, **68**, 621 (2002); https://doi.org/10.1055/s-2002-32906
165. A.N.Panche, A.D.Diwan, S.R.Chandra. *J. Nutr. Sci.*, **5**, e47 (2016); https://doi.org/10.1017/jns.2016.41